GEORGIA INSTITUTE OF TECHNOLOGY
OFFICE OF CONTRACT ADMINISTRATION
SPONSORED PROJECT INITIATION

Date: March 31, 1978

Project Title: The Effect of Ion Plating and Ion Implantation on the Cyclic Response and Fatigue Crack Initiation of Metals & Alloys

Project No: E-19-664

Project Director: E.A. Starke

Sponsor: Office of Naval Research

Agreement Period: From 3/1/78 Until ~~2/29/81~~ 2/28/84

Type Agreement: Contract No. N00014-78-C-0270

Amount: $157,100 (Partially funded at $50,000 through 2/28/79)

Reports Required: Progress Reports, Final Report

Sponsor Contact Person (s):

Technical Matters

Director, Metallurgy & Ceramics
Material Sciences Division
Office of Naval Research
Arlington, Va. 22217

Contractual Matters

(thru OCA)
Henry S. Cassell, III
Office of Naval Research
325 Hinman Research Bldg.
Ga. Institute of Technology
Atlanta, Ga. 30332

Defense Priority Rating: DO-C9 under DMS Reg. 1

Assigned to: Chemical Engineering (School/Laboratory)

COPIES TO:

- Project Director
- Division Chief (EES)
- School/Laboratory Director
- Dean/Director—EES
- Accounting Office
- Procurement Office
- Security Coordinator (OCA)
- Reports Coordinator (OCA)
- Library, Technical Reports Section
- EES Information Office
- EES Reports & Procedures
- Project File (OCA)
- Project Code (GTRI)
- Other

CA—3 (3/75)

GEORGIA INSTITUTE OF TECHNOLOGY — OFFICE OF CONTRACT ADMINISTRATION

SPONSORED PROJECT TERMINATION/CLOSEOUT SHEET

Date 2/22/85

Project No. E-19-664 — School/~~XXX~~ Chemical Engineer

Includes Subproject No.(s) N/A

Project Director(s) Dr. E.A. Starke, Jr. — GTRC /~~XXXX~~

Sponsor Office of Naval Research

Title The Effect of ~~Ion~~ ion Plating and ~~Ion~~ ion Implantation of the Cyclic Response and Fatigue ~~Crack~~ Crack Initiation of Metals and Alloys

Effective Completion Date: 2/28/84 (Performance) 4/28/84 (Reports)

Note: All closing documents submitted under E-19-672 which is same contract.

Grant/Contract Closeout Actions Remaining:

- [X] None
- [ ] Final Invoice or Final Fiscal Report
- [ ] Closing Documents
- [ ] Final Report of Inventions
- [ ] Govt. Property Inventory & Related Certificate
- [ ] Classified Material Certificate
- [ ] Other

Continues Project No. — Continued by Project No. E-19-672

COPIES TO:

Project Director
Research Administrative Network
Research Property Management
Accounting
Procurement/GTRI Supply Services
Research Security Services
Reports Coordinator (OCA)
Legal Services
Library
GTRC
Research Communications (2)
Project File
Other M. Heyser

A. Jones

FORM OCA 69.285

Technical Report 1
For the Period
1 March 1978 – 28 February 1979

THE EFFECT OF ION PLATING AND ION IMPLANTATION ON THE CYCLIC RESPONSE AND FATIGUE CRACK INITIATION OF METALS AND ALLOYS

By

S. Spooner, H. Solnick-Legg and E. A. Starke, Jr.
Fracture and Fatigue Research Laboratory

RESEARCH REPORT
CONTRACT N00014–78–C–0270

Prepared for

OFFICE OF NAVAL RESEARCH
DEPARTMENT OF THE NAVY

Approved for Public Release;
Distribution Unlimited

Permission is granted the U. S. Government
to reproduce this report in whole or in part.

GEORGIA INSTITUTE OF TECHNOLOGY
SCHOOL OF CHEMICAL ENGINEERING
ATLANTA, GEORGIA 30332

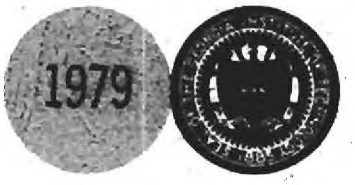

SECURITY CLASSIFICATION OF THIS PAGE *(When Data Entered)*

REPORT DOCUMENTATION PAGE		READ INSTRUCTIONS BEFORE COMPLETING FORM
1. REPORT NUMBER Technical Report No. 1	2. GOVT ACCESSION NO.	3. RECIPIENT'S CATALOG NUMBER
4. TITLE *(and Subtitle)* The Effect of Ion Plating and Ion Implantation on the Cyclic Response and Fatigue Crack Initiation of Metals and Alloys		5. TYPE OF REPORT & PERIOD COVERED Technical 1 March 78 - 28 Feb. 79 6. PERFORMING ORG. REPORT NUMBER
7. AUTHOR(s) S. Spooner, H. Solnick-Legg, and E. A. Starke, Jr.		8. CONTRACT OR GRANT NUMBER(s) N00014-78-C-0270
9. PERFORMING ORGANIZATION NAME AND ADDRESS Fracture and Fatigue Research Laboratory Georgia Institute of Technology Atlanta, Georgia 30332		10. PROGRAM ELEMENT, PROJECT, TASK AREA & WORK UNIT NUMBERS
11. CONTROLLING OFFICE NAME AND ADDRESS Office of Naval Research 800 N. Quincy Street Arlington, Virginia		12. REPORT DATE March 1979 13. NUMBER OF PAGES 30
14. MONITORING AGENCY NAME & ADDRESS*(if different from Controlling Office)*		15. SECURITY CLASS. *(of this report)* Unclassified 15a. DECLASSIFICATION/DOWNGRADING SCHEDULE

16. DISTRIBUTION STATEMENT *(of this Report)*

Approved for Public Release; Distribution Unlimited

17. DISTRIBUTION STATEMENT *(of the abstract entered in Block 20, if different from Report)*

18. SUPPLEMENTARY NOTES

19. KEY WORDS *(Continue on reverse side if necessary and identify by block number)*

Ion Implantation
Ion Plating
Fatigue Crack Initiation
Copper

20. ABSTRACT *(Continue on reverse side if necessary and identify by block number)*

X-ray diffuse scattering and transmission electron microscopy have been used to study the defect state of copper implanted with aluminum and argon ions. Electron microscopy studies of argon implanted thin foils reveals vacancy loops in the size range of 70Å to 350Å diameter for a dose of $2X10^{15}$ ions cm^{-2} at 100 kev. X-ray diffuse scattering measured around the 222 Bragg reflection reveals a combination of microalloying and dislocation loop effects from implantation of aluminum ions to a dose of $2X10^{16}$ ions cm^{-2} at 100 kev. Loop densities on the order of 10^{17} cm^{-2} and an average loop size of 25Å was

DD FORM 1 JAN 73 1473 EDITION OF 1 NOV 65 IS OBSOLETE

SECURITY CLASSIFICATION OF THIS PAGE *(When Data Entered)*

The Effect of Ion Plating and Ion Implantation on the Cyclic Response and Fatigue Crack Initiation of Metals and Alloys

Technical Report 1
For the Period
1 March 1978 - 28 February 1979

March 1979

by

S. Spooner, H. Solnick-Legg and E. A. Starke, Jr.

Prepared for the Office of Naval Research
Department of the Navy, under Contract
N00014-78-C-0270

Approved for public release; distribution unlimited

Permission is granted the U.S. Government to
reproduce this report in whole or in part.

Fracture and Fatigue Research Laboratory
Georgia Institute of Technology
Atlanta, Georgia 30332

TABLE OF CONTENTS

LIST OF FIGURES

ABSTRACT

X-ray diffuse scattering and transmission electron microscopy have been used to study the defect state of copper implanted with aluminum and argon ions. Electron microscopy studies of argon implanted thin foils reveals vacancy loops in the size range of 70Å to 350Å diameter for a dose of $2X10^{15}$ ions cm^{-2} at 100 kev. X-ray diffuse scattering measured around the 222 Bragg reflection reveals a combination of microalloying and dislocation loop effects from implantation of aluminum ions to a dose of $2X10^{16}$ ions cm^{-2} at 100 kev. Loop densities on the order of 10^{17} cm^{-3} and an average loop size of 25Å was estimated from the x-ray data. The aluminum ion damage is largely unchanged upon annealing for 30 minutes at 500° and 600°C. Alloying appears to stablize the surface radiation damage relative to damage produced in self-ion bombardments. The possible effectiveness of implanted layers in affecting fatigue crack initiation is being assessed.

I. BACKGROUND

Modern design philosophies, which are greatly affected by economical and safety factors, require the use of materials having an optimum combination of properties, e.g., fabricability, strength, facture toughness, corrosion and fatigue resistance. It is difficult to obtain alloys, either by design or through empirical development, having the required combination since the alloy chemistry and microstructure desired for certain properties may be detrimental to others. For example, aluminum alloys which show the highest static strength are inherently susceptable to stress corrosion cracking[1] and have poor fatigue resistance.[2] However, for most alloy systems corrosion and fatigue behavior are greatly affected by the surface condition and surface related phenomena, and may be improved (or controlled) by altering the state of the surface without adversely changing bulk properties, e.g., fracture toughness, yield strength, and ductility.

Metallic coatings have been widely used in industry for controlling corrosion and errosion. The principle of this technique is to separate the metal being protected from the unfavorable surroundings. An improvement arises from the inertness of the coating material with the environment. Many coating techniques are now available, and include hot dipping, metal spraying, electroplating, vacuum deposition, and diffusion coatings. These methods can be divided into two general groups: those which create an abrupt interface with a composition discontinuity between the coating surface and the substrate, and those which create a composition varation at the interface. Most of these coating methods produce an undesired contaminated interface which may prove detrimental when the sample is under static or dynamic loading. For example, during electroplating there may be a simultaneous reaction (e.g., water is

often reduced to form hydrogen) which may have a considerable influence on the mechanical properties. In addition, electroplated layers can have a wide range of compressive and tensile stresses depending upon the plating parameters, and may contain networks of microcracks with varying depths and spacing.[3] The more recent ion plating and ion implantation methods produce a clean, strongly-adherent interface between the coating material and substrate. The compositional variation at the interface can be controlled by controlling the energy of the ions.

Although it is generally agreed that fatigue cracks originate and propagate from a free surface and that the surface condition has a considerable effect on fatigue life, research on the influence of surface films on fatigue behavior has been lacking. The fatigue process may be divided into two general areas: crack initiation and crack propagation. Improvements in fatigue life can be obtained by increasing the time to crack initiation or reducing crack growth rates, or both. However, crack initiation is more affected by the surface condition than is crack propagation, and consequently the possibility exists for improving the fatigue performance by altering the state of the surface, without greatly changing bulk properties. The present ONR program is concerned with the effects of various ion-plated and ion implanted surfaces, and their microstructure, on the CSSR and fatigue crack initiation of a copper substrate. To meet the program objectives we have selected surface film-substrate combinations designed to separate the various parameters which control near surface deformation and associated crack initiation.

The influence of ion-plated surface films and/or implanted surfaces on fatigue crack initiation depends on such parameters as: crystal structure,

stacking fault energy, composition, and mechanical properties of the surface region and the substrate; the degree of misfit and cleanliness at the interface, the residual stresses in the film and substrate (due to radiation damage and the accommodation dislocation network) and the adhesion of the film. The complex interrelationships between these parameters, as well as which ones dominate for a given system, are presently not well understood. Consequently, the behavior of such composites is now largely unpredictable. Our effort during the first year of this program has been mainly concerned with studying the surface structure of copper single crystals implanted with aluminum and argon ions. Studies of fatigue crack initiation in similarily implanted crystals is now underway. Concurrently, we are studying the effect of ion plating on the low cycle fatigue behavior of polycrystalline copper. However, this report is concerned only with our preliminary results on the characterization of ion implanted copper single crystals.

II. INTRODUCTION

Although ion implantation effects are confined to very thin layers, several kinds of property improvements are effected by this method of surface treatment. Mechanical wear resistance dramatically increases so that wire drawing die life is quantitatively extended in the case of ion implantation of steel dies.[4] Ion plating which combines aspects of vaper deposition with aspects of low energy implantation at the substrate/plating interface has been demonstrated to modify the fatigue crack initiation resistance in copper single crystals.[5] Vapor deposition alone can change mechanical properties of copper[6] but the additional effects of ion damage on mechanical properties remains unexplored. There are many fundamental studies of the structure of ion implantation damage

related neutron damage simulation[7] and semi-conductor device physics.[8] The structure of the implanted layer can be modified in a controlled way by choice of ion, energy and dose. In approaching the possible application of implantation alloying and damage effects to fatigue crack initiation, one must answer several fundamental questions: (1) How do ion-type and implantation energy affect surface layer structure and structure stability, (2) How do the various implantation structures affect fatigue crack initiation mechanisms, and (3) which structures are helpful or detrimental to mechanical property improvements. A partial answer is given in a recent presentation on the effects of platinum ion plated titanium in which subsurface crack initiation was reported.[9]

A basic inquiry into the first question has been initiated with transmission electron microscopy and diffuse x-ray scattering studies of ion damage structure in copper. The single crystal method adopted for this investigation[10] is capable of measuring surface layer distortion and the density of dislocation loop produced by ion damage. The combination of these two methods aims at direct characterization of damage type and density and surface strain state measurement. This preliminary work describes some findings on the nature of sessile loops produced in copper by argon ion damage and the character of combined microalloy and sessile loop structure in aluminum-implanted copper. There are indications of irradiation damage stability in x-ray difuse scattering from annealed microalloys.

III. EXPERIMENTAL

Aluminum ion implantation of copper was selected on the basis of a favorable substitutional solubility combined with an easily measured alloy lattice parameter change. In addition, the relatively light ion can penetrate deeply into the copper substrate.

Copper single crystal surfaces parallel to (111) were prepared in bulk material or thin foil TEM discs for ion implantation. TEM discs were mechanically cut, electropolished and then teepanned into 3 mm discs. These discs were etched chemically and then finally thinned with a TENUPOL double-jet electro polisher until perforation. These foils were examined in the JEOL 100C electron microscope for selection of low dislocation density samples for later implantation.

Highly perfect crystals were selected for x-ray studies in order to ensure that pre-existing dislocation effects would not interfere with ion-implantation effects. Bulk copper crystals were provided by F. W. Young of Oak Ridge National Laboratory. These crystals were grown by Bridgeman technique and then annealed for two weeks at a few degrees below the melting point. The crystals were radiation hardened with neutrons before final cutting to orientation. Chemical cutting techniques were used to shape the crystal. The dislocation densities measured after final sample preparation, but prior to ion implanation, was less than 10^3 cm^{-2}.

The TEM discs and bulk crystals were oriented with (111) surface normals 6° from the incident beam direction to prevent channeling (even through [111] channeling in copper is very unfavorable). The Accelerators, Inc. 200 kev Ion Implanter was used to irradiate the crystal surfaces at 25°C. Temperature rises in these samples have not been measured. However, bulk samples are not expected to see more than a few degrees centigrade rise since the crystal substrate is a good heat sink. The TEM foils are mounted in mechanical contact with a good heat sink, but since the degree of thermal contact is unknown a temperature rise of several 10's of degrees C is possible at a high dose rate. Argon dose rates

at 100 kev were $3X10^{12}$ ions cm^{-2} sec^{-1}. The total dose was $2X10^{15}$ ions cm^{-2}. Bulk crystals were implanted with three doeses for the purpose of providing an approximately level implanted ion concentration from the surface to the maximum depth range at 200 kev. The implantation area of 3 mm diameter was placed to one side of the surface in order that x-ray diffraction measurement could be made on both implanted and unimplanted areas on the same crystal surface. Dose rates were as follows: $19.7X10^{13}$ ions cm^{-2} sec^{-1} at 200 kev, $9.9X10^{12}$ ions cm^{-2} sec^{-1} at 100 kev and $2.4X10^{11}$ ions cm^{-2} sec^{-1} at 50 kev. The does were $2X10^{16}$ ions cm^{-2}, $4X10^{15}$ ions cm^{-2} and $5.5X10^{15}$ ions cm^{-2} respectively. An aluminum concentration of 2 atomic percent is calculated to have been generated to a thickness of 1000 Å. The ion implanter beam line vacuum was $2X10^{-5}$ Torr during implantations. The ion implantation machine is now being modified to provide implant concentration profile determinations. In these studies theoretical estimates of implant distribution were used. Annealing studies were carried out on the bulk crystals at 500°C, 600°C, and 900°C in a vacuum of $\sim 10^{-6}$ Torr for 30 minutes.

The x-ray measurements were carried out with apparatus at the Oak Ridge National Laboratory. The diffuse scattering was measured in a two-axis x-ray spectrometer with Cu Kα radiation monochromated with the 333 reflection of a silicon crystal. The x-rays impinge on the (111) surface at approximately 45° and radiation scattered in the vicinity of the 222 reflection is intercepted by an open detector set at 90° from the incident beam. The scattering geometry is shown in Figure 1. The scattered intensity is measured as a function of the copper crystal rocking angle, $\Delta\Theta$, after the crystal has been carefully oriented to give a maximum peak reflectivity. The measured intensities are scaled to

the incident beam intensity of an approximately 2 mm diameter beam measured by the open detector positioned to intercept the beam through a calibrated filter.

TEM investigations concentrated on the observation of the relatively large loops found in the argon implanted foils. The theoretical argon ion distribution is peaked at 350 Å for 100 kev. Therefore it is estimated that a significant fraction of the damage will be deposited in the TEM foil. Sessile loops were identified by observing the variation of loop contrast with changing diffraction vector used for image contrast. The loop-type was identified by assuming a Burgers vector b = a/3 <111> and the collapse planes of {111}. Use of single crystals greatly facilitates the orientation analyses.

IV. RESULTS

The diffuse scattering measurements made on an aluminum implanted copper crystal are shown in Figure 2. The logarithm of the normalized scattering intensities of the implanted and un-implanted crystals are plotted as a function of the rocking angle $\Delta\Theta$ relative to the substrate Bragg peak position. An intensity increase arising from implantation is seen on both low and high angle sides of the Bragg peak. A general intensity increase is larger at low angles and no obvious side peak is seen. The qualitative character of the intensity is consistent with scattering from a Cu(Al) alloy whose lattice parameter is larger than that of the pure copper substrate. As will be discussed below, calcuated alloy layer scattering effects predict scattering in the form of a low angle peak with $I^S/I_o \sim 0.01$ with much smaller contribution, at high angles (I^S = scattered intensity and I_o is incident power). Therefore, additional diffuse scattering is present in the form of dislocation loop scattering. Such scattering arises from damage within the microalloy region. Thus, this diffuse

scattering must be peaked at an angle which is displaced toward the low-angle side from the substrate Bragg peak position. Presently no quantitative calculation of combined microalloying and damage effect scattering can be made. But recent self-ion damage results on nickel[11] provides some guidance on effects to be expected from loops alone. For the nickel study in which $5X10^{13}$ ions cm^{-2} were implanted at 4 Mev, points defects produced[12] were a factor of 20 less than that of the aluminum implantation of this study. The scattering intensity (I^S/I_o) seen in the nickel study was on the order of 10^{-3} in the angular range of interest. If the nickel scattering intensities were scaled up in proportion to the number of point defects produced then the scaled intensity would be in the range of scattering observed in our experiments. Thus, loop scattering and microalloying effects are comparable in their contribution to the integral diffuse scattering effect.

The results from integral diffuse scattering measurements for as-implanted and 500°C (T/T_M = 0.56) for 30 minutes annealed material is shown in Figure 3. This curve shows the difference between intensities taken from the implanted and unimplanted areas. Figure 4 shows similar data for a second crystal which was annealed at 600°C (T/T_M = 0.64) for 30 minutes. (The data in this figure may be compromised by the surface roughness of the sample although the trend shown in the annealing effects is at least qualitatively correct). The important finding is that the loop scattering (which is indicated most cleanly on the high angle side of the rocking curve) does not significantly change with annealing. This result should be compared with the observation that a 25% decrease in scattering from nickel self-ion implanted crystals was observed upon annealing at 450°C (T/T_M = 0.42) for one hour. Finally, although not shown, it

was observed that a 900°C (T/T_M = 0.86) annealled for 30 minutes entirely removed scattering effects from the crystal which was initially annealed at 500°C.

TEM micrographs of argon implanted foils are shown in Figure 5. Dislocation loops are visible near bend contours which contribute to the contrast. At least one-third of the larger loops present will not be visible due to image contrast geometry and no analysis for "black dot" loops was attempted. Several of the more easily seen loops (up to 350 Å diameter) were analyzed as vacancy type. This was determined on the basis of an "inside-outside" contrast variation with a change from one known diffraction vector to another. An estimate of the loop density of the larger loops was done assuming that one-third of the dislocations were observed in the damage thickness of 350 Å. The calculation gave $4X10^{10}$ loops cm^{-3}. If an average loop size of 100 Å diameter is assumed, then the number of point defects residing in loops is $2X10^{14}$ cm^{-3} which is lower than the density of Frenkel pairs which one calculates for the argon implantation dose. A calculation of dislocation density gives 10^6 cm^{-2} which is a density found in moderately annealed material.

V. DISCUSSION

TEM is essential for the determination of the dislocation loop type through contrast analysis. This kind of determination is not feasible with the present diffuse scattering method and would be difficult under the best of circumstances in the case of mixed vacancy and interstitial loop population. The observation of large loops in the estimated density found in argon implanted copper is consistent with the possibility of thin foil heating during implantation. The interstitials have enough mobility to leave the foil surfaces which are but a few tens of atomic diameters away from an average interstitial. A small amount of temperature rise may allow vacancy migration to go to larger loops which is

energetically favorable. In summary, one can expect to see elimination of interstitials and their loops and the growth of vacancy loops. Such a plausibility is born out in the TEM results which indicate vacancy loops at a density corresponding to moderately annealed material. As these studies progress, TEM methods employing back thinning will be used increasingly for the purpose of complementary TEM and x-ray studies of a identically implanted copper.

The x-ray diffuse scattering measurements can be compared against microalloy scattering estimates and loop scattering measurements made on self-ion implanted nickel.[11] Microalloy effects were estimated on the basis of a dynamical diffraction calculation originally done for elastically bent crystals.[13] Larson et al[14] have applied this approach to boron implanted silicon. Two coupled differential equations are written for the derivatives of the real and imaginary components of the scattering amplitude with respect to distance normal to the surface. These equations include a term describing the lattice strain as a function of depth due to a distribution of implanted solute. The lattice strain was taken to arise from the aluminum alloying lattice parameter change. The aluminum distribution was described by an approximation to the theoretical implantation profile. Numerical integration of the coupled differential equations was done with a differential equation solver available from the computer center library. The calculation sequence was as follows. At a given rocking angle, the real and imaginary components of the scattering amplitude was calculated for a perfect crystal[15,16]. These components were used as initial values for the integration into the crystal to a depth below the implanted ions. The real and imaginary components at this depth were then used as initial values for integration back to the free surface but with the intervening material now modified to include lattice distortions. The resulting amplitude at the free

surface gave the reflectivity of the crystal at the particular rocking. A sequence of these calculations gives the rocking curve shown in Figure 6. The small peak appearing at low angle has an associated d-spacing corresponding to the assumed 1 atomic percent alloy. The peak reflectivity of approximately 1% is of the right magnitude to correspond to observed scattering intensity. The model for the lattice strain used in the calculation does not take lattice relaxation at the interface between implanted and unimplanted material into account. There is expected to be a gradient in lattice parameter which would tend to broaden the scattering peak and therefore the scattering is distributed over wider angles at a lower intensity. When quantitative measurements of implantation profiles can be made with the implantation device on identically prepared material, further refinements of the above calculation will be attempted.

The diffuse scattering (I^S/I_0) from dislocation loops seen in self-ion implanted nickel is in the range of 10^{-3} over a wide angular range. The scattering of small rocking angles--Huang scattering--arises from the long-range loop strain fields and is characterized by a proportionality to $-\ln(\Delta\Theta)$. A larger angle scattering proportional to $(\Delta\Theta)^{-2}$ arises from short-range strain fields. In the aluminum implantation of copper, dislocation loops are created within the microalloy region. Thus, loop scattering build-up centers at the Bragg peak angle of the microalloy. This explains why there is a broad asymmetry of scattering in Figures 3, 4 and 5. It was necessary to estimate the Bragg peak center from the lattice expansion expected in a 2 atomic percent alloy with the result that $\Delta\Theta_{Bragg} = 3.9$ min. The diffuse scattering was plotted in Figure 7 where $\Delta\Theta$ was measured relative to the displaced microalloy Bragg peak. The average scattering calculated from

$$\bar{I} = (I^S(+)/I_o + I^S(-)/I_o)/2$$

was extrapolated to zero on the $\bar{I}$ vs $\ln(\Delta\theta)$ curve to obtain $\Delta\theta^*$. This value can then be used to obtain an average loop diameter from the relation[10] where

$$R_o = (e^{\frac{1}{2}} q_o^*)$$

where $q_o^* = h\,\Delta\theta^* \cos\theta_B$ and $h = 2\pi/d_{222}$. The average loop radius obtained in this calculation is 25 Å, but it must be kept in mind that loop radius size distributions have been found to be a strongly decreasing exponential[11] in form so that the average loop radius must be interpreted carefully.

An advantage in this scattering technique is that the measured intensity can be calculated with no arbitrary constants. Thus, parameters used for describing the loop size distribution can be obtained from an analysis of the measurements. For example, the Huang scattering occurring at small rocking angles can be calculated for a single loop size, R, having a specified loop density, C_r, which comes from the above described intensity extrapolation method. Hence

$$I^3(q_o)/I_o = K\,C_L R^4 \ln(q_o^*/q_o)$$

where $q_o = hq_o \cos\theta_B$ and K is a calculable constant which depends on known physical constants of the material. More physical models of loop size distribution such as the exponential form mentioned above ($C_L(R)\,C^{-R/R_o}$) can be used in similar equations to make quantitative comparisons with scattering data. For the time being it will be simpler to make qualitative comparisons of aluminum implant scattering with nickel self-ion implant scattering[11].

A simple Kinchen-Pease model for Frenkel defect (vacancy-interstial) production can be used to scale the expected scattering effects.( ) The number of defects per ion is given by

$$\nu(E_R) = \frac{0.8\ E_d}{2\ E_D^{avg}}$$

where E_R is the recoil energy, E_d is the recoil energy corrected for electronic energy loss, and E_D^{avg} is the average displacement energy. The ratio of defects produced in copper by 200 kev aluminum ions and in nickel by 4 Mev nickel ions is approximately 20 after dose differences are taken into account. A comparison of Huang scattering for the two cases is shown in Figure 8. Only a factor of 7 is seen which can be justified on several grounds. First, displacement cascades are smaller and distributed more deeply for aluminum in copper suggesting a tendency toward smaller loops. Second, saturation effects due to dose rate may lead to more point defect anhililation. Third, copper is at a higher homologous temperature at room temperature thus favoring point defect loss. Thus, loop scattering at low angles which favors large loops may be relatively lower in the aluminum implantation case. Nevertheless, loop densities on the order of 10^{17} cm^{-3} are estimated on the basis of densities quoted in the work on nickel. The x-ray results on as-implanted copper are satisfactorally interpreted in terms of a microalloy lattice parameter expansion and creation of a high dislocation loop density with an average loop size of 25 Å. More quantitative loop density interpretations are possible with measurements of scattering to larger rocking angles.

The annealing response of the aluminum implants shown in Figure 3 and Figure 4 points out that the dislocation loops are in a thermally stable

configuration. Both aluminum alloying and loop entanglement at high doses may account for this stability. Annealing at 500°C produces only subtle intensity changes, indicating that little or no aluminum transport has occurred to smooth out the composition gradient. Neither has there been a quantitative change in loop density or size distribution change. At 600°C, however, there has been a clear change in the asymmetry of scattering with only a 20% to 30% decrease in diffuse scattering tails. This suggests that the aluminum impurity transport is fast enough for aluminum to diffuse into the substrate. This results in a restortation of the original lattice parameter but since the loop structure remains largely intact, loop scattering persists but is now centered at the main Bragg peak position. With carefully chosen annealing treatments, it appears possible to eliminate microalloy affects and thereby a separation of the two effects becomes possible. Of more practical significance is the observation of a high thermal loop structure stability and hopefully a high mechanical stability for aluminum implantation. A comparable reduction of loop scattering was observed for one hour in nickel at 425°C with a homologous temperature of 0.42. The changes at 600°C in copper at a homologous temperature of 0.64 attest quantitatively to an appreciable stability.

The strain effects seen in aluminum implanted copper can be divided into a net strain due principally to microalloying and a fluctuating strain arising from dislocation loops. In the case studied by x-rays the net strains put the surface layer in compression as the copper lattice attempts to maintain coherency with the implanted layer. This is the desired stress condition for fatigue prevention. The loop distribution is likely to respond to this stress field although it is not obvious what response in loop density or loop-type distribution might be found. Further characterization of the surface layer will be needed.

Electron channeling is under consideration as a method for eventual use in our laboratory. Sensitive measurements of lattice strain are possible by this technique and results could corroborate x-ray diffraction trends.

As more implantation species are investigated, the relation between micro-alloying and loop stability will be explored. Detailed characterization of interstitial or substitutional implants will be needed especially in cases of highly metastable alloy combinations. To this end, consideration is being given to ion channeling for indification of lattice disruption effects.

VI. SUMMARY

The feasibility of TEM and x-ray scattering methods to characterize implantation microstructure has been demonstrated. Preliminary results indicate that substantial surface damage is induced in copper by aluminum implantation. Annealing response demonstrates that the damage state is stable. However, the observed stability is a function of the implantation ion. We are now in a position to quantitatively investigate surface strain, loop type and density of new implants. Fatigue crack initiation experiments will soon be started on implanted copper samples so that favorable microstructures can be identified.

VII. ACKNOWLEDGEMENTS

The authors would like to thank Dr. B. C. Larson and Mr. Jim Barhorst of ORNL for considerable aid in collection of the scattering data and many useful discussions. In addition, we would like to express our appreciation to Dr. Keith Legg for performing the implantations used in these investigations.

VIII. REFERENCES

1. M. O. Speidel, Met. Trans. A, 1975, Vol. 6A, p. 631.

2. M. E. Fine, Met. Trans. A., 1975, Vol. 6A, p. 625.

3. R. W. Staehle, in Surface Effects in Crystal Plasticity, R. M. Latanision and J. T. Fourie, eds., NATO Advanced Study Institute Series No. 17, Noordhoff-Leyden, 1977, p. 589.

4. G. Dearnaley and N. E. W. Hartley, Thin Solid Films, 1978, Vol. 54, p. 215.

5. E. Y. Chen and E. A. Starke, Jr., Materials Sci. Eng., 1976, Vol. 24, p. 209.

6. B. R. Livesay and E. A. Starke, Jr., Acta Met., 1973, Vol. 21, p. 247.

7. P. D. Townsend, J. C. Kelly and N. E. W. Hartley, Ion Implantation, Sputtering and Their Application, 1976, Chp. 4.

8. J. Stephen, in Ion Implantation, G. Dearnaley et al. eds, North-Holland Publ. Co., 1973, Chp. 5.

9. S. Fujishiro, "Improved High Temperature Mechanical Properties of Titanium Alloys by Pt Ion Plating," paper 9/18 in Int. Conf. Metallurgical Coatings, April 3-7, 1978, San Francisco.

10. B. C. Larson, J. Appl. Cryst., 1975, Vol. 8, p. 150.

11. J. Naryan and B. C. Larson, J. Appl. Phys., 1977, Vol. 48, p. 4536.

12. K. L. Merkle, in Radiation Damage in Metals, N. L. Peterson and S. D. Harkness eds., ASM, 1976, pp. 58-88.

13. B. Klar and F. Rustichelli, Nvovo Cimento, Vol. 13B, 1973, p. 249.

14. B. C. Larson, C. W. White and B. R. Appleton, Appl. Phys. Lett., 1978, Vol. 32, p. 801.

15. B. E. Warren, X-Ray Diffraction, Addison-Wesley, 1969, Chp. 14.

16. W. H. Zachariasen, Theory of X-Ray Diffraction in Crystals, Dover, 1967.

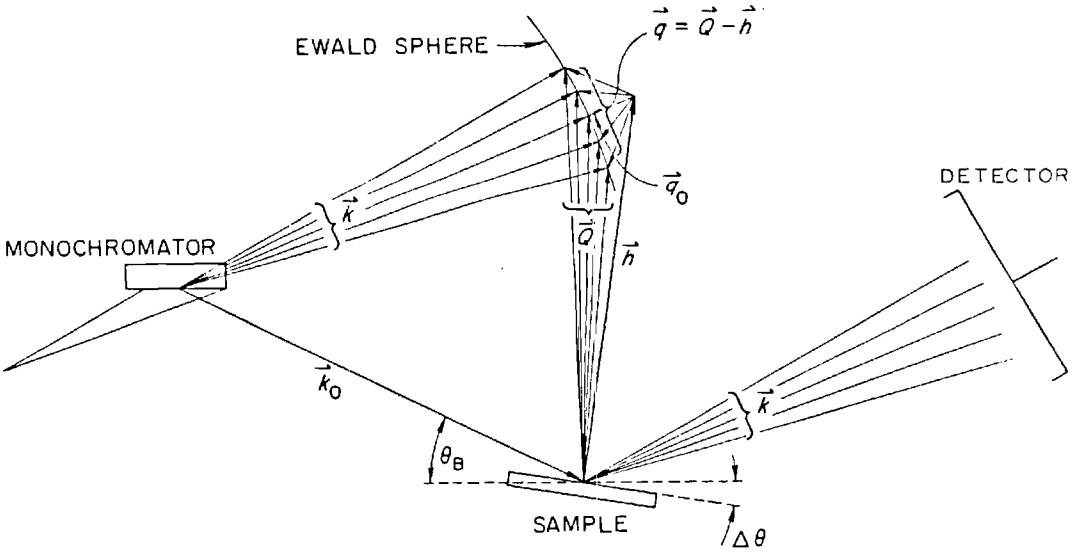

Figure 1. X-Ray Scattering Geometry for the Double-Crystal Measurements.

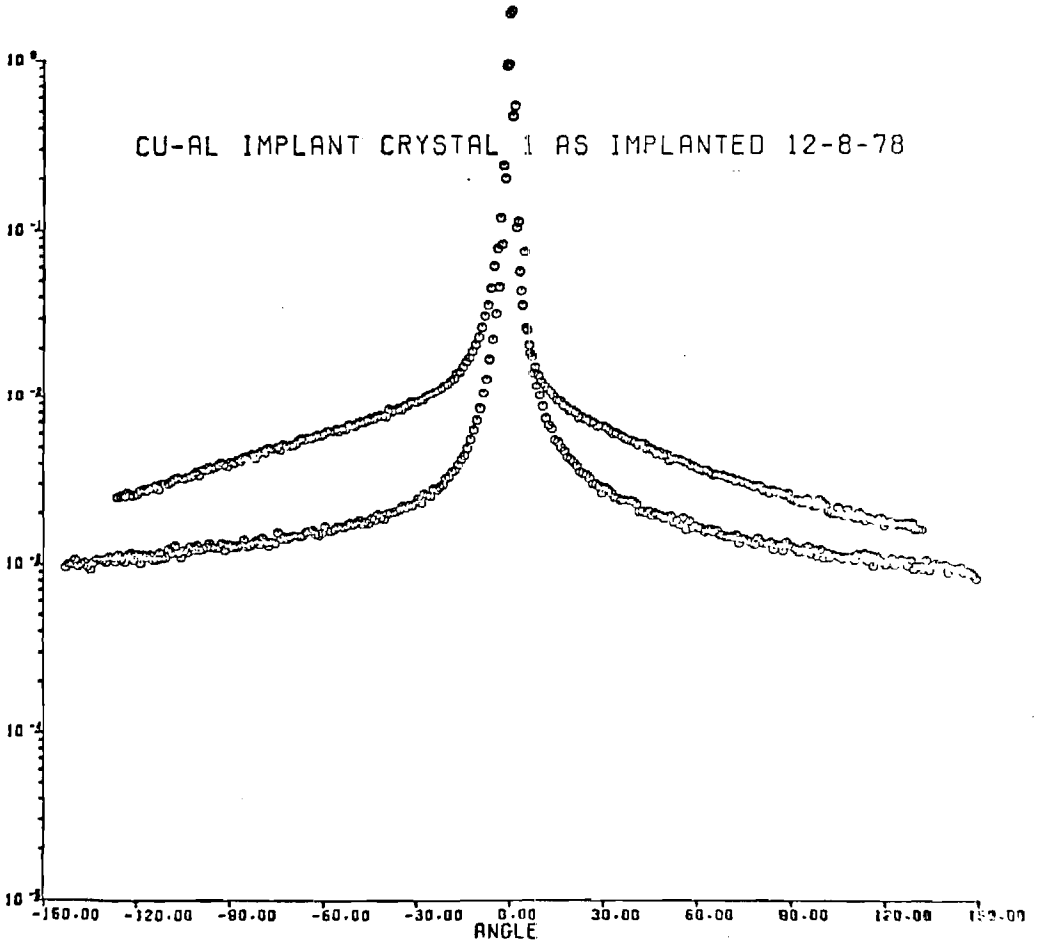

Figure 2. Scattering Rocking Curves (a) First Crystal Implanted and (b) Unimplanted.

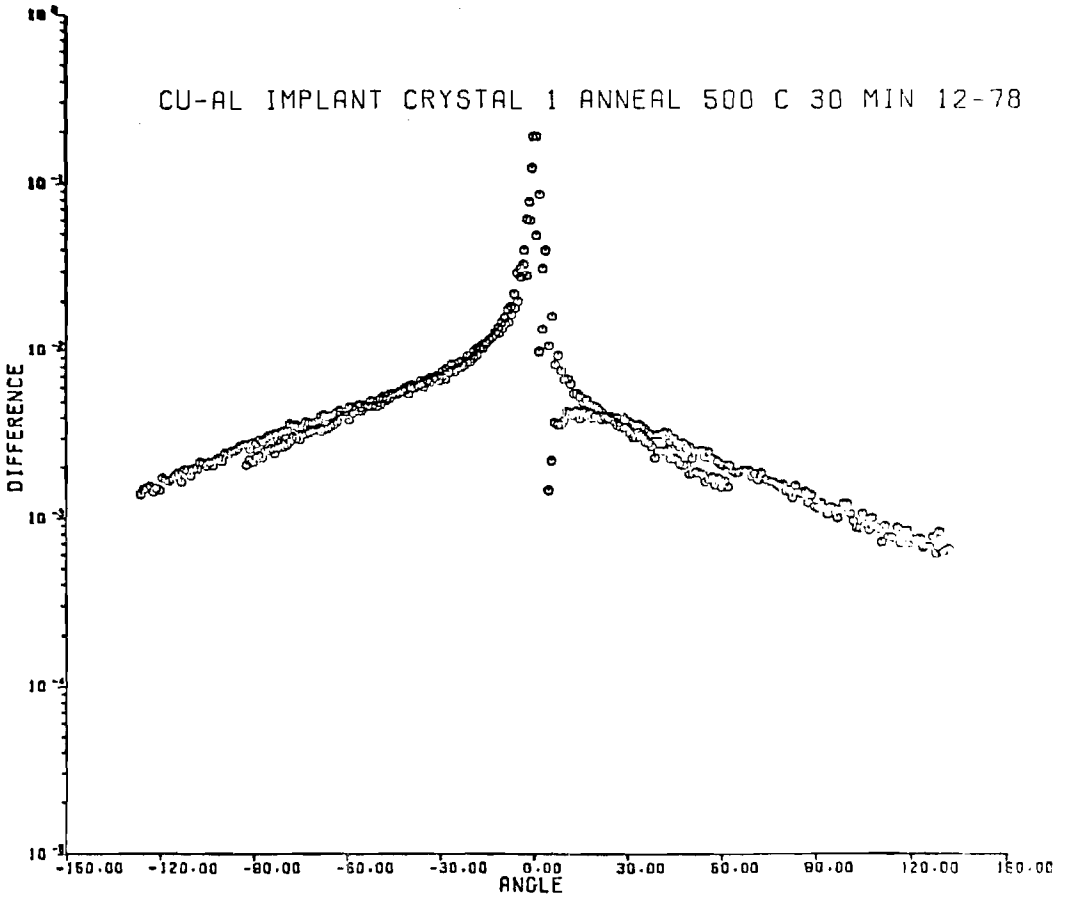

Figure 3. Implantation Scattering Intensity (a) First Crystal as Implanted and (b) Annealed at 500°C for 30 Minutes.

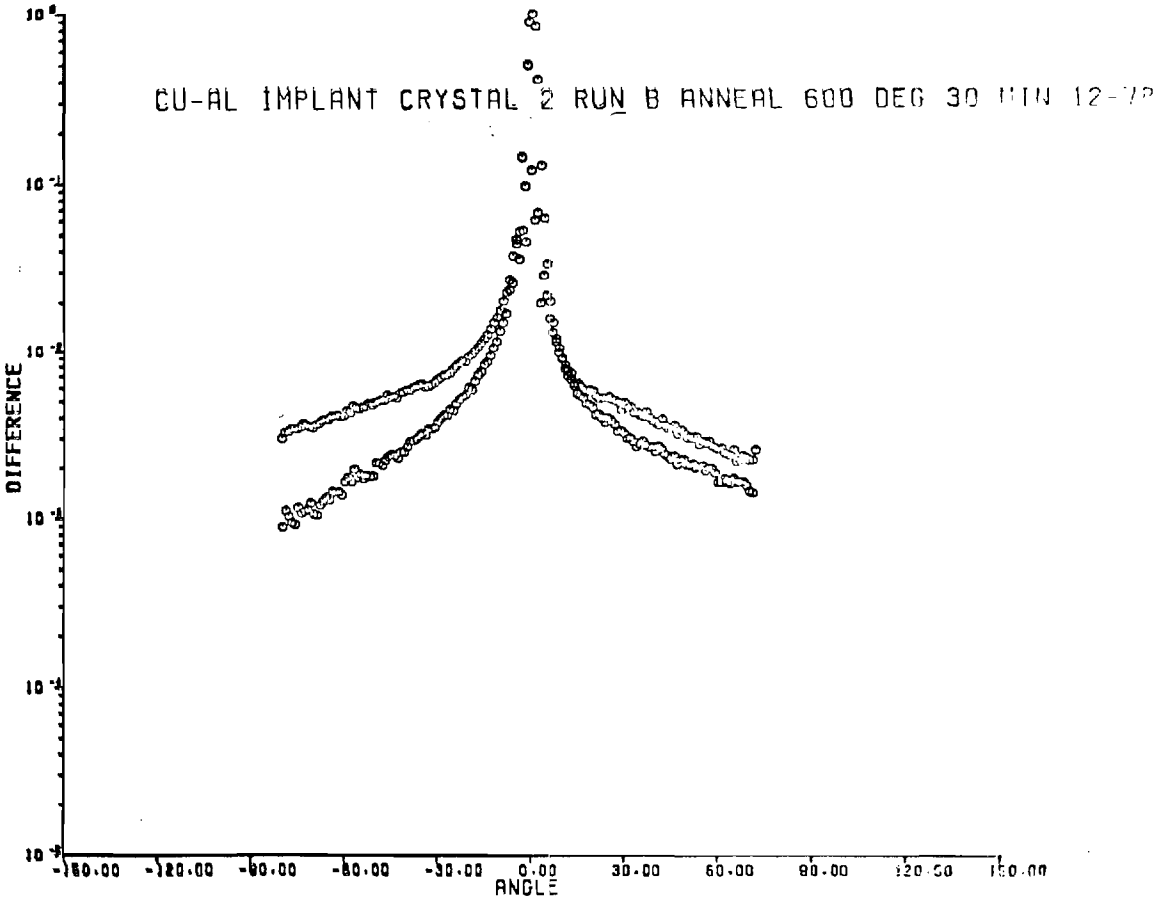

Figure 4. Implantation Scattering Intensity (a) Second Crystal As-Implanted and (b) Annealed at 600°C for 30 minutes.

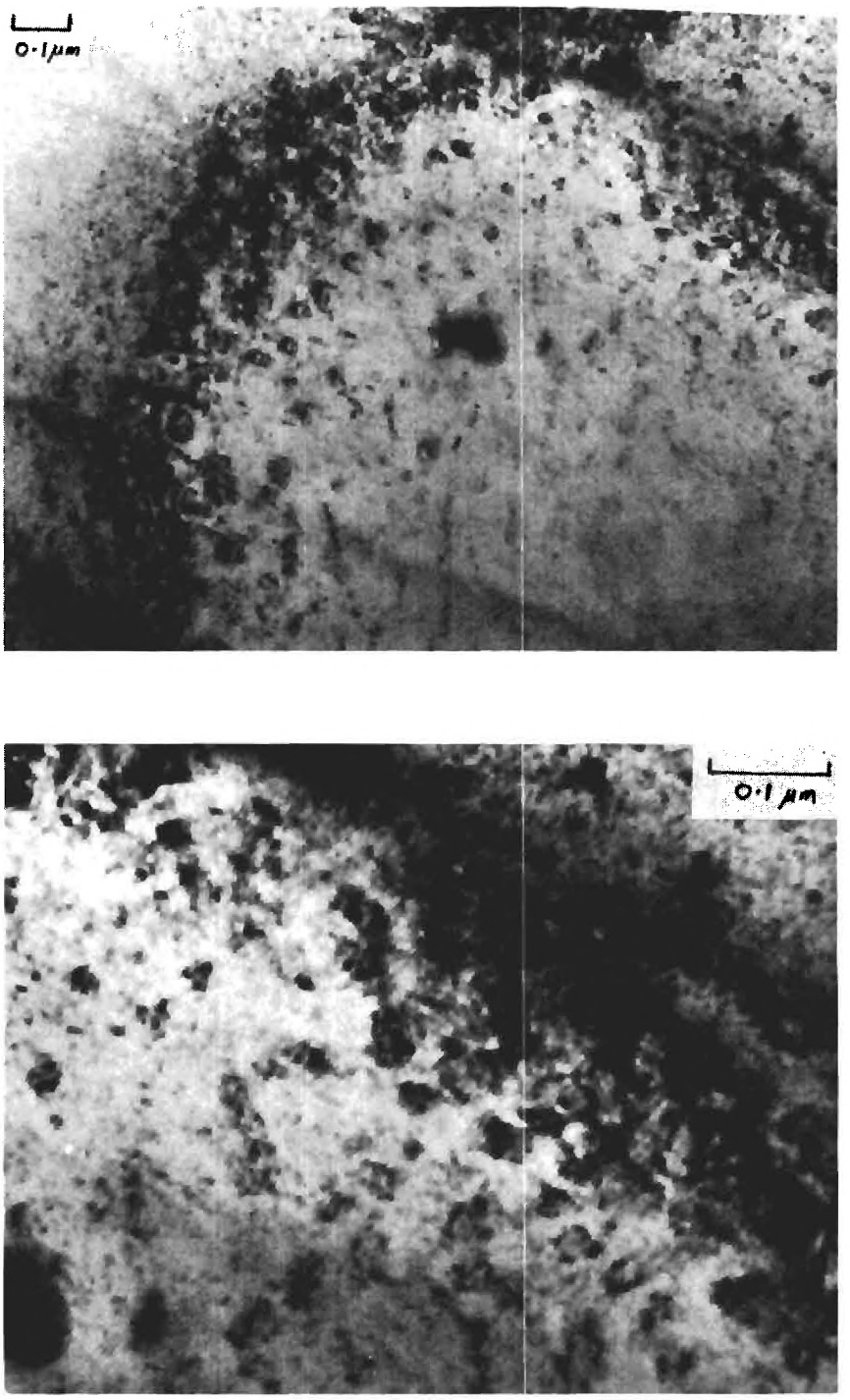

Figure 5. Transmission Electron Microscopy Micrographs Showing Effects of Argon Implantation ($2X10^{15}$ ions cm^{-2} at 100 kev). Many Large Loops Can Be Seen.

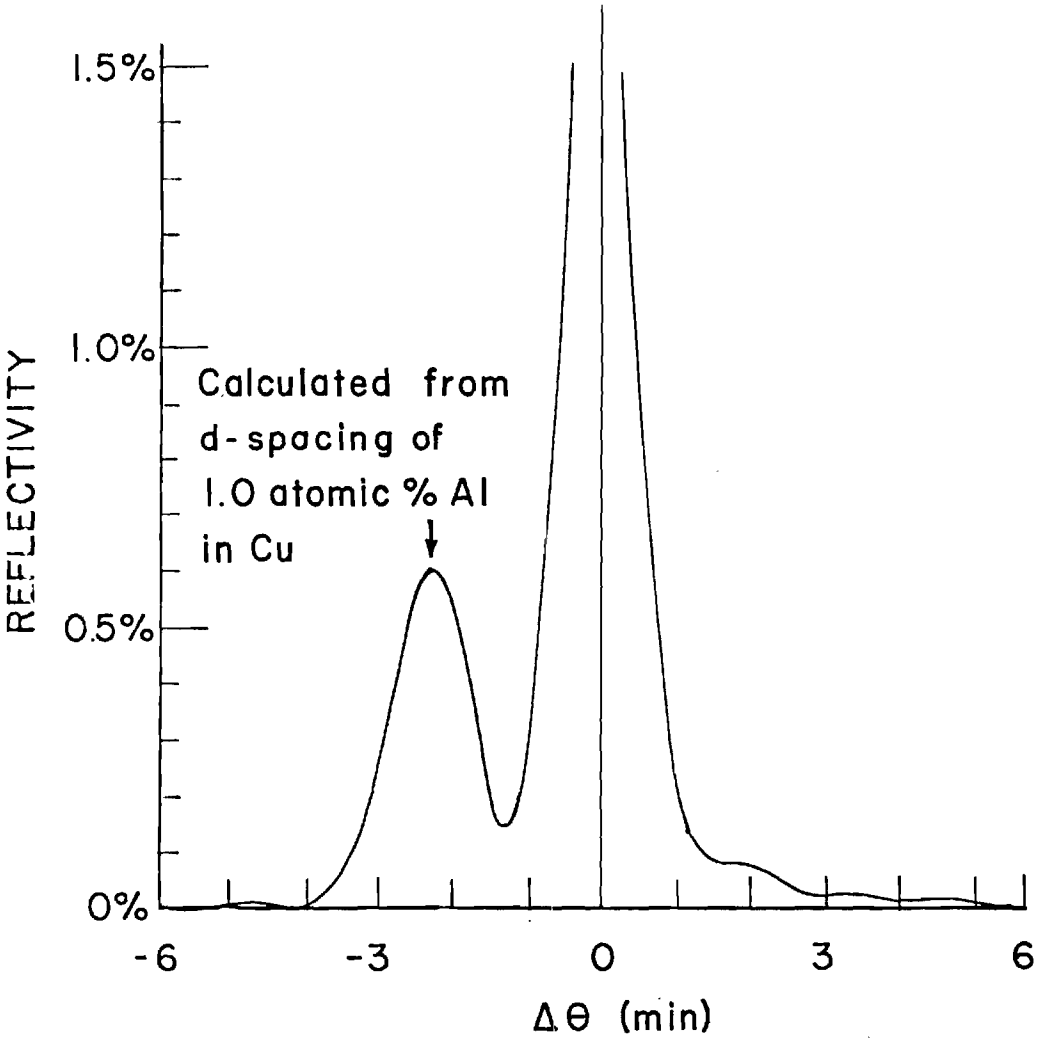

Figure 6. Calculated Reflectivity Versus Rocking Angle for a Copper Crystal Implanted With Aluminum to a Depth of 1300 Å at a Microscopic Concentration of 1 Atomic Percent.

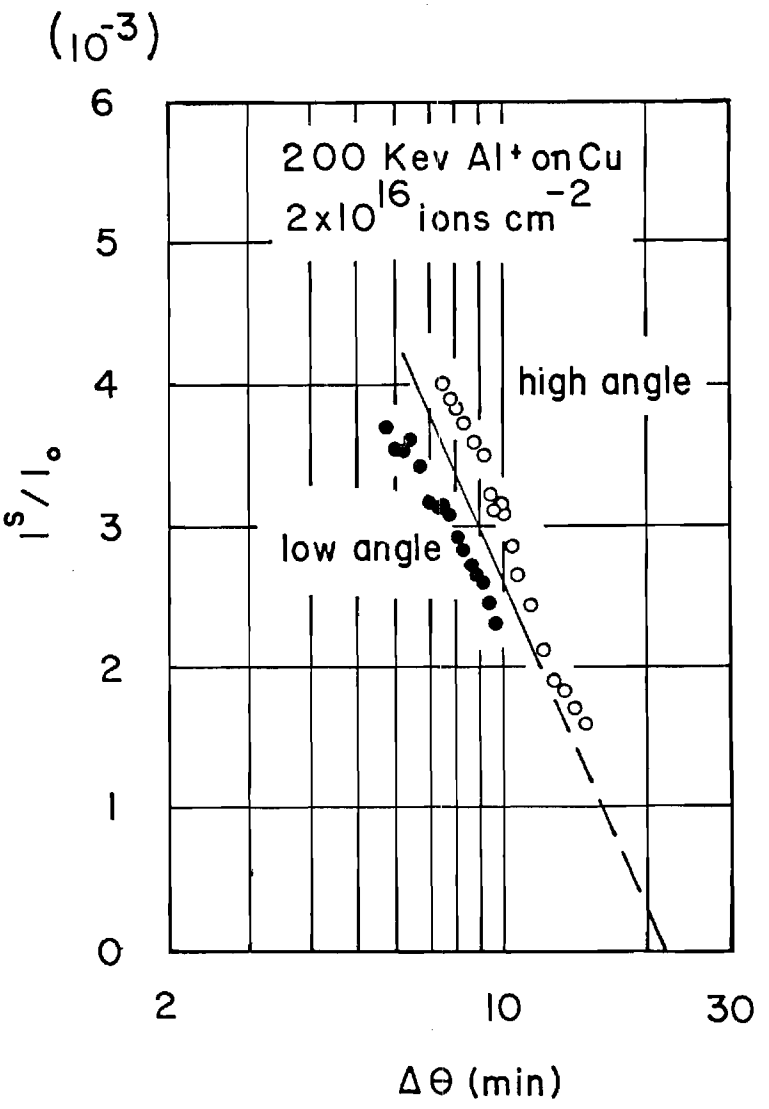

Figure 7. Diffuse Scattering From As-Implanted Sample Plotted as a Huang Scattering Curve I^S/I_0 vs ln $\Delta\Theta$.

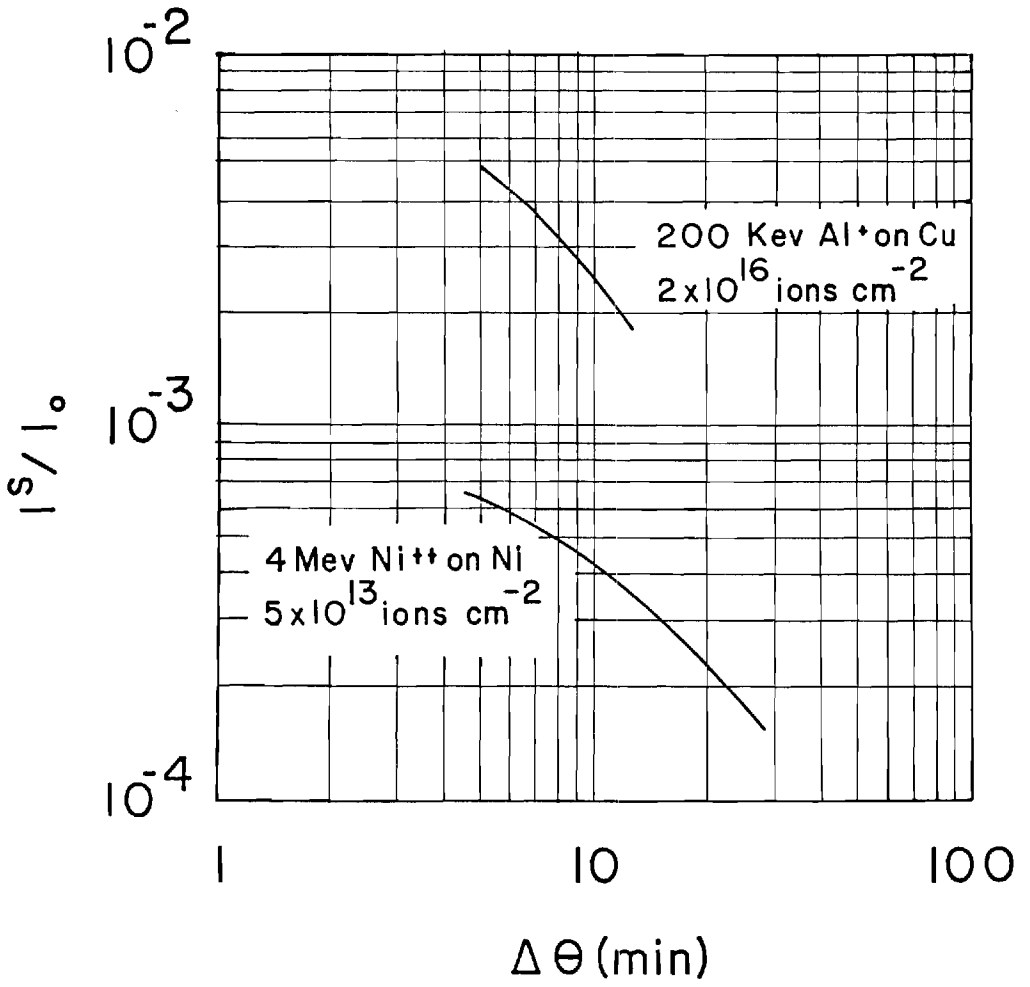

Figure 8. A Comparison of Huang Diffuse Scattering From Aluminum Implanted Copper (200 kev, $2X10^{16}$ ions cm^{-2}) and Nickel Implanted Nickel (4 Mev, $5X10^{13}$ ions cm^{-2}).

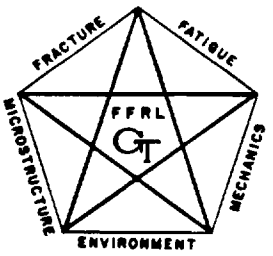

TECHNICAL REPORT 2
FOR THE PERIOD
1 MARCH 1979 - 29 FEBRUARY 1980

THE EFFECT OF ION PLATING AND ION IMPLANTATION ON THE CYCLIC RESPONSE AND FATIGUE CRACK INITIATION OF METALS AND ALLOYS

BY

S. B. CHAKRABORTTY, S. SPOONER, AND E. A. STARKE, JR.
FRACTURE AND FATIGUE RESEARCH LABORATORY

RESEARCH REPORT
CONTRACT N00014-78-C-0270

PREPARED FOR
OFFICE OF NAVAL RESEARCH
DEPARTMENT OF THE NAVY

APPROVED FOR PUBLIC RELEASE;
DISTRIBUTION UNLIMITED

PERMISSION IS GRANTED THE U.S. GOVERNMENT
TO REPRODUCE THIS REPORT IN WHOLE OR IN PART.

GEORGIA INSTITUTE OF TECHNOLOGY
ATLANTA, GEORGIA 30332

TABLE OF CONTENTS

ABSTRACT

Fatigue crack initiation can be affected by surface phenomena and the possibility exists for improving the fatigue performance by altering the state of the surface without greatly changing bulk properties. This program was initiated on 1 March 1978, with the objective of determining the effect of ion implantation and ion plating on the cyclic stress-strain response and fatigue crack nucleation of a metal substrate. To meet this objective, we have selected surface film-substrate combinations designed to separate the various parameters, e.g., crystal structure, SFE, shear modulus, misfit, residual stress, etc., which control near surface deformation and associated crack initiation. This report summarizes our progress during the period 1 March 1979 - 29 February 1980. Three aspects of the program are discussed: (1) The effect of silver and nickel ion plating on the low and high cycle fatigue behavior of polycrystalline copper, (2) x-ray diffraction analysis of ion implanted crystals, and (3) the effect of aluminum-ion implantation on the fatigue crack initiation of polycrystalline copper.

I. BACKGROUND

Modern design philosophies, which are greatly affected by economical and safety factors, require the use of materials having an optimum combination of properties, e.g., fabricability, strength, fracture toughness, corrosion and fatigue resistance. It is difficult to obtain alloys, either by design or through empirical development, having the required combination since the alloy chemistry and microstructure desired for certain properties may be detrimental to others. For example, aluminum alloys which show the highest static strength are inherently susceptable to stress corrosion cracking and have poor fatigue resistance. However, for most alloy systems corrosion and fatigue behavior are greatly affected by the surface condition and surface related phenomena, and may be improved (or controlled) by altering the state of the surface without adversely changing bulk properties, e.g., fracture toughness, yield strength, and ductility.

Metallic coatings have been widely used in industry for controlling corrosion and errosion. The principle of this technique is to separate the metal being protected from the unfavorable surroundings. An improvement arises from the inertness of the coating material with the environment. Many coating techniques are now available, and include hot dipping, metal spraying, electroplating, vacuum deposition, and diffusion coatings. These methods can be divided into two general groups: those which create an abrupt interface with a composition discontinuity between the coating surface and the substrate, and those which create a composition variation at the interface. Most of these coating methods produce an undesired contaminated interface which may prove detrimental when the sample is under static or dynamic loading. For example, during electroplating there may be a simultaneous reaction (e.g.,

water is often reduced to form hydrogen) which may have a considerable influence on the mechanical properties. In addition, electroplated layers can have a wide range of compressive and tensile stresses depending upon the plating parameters, and may contain networks of microcracks with varying depths and spacing. The more recent ion plating and ion implantation methods produce a clean, strongly-adherent interface between the coating material and substrate. The compositional variation at the interface can be controlled by controlling the energy of the ions.

Although it is generally agreed that fatigue cracks originate and propagate from a free surface and that the surface condition has a considerable effect on fatigue life, research on the influence of surface films on fatigue behavior has been lacking. The fatigue process may be divided into two general areas: crack initiation and crack propagation. Improvements in fatigue life can be obtained by increasing the time to crack initiation or reducing crack growth rates, or both. However, crack initiation is more affected by the surface condition than is crack propagation, and consequently the possibility exists for improving the fatigue performance by altering the state of the surface, without greatly changing bulk properties. The present ONR program is concerned with the effects of various ion-plated and ion implanted surfaces, and their microstructure, on the CSSR and fatigue crack initiation of a copper substrate. To meet the program objectives we have selected surface film-substrate combinations designed to separate the various parameters which control near surface deformation and associated crack initiation.

The influence of ion-plated surface films and/or implanted surfaces on fatigue crack initiation depends on such parameters as: crystal structure,

stacking fault energy, composition, and mechanical properties of the surface region and the substrate; the degree of misfit and cleanliness at the interface, the residual stresses in the film and substrate (due to radiation damage and the accommodation dislocation network) and the adhesion of the film. The complex interrelationships between these parameters, as well as which ones dominate for a given system, are presently not well understood. Consequently, the behavior of such composites is now largely unpredictable. Our effort during the past year has been concerned with studying the effect of ion plating on the low cycle fatigue behavior of polycrystalline copper; characterizing the surface structure of copper single crystals implanted with aluminum and argon ions; and determining the effect of this implantation on fatigue crack initiation.

II. THE EFFECT OF SILVER AND NICKEL ION PLATING ON LOW AND HIGH CYCLE FATIGUE BEHAVIOR OF POLYCRYSTALLINE COPPER.

The results of our previous strain controlled, LCF studies [1] have shown that silver and nickel ion plating on copper single crystals has a significant effect on low cycle fatigue life (Figure 1). Silver plating, which has low SFE, reduces the propensity of PSB formation in the surface region and extends the fatigue life over that of unplated copper crystals. Nickel plating, which has a high SFE, has the opposite effect.

This aspect of the program was undertaken to see if similar results are possible for polycrystalline copper. In addition, stress controlled high cycle fatigue studies were made to see if similar changes in the fatigue life occur in the long-life regime.

Experimental

LCF and HCF specimens were machined from annealed, electrical grade, polycrystalline copper rod obtained from Southwire Company. The specimens were

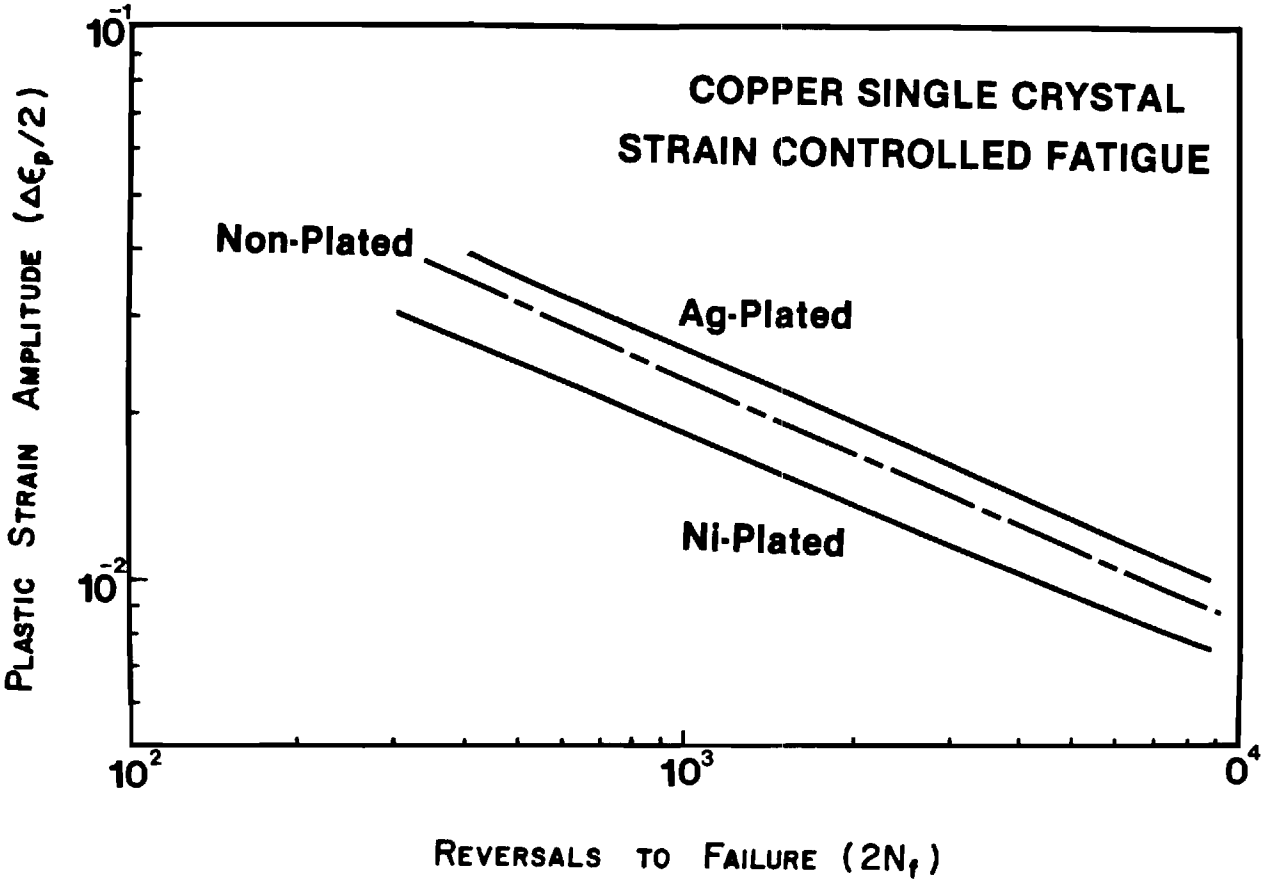

Figure 1. Strain-life curves for Ni- and Ag plated and non-plated copper single crystals.

mechanically polished and then electropolished. Some of the specimens sputter cleaned by argon ions at 2kv. Others were sputter cleaned and then ion plated with either silver or nickel. A 2.5kv potential was used for obtaining a plating thickness of 1μm. Low cycle (strain-controlled) or high cycle (stress-controlled) fatigue tests were conducted using a servohydraulic closed-loop testing machine. Optical and scanning electron microscopy were performed on the fatigued samples in order to characterize the surface and near surface defromation and crack nucleation behavior.

Results and Discussion

Several silver-plated samples have been studied and the results compared with those obtained from non-plated samples. A limited number of nickel-plated samples have been examined to date. However, one HCF and one LCF result

is included for comparison.

The stress-response under strain-control shows considerable cyclic hardening followed by saturation for both non-plated and plated samples, Figure 2. The cyclic stress-strain curves, Figure 3, show that the extent of hardening for the non-plated and plated samples is slightly different. Silver plating is observed to reduce the extent of hardening compared the non-plated copper, whereas nickel plating seems to have the opposite effect. The cyclic strain-life curves derived from the data, Figure 4, appear to follow the Coffin-Manson [2,3] relationship. Ag-plating improves the fatigue life and nickel plating seems to have the opposite effect. The cyclic stress-life curves, Figure 5, show an analogous effect, which is most significant at lower stresses (near the fatigue limit).

Surface slip markings on low cycle fatigue samples, Figure 6, show that silver plating leads to more homogeneous slip and reduces the propensity of persistant slip band formation. Grain boundary cracking appears to be the predominent mode of crack initiation for both the plated and nonplated materials. Surface slip markings on the high-cycle fatigue samples, Figure 7, show that slip band cracking is the predominate mode of crack initiation. at long lives. Although the density of PSB's appear to be similar for both the Ag-plated and nonplated materials the Ag-plated sample was examined after a considerably larger number of cycles. Consequently, it appears that Ag-plating reduces the propensity of PSB formation.

Deformation near the free surface has a dominate effect on the cyclic behavior of materials, especially at low strains. A surface coating of a low SFE material (e.g., Ag) modifies the surface deformation of copper towards that of silver. Under cyclic deformation slip in the surface and near surface region becomes more reversible due to a lower incidence of cross-slip. This

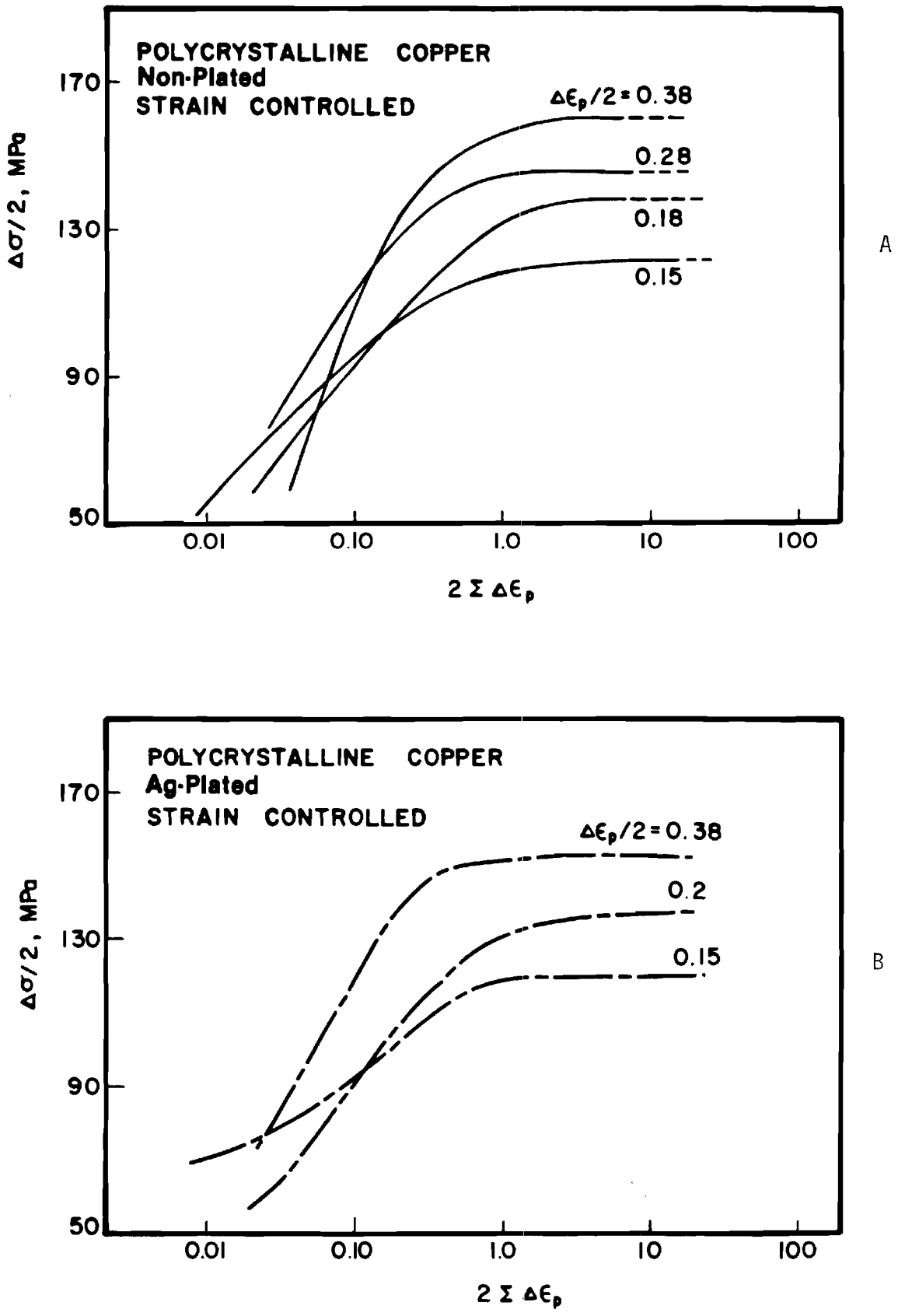

Figure 2. Cyclic stress response curves during strain controlled LCF testing.

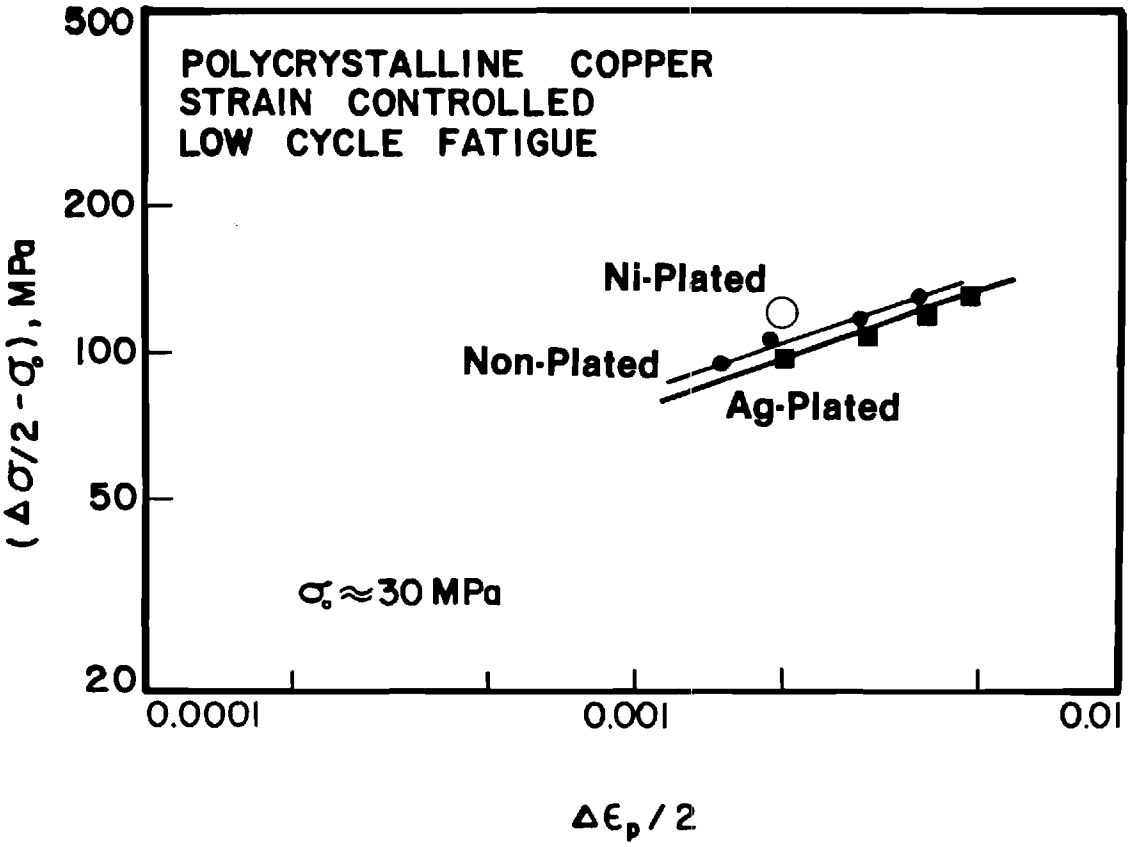

Figure 3. Cyclic stress strain curves for non-plated and Al plated polycrystalline copper.

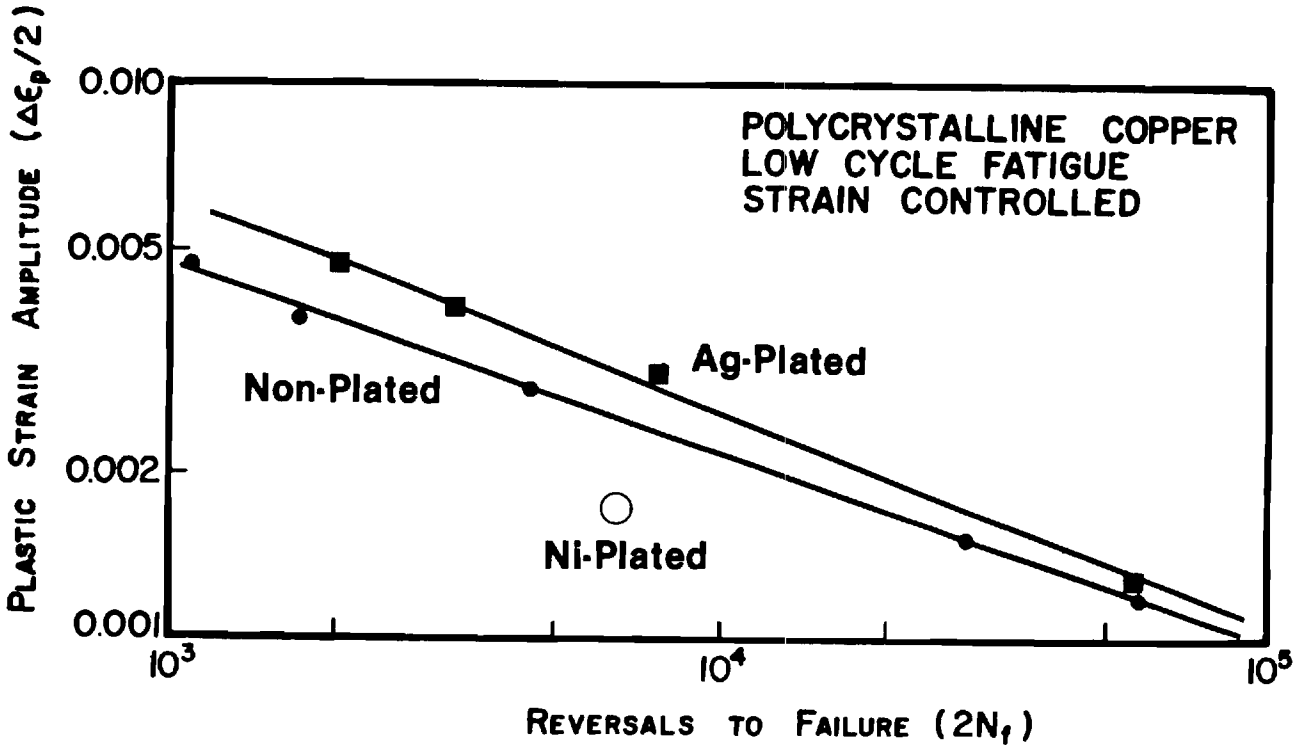

Figure 4. Strain life curves for non-plated and Ag-plated polycrystalline copper.

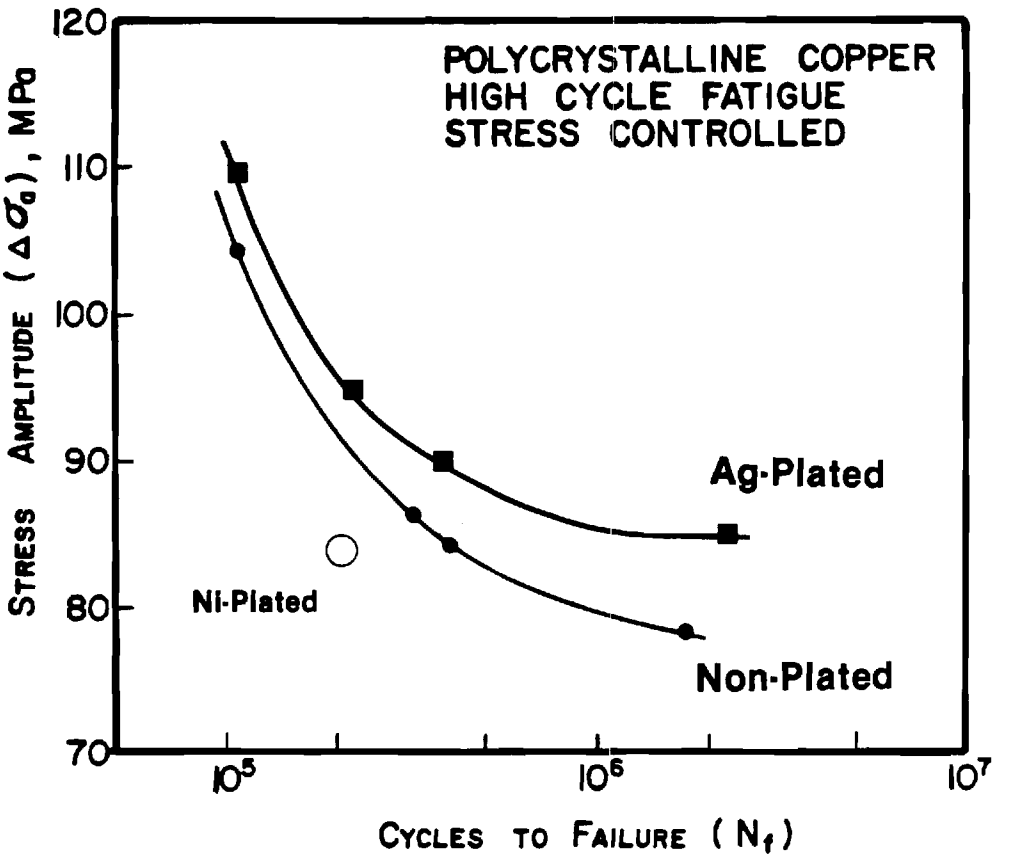

Figure 5. Stress-life curves for non-plated and Ag-plated polycrystalline copper.

gives rise to more homogeneous cyclic deformation and a reduced propensity for PSB formation. Therefore, silver plating produces (1) lower cyclic hardening as a result of reduced dislocation interactions, and (2) longer fatigue life as a result of more homogeneous and reversible surface slip. These results indicate that ion plating has similar effects on the fatigue properties of both single and polycrystalline copper.

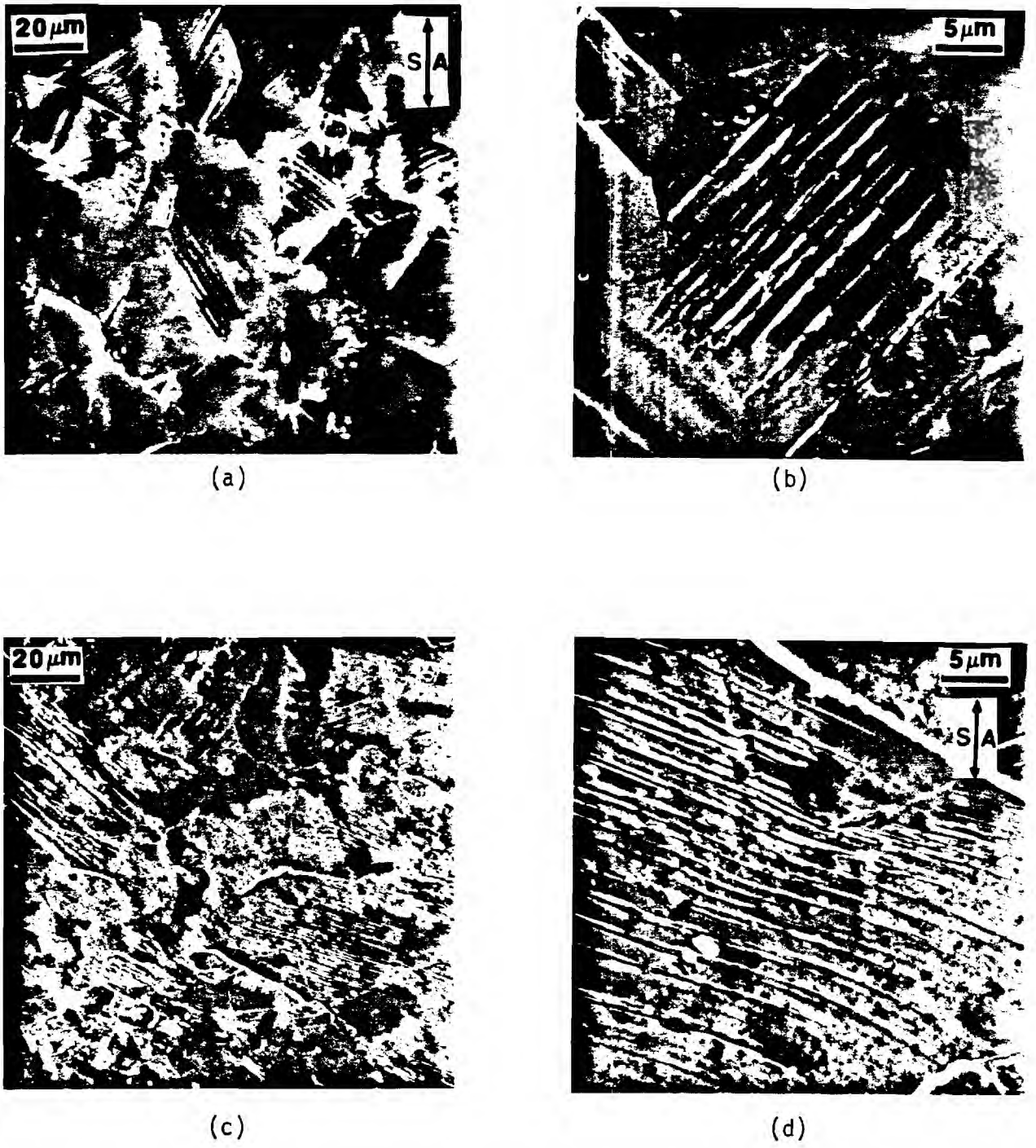

Figure 6. Scanning electron micrographs of the surface slip features of strain-cycled polycrystalline copper samples; $\Delta\varepsilon_p/2 \simeq 0.3\%$. (a) and (b) non-plated and sputter cleaned; (c) and (d) silver plated.

(a)

(b)

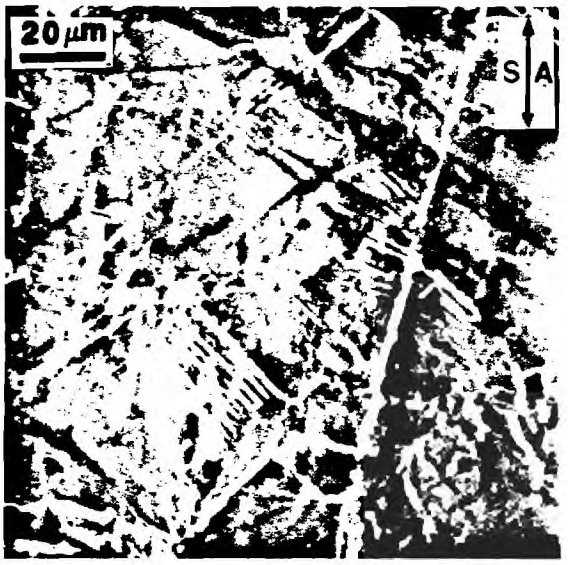

(c)

(d)

Figure 7. Scanning electron micrographs of the surface slip features on stress-cycled polycrystalline copper samples. (a) non-plated, (b) nickel-plated, (c) and (d) silver-plated.

III. X-RAY DIFFRACTION ANALYSIS OF ION IMPLANTED CRYSTALS

Some results of this aspect of our research have been prepared for publication in the proceedings of two symposia. These are included in this report as Appendices A and B. The main features of this type of analysis and our most recent results are summarized below.

The state of stress at the surface of the implanted crystal can be inferred from the lattice strain which in turn is measured by a shift in the Bragg angle. Implantation not only modifies the lattice parameter by microalloying but can severely damage the surface with the production of point defects which can also shift the lattice parameter and give a large diffuse scattering. All these effects are confined to depths much less than a micron. Non-destructive methods of implantation characterization with x-rays must employ special approaches to obtain the structural information. X-rays would not normally be useful for analysis of implantation since the sampling depth is many times the depth of the implantation affected volume. In order to avoid obscuring the scattering effects from the implanted layer, a perfect crystal substrate is used in a double-crystal diffraction arrangement. When a perfect crystal and an implanted crystal are arranged so that maximum intensity is obtained by the second reflection, the angular resolution in diffuse scattering measurements and peak shifts is measured in seconds of arc. In this way, both Bragg peak shifts and diffuse scattering from defects associated with the implanted layers can easily be measured.

Scattering from an Implanted Crystal

The two principal sources of extra scattering from an implanted single crystal are (1) the scattering from the implanted layer whose Bragg angle is changed by alloying and (2) the scattering from point defect clusters (interstital and vacancy loops). Analysis of the scattering attributed to lattice

strain due to alloying has been done in several cases where point defect scattering was not present [4]. A modification of dynamical diffraction theory can be used to calculate the reflectivity of the alloyed crystal as a function of rocking angle. To a first approximation the results of such calculations resemble the results which one might obtain using kinematic diffraction theory for a very thin crystal. In detail, however, there are interference effects which can be analyzed in terms of strain distribution to get a more detailed description of alloy distribution.

The second source of scattering dominates in the measured scattering in the implanted metals under investigation in this program. One result is that alloy distribution and strain effects are somewhat obscured. Nevertheless quantitative analysis of the damaged state of the implanted layer can be done. Scattering theory (kinematic) for scattering from dislocation loops and spherical precipitates has been worked out [5]. Diffuse scattering measured as "integral diffuse" intensity in a double-crystal experiment is given in the following formulas:

$$I^S(q_o)/I_o = 1/(2\mu_o)\,(r_e f_h e^{-M_h})^2 (h/k)^2\, 2\pi\tau \sum_i (c_i/V_c)\,(b\pi R_i^2/V_c)^2 \ln(e^{\frac{1}{2}} q_L^i/q_o)$$

for $q_o < q_L$ and,

$$I^S(q_o)/I_o = (1/2\,\mu_o V_c)\,(re f_m e^{-M_h})^2\,(h/k)^2\, 2\pi\tau\,(b\pi/V_c)\,\alpha^2/2q_o^2\, n_{PD}$$ for

$q_o > q_L$ where, $I^S(q_o)$ is the average diffuse scattering intensity calculated from $(I(+q_o) + I(-q_o))/2$, $q_o = h\cos\theta_B\,\Delta\Theta$, $\Delta\Theta = \Theta - \Theta_B$, $h = 4\pi\sin\Theta_B/\lambda$, μ_o absorption, r^e Thompson electron radius, f_h structure factor, e^{-M_h} Debye-Waller factor, $k = 2\pi/\lambda$, $2\pi\tau$ is an averaging parameter for dislocation loops, C_i/V_c is the number density of loops of radius R_i, b Burgers vector V_c unit all volume, q_L^i is α/R_i, with $\alpha = \sqrt{2}$ for the (222) reflection and n_{PD} the density of point defects. The first equation can be used to determine the loop size

distribution for the case of well determined diffuse scatterings. A simpler application uses the assumption of a single average loop radius size which can be obtained from the extrapolation of $I^S(q_o)$ vs $\ln(q_o)$ to zero where $q_o = e^{\frac{1}{2}} q_L$ and $R^2 = \alpha/q_L$.

The second equation can be used to obtain the total point defects per volume; $I^S(q_o)\ q_o^{\ 2}$ is proportional to n_{PD}. These formulas do not distinguish between vacancy and interstital loops since differential symmetrically averaged intensity is employed. A detailed measurement of the differential diffuse scattering rather than integral diffuse scattering is required for such distinctions to be made unambiguously.

Since the loop scattering originates in the implanted layer, the q_o value must be adjusted for the Bragg angle shift. Since shifts are small (a few minutes) the measurement of n_{PD} which uses large q_o values is unaffected. At small angles (q_o) asymmetry in the scattering can be used to infer Bragg angle changes. But, one must recognize that it is possible to produce asymmetry in the scattering at small angles by certain combinations of interstitial and vacancy loop scattering, each of which has opposing asymmetry.

Double Crystal Method

As mentioned earlier, the double-crystal method which uses perfect crystals has the advantage of permitting the observation of scattering at angles very close to the Bragg peak. The scattering which is measured is, in fact, diffuse scattering measured over the Ewald sphere in the vicinity of the Bragg point in reciprocal space. The range of the integration is determined by the solid angle defined by the solid angle subtended by the detector. A major portion of the measured scattering at small angles is reflected (in the dynamical theory sense) from the unimplanted subtrate and can be corrected by subtraction of scattering measured from an unimplanted surface. Fig. 8 shows

the curves for implanted and unimplanted crystal as a log intensity scale. The excess scattering although obvious on a log scale is nevertheless small (a few tenths of a percent reflectivity) over an angular range of less than a degree. The asymmetry that may be attributed to Bragg angle shift can only be measured within an angular range of ten minutes of the substrate Bragg peak.

The experimental arrangement needed for such measurements is simple. Two crystals are mounted on adjustmable goniostats. The first crystal reflects intensity from the x-ray source to the second crystal and is adjusted only once to maximize the intensity at the second crystal position. The second crystal can then be focused to reflect the incident rays into the detector (actually 85 to 90% according to theory). This is the "antiparallel" arrangement which simply means that the Bragg plane normals are perfectly parallel but are directionally opposite. As Fig. 9 shows the peak is sharp - a full width at half maximum of approximately 10 seconds. The second crystal - which is the implanted crystal - is rotated on a goniometer to give the rocking curve. Simple adjustments are sufficient to keep the detector centered on the Bragg peak intensity. Upon mounting a new sample crystal, some care must be taken to find maximum reflectivity.

Equipment

Two goniostats, motorized goniometer and conventional x-ray equipment are assembled into a double crystal apparatus. The only critical part of the apparatus is the motorized goniometer. A Huber goniometer was used with a 10-to-1 gear reducer and was driven by a SLO-SYN pulsed motor. Backlash in the goniometer gearing is but a few seconds and can be removed effectively by running rocking curves in a fixed direction. No absolute angular measurements are made since the Bragg peak from the substrate is a satisfactory internal standard. Data are collected by step-counting mode. Figure 10 shows

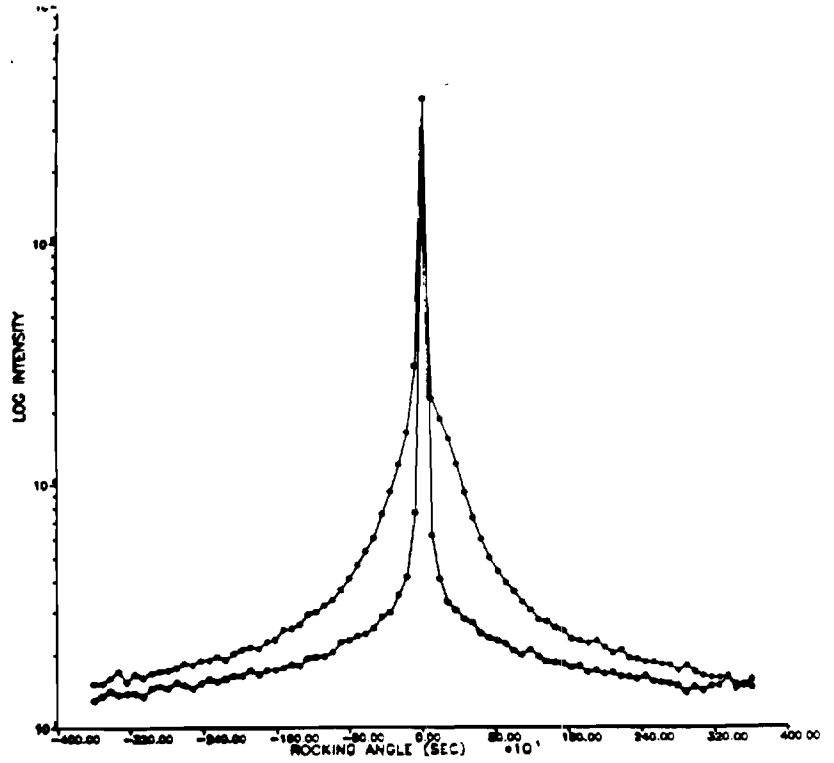

Figure 8. Log integral diffuse scattering vs. rocking angle for copper implanted with $3.4X10^{15}$ boron ions/cm^2.

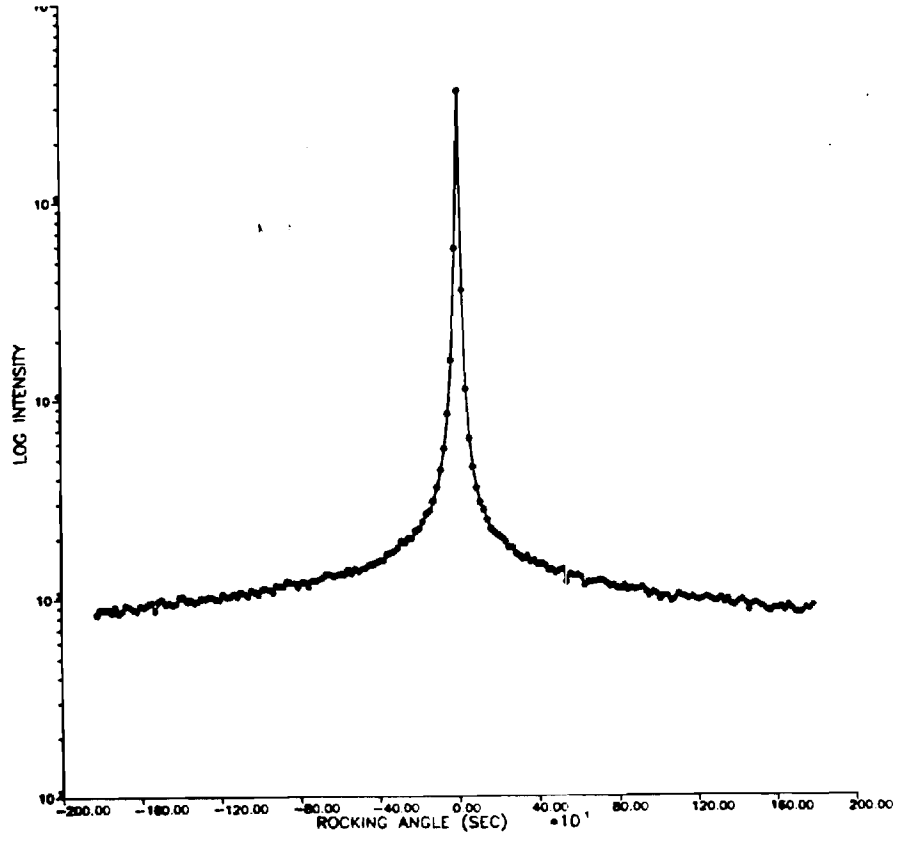

Figure 9. Sharpness of resolution is shown in the rocking curve of unimplanted copper.

a photograph of the arrangement operating with the GE XRD-7 system.

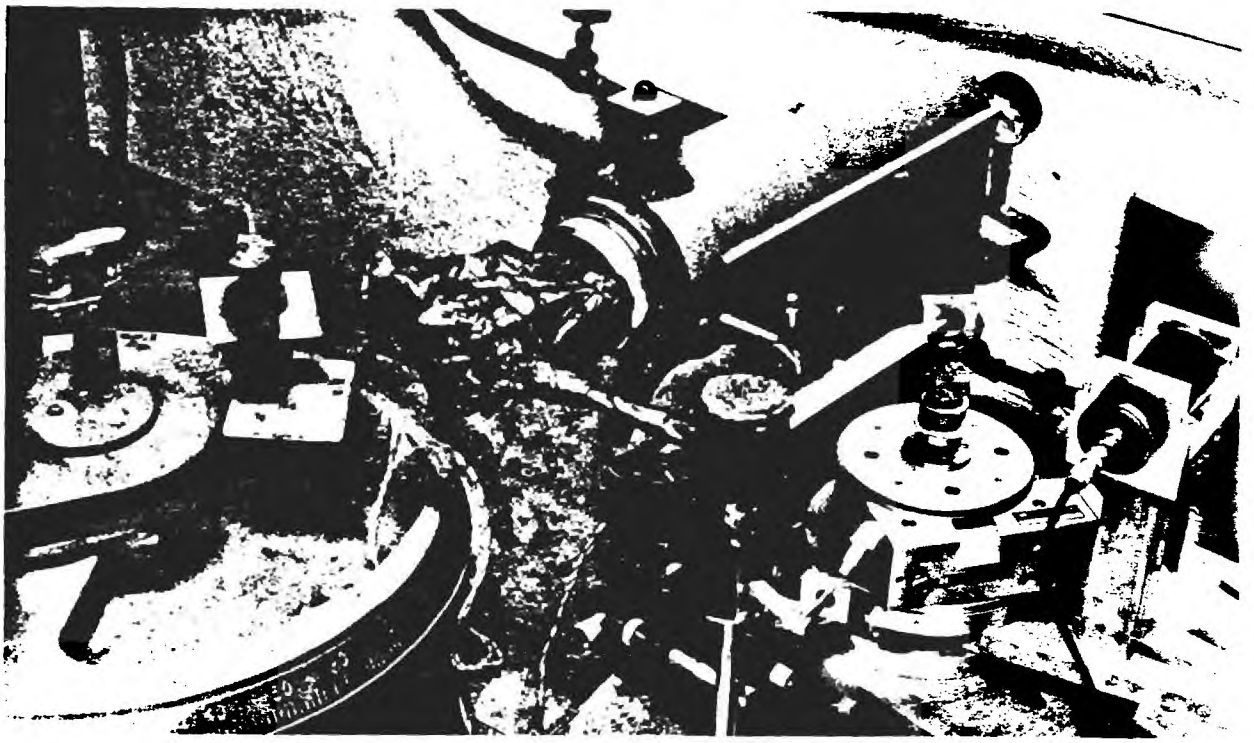

Figure 10. Layout of double crystal apparatus. The monochromating (first) crystal is enclosed in the cylindrical lead shield. A 2 mm diameter apparature near the second crystal defines the sampled area. No collimation is placed between the second crystal and the detector.

Interpretation of Boron Implantation Results

Boron implantation produces a surface alloy whose lattice parameter is less than that of copper. This can be seen in Figure 11 in which the intensity is shifted by approximately 50 arc seconds. The shift is somewhat smaller in the 1.25 dose than in the 1.00 dose and might be attributed to second order lattrice parameter changes due to a greater number of point defects. The fractional lattice parameter change calculated from this shift is -2.6×10^{-4} ($\Delta a_o/a_o$) and with the estimated alloy composition represents a large change (10% per atomic per cent of boron). The implication of this finding is that the implanted layer will be under tensile stress by virtue of lattice parameter coherency between the implanted layer and the copper substrate (matrix).

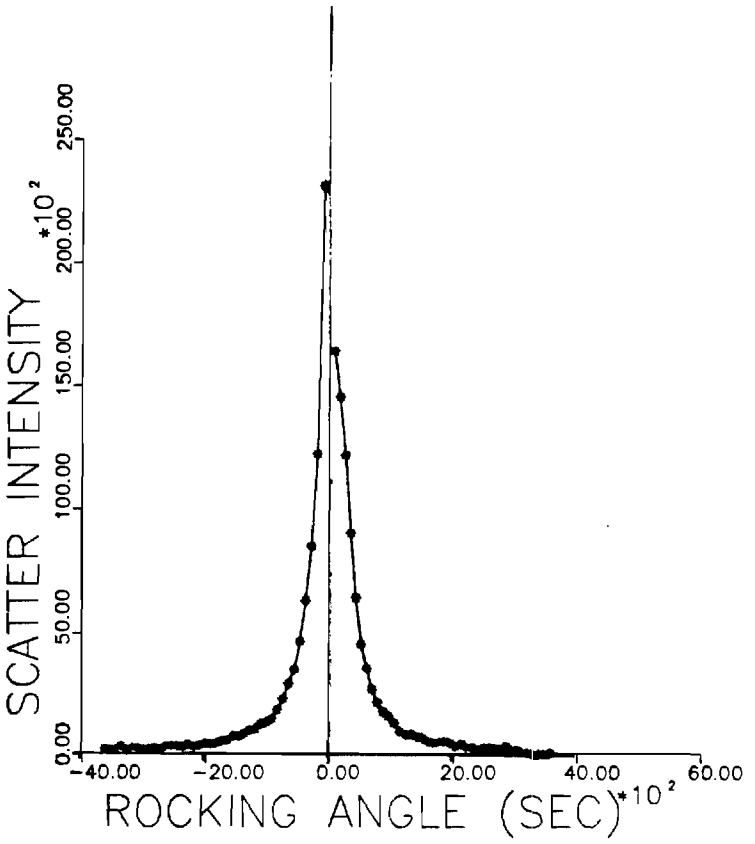

Figure 11. The angular shift toward larger angle is shown in the excess diffuse scattering curve for copper implanted with $3.4X10^{15}$ boron ions/cm^2.

These data have been analyzed in terms of dislocation loop structure and total point defect density. In Fig. 12 the symmetric excess intensity is plotted versus ln q_o and the intercept at zero intensity (q_o*) is used in the relation

$$q_o^* R_{loop} = e^{\frac{1}{2}\alpha}$$

with $\alpha = \sqrt{2}$ for the (222) reflection. It is found that loop radii become smaller with dose even though the number of point defects increase with dose. Table 1 summarizes the preliminary findings for these doses. Note that the peak boron content in the highest dose is still smaller that the quoted solubility limit (0.34 atomic %).

TABLE I

Dose (ions/x-rayed area)	$\bar{R}_{loop}$	Point Defects (per x-rayed area)
$0.4X10^{14}$	93 Å	$0.4X10^{15}$
$1.6X10^{14}$	80 Å	$3.6X10^{15}$
$2.0X10^{14}$	73 Å	$3.9X10^{15}$

The number of defects produced per ion is approximately 18 to 20 and is between 2 and 5% of the point defects produced as estimated by simple LSS collision theory. The density of dislocations in the implanted layer was estimated by using a 80 Å loop circumference to contain measured point defects in a layer assumed to be 3000 Å thick. The resulting dislocation density is $2.5X10^{12}$ cm^{-2}.

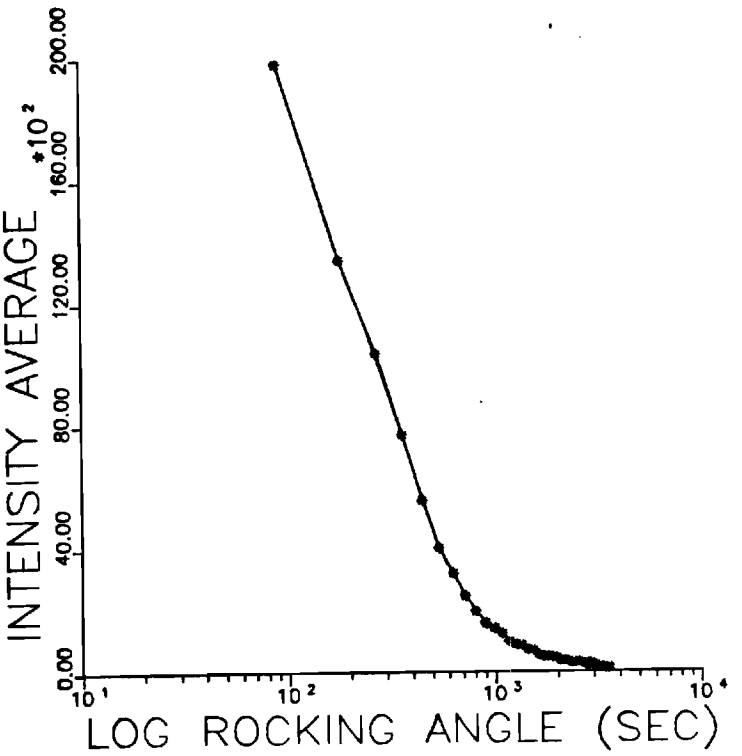

Figure 12. An average loop radius is determined from the extrapolation of intensity to zero in this plot. A llop radius of 90 A is obtained for an implantation of $3.4X10^{15}$ boron ions/cm^2.

IV. THE EFFECT OF ION IMPLANTATION ON THE FATIGUE CRACK INITIATION OF POLYCRYSTALLINE COPPER

Some of the results of this aspect of our research have been prepared for publication in the proceedings on the Symposium on Surface Modifications of Materials by Ion Implantations. The manuscript is included in this report as Appendix C. The main features can be summarized as follows:

Aluminum ion implantation did not seem to effect the monotonic yield stress, but did decrease the extent of work hardening in the low strain range. A similar decrease was observed in the cyclic hardening behavior. Aluminum ion implantation produced a significant improvement in fatigue life for both strain and stress controlled tests. This improvement is associated with modifications of the deformation behavior in the surface and near surface regions of the implanted copper, and its subsequent effect on fatigue crack initiation. For details, see Appendix C.

V. PROFESSIONAL PERSONNEL

Dr. Edgar A. Starke, Jr.
Dr. Saghana B. Chakrabortty
Dr. Stephen Spooner
Dr. Keith O. Legg

VI. GRADUATE STUDENTS

Fred Anderson
A. Kujore
P. Heydari-Darani

VII. PUBLICATIONS AND PRESENTATIONS

1. A.Kujore, S. B. Chakrabortty, E. A. Starke, Jr., and K.O. Legg, "The Effect of Aluminum Ion Implantation on the Fatigue Crack Initiation of Polycrystalline Copper," presented at the Materials Research Society's Symposium on Surface Modification of Materials by Ion Implantation, Cambridge, MA, November 30, 1979. To be published in the Proceedings of the Symposium.

2. Stephen Spooner and Keith O. Legg, "X-Ray Diffraction Characterizations of Aluminum Implanted Copper Crystals," presented at the Materials Research Society's Symposium on Surface Modifications of Materials by Ion Implantation, Cambridge, Ma, November 30, 1979. To be published in the Proceedings of the Symposium.

3. S. Spooner, "X-Ray Scattering Investigation of Microalloying and Defect Structure in Ion Implanted Copper," presented at the AIME Symposium on Advanced Techniques for the Characterization of Microstructures, Los Vegas, Nevada, February 24-28, 1980. To be published in the Proceedings of the Symposium.

4. P. Heydari-Darani, A. Kujore, S. B. Chakrabortty, E. A. Starke, Jr., and K. Legg, "The Effect of Ion Implantation on the Cyclic Stress Strain Response and Fatigue Crack Initiation of Copper," presented at the 109th AIME Annual Meeting, Las Vegas, Nevada, February 24-28, 1980.

5. A. Kujore, S. B. Chakrabortty, and E. A. Starke, Jr.,"Low Cycle and High Cycle Fatigue Behavior of Ion Plated Polycrystalline Copper," presented at the 109th AIME Annual Meeting, Las Vegas, Nevada, February 24-28, 1980.

6. S.B. Chakrabortty, A. Kujore, and E. A. Starke, Jr., "The Effect of Ion Implantation on the Cyclic Stress-Strain Response of Polycrystalline Copper," to be presented at the International Conference on Metallurgical Coatings, April 21-25, 1980, San Diego, California.

7. S. B. Chakrabortty, K. Legg, and E. A. Starke, Jr., "The Effect of Ion Implantation on the Fatigue Properties of Polycrystalline Copper," to be presented at the Ion Beam Modification of Materials, July 14-18, 1980, Albany, N.Y.

8. E. A. Starke, Jr., S.B. Chakrabortty, and A. Kujore, "The Effect of Ion Implantation on the Fatigue Behavior of Metals and Alloys," to be presented at the Sixth Conference on the Applications of Accelerators in Research and Industry, November 3-5, 1980, Denton, Texas.

VIII. REFERENCES

1. E. Y. Chen and E. A. Starke, Jr., "Effects of Ion-Plating on the Low Cycle Fatigue Behavior of Copper Single Crystals," Materials Science and Engineering, 24 (1976) pp 209-221.

2. L. F. Coffin, Trans. AIME, 76 (1954) pp 931-950.

3. S. S. Manson, NASA, Technical Note 2933 (1954).

4. B. C. Larson, C. W. White and B. R. Appleton, "Unidirectional Contraction in Boron-Implanted Laser Annealed Silicon," Appl. Phys. Lett., 32, pp. 801-803 (1978).

APPENDIX A

X-RAY DIFFRACTION CHARACTERIZATIONS OF ALUMINUM ION IMPLANTED COPPER CRYSTALS

By

Stephen Spooner
and
Keith O. Legg

Presented at the MaterialsResearch Society's Symposium on Surface Modifications of Materials by Ion Implantation, Cambridge, MA, November 30, 1979. To be published in the Proceedings of the Symposium.

X-RAY DIFFRACTION CHARACTERIZATION OF ALUMINUM ION IMPLANTED COPPER CRYSTALS

Stephen Spooner
Fracture and Fatigue Research Laboratory
and
Keith O. Legg
School of Physics
Georgia Institute of Technology

X-ray diffraction from aluminum ion implanted copper is analyzed in single crystals in terms of microalloying and radiation damage effects. Sessile dislocation loop scattering dominates scattering, although asymmetry in diffuse scattering distribution can be attributed to the lattice expansion due to alloying. Annealing at 500°C for 30 minutes produces no significant change in the structure. Annealing at 600°C for 30 minutes appears to remove microalloying effects while leaving damage structure having a stability which may be effective in inhibiting fatigue crack initiation.

Introduction

Ion plating has been demonstrated to modify the fatigue crack initiation resistance in copper single crystals (1). Vapor deposition alone can change mechanical properties of copper (2) but the damage effects of ion implantation on mechanical properties remains unexplored. Studies of the structure of ion implantation damage in connection with neutron damage simulation (3) and semi-conductor device physics (4) provide a basis for such investigations. The structure of the implanted layer can be modified by choice of ion, energy, and dose. The application of implantation to the control of fatigue crack initiation must consider several fundamental questions: How do ion-type and implantation energy affect surface layer structure and structure stability? How do the various implantation structures affect fatigue crack initiation mechanisms? Which structures are helpful or detrimental to mechanical property improvements? A partial answer to some of these questions can be found in a recent presentation on the effects of platinum implantation on subsurface crack initiation in titanium. (5) In this case the treatment brings mixed benefits to the control of fracture initiation.

This x-ray diffraction investigation is part of a study on the effects of ion plating and ion implantation on fatigue crack initiation. Conventional x-ray diffraction methods depend either on measurement of peak shifts to reveal the state of residual stress (6) or peak profile analysis (e.g., the Warren-Averbach analysis) to characterize effective particle sizes and strains (7) in the material of a surface. In these investigations the property controlling imperfections are distributed over depths much greater than the penetration depth of the x-rays. However, in the case of an implanted layer, the affected material is much shallower than the x-ray penetration depth and, unless some special conditions are used, the diffraction effects from the damaged layer would be lost in the tails of the diffraction peak from the unmodified substrate sampled by the x-rays. We have adopted the use of rather perfect crystals in a double-crystal technique (8-10) used in radiation damage investigations which successfully circumvents the problems in the conventional x-ray diffraction methods. Experiments are described in which aluminum implantation effects in copper crystals including response to annealing are analyzed. It is shown that the damaged state produced by ion implantation is relatively stable against annealing and therefore may provide an effective inhibitor to surface fatigue crack initiation. The effects of aluminum implantation in polycrystalline copper is discussed in a companion paper (11).

Experimental

Implantation of copper with aluminum ions was selected for this study because of high solubility of aluminum in copper, because of an appreciable lattice parameter change upon alloying aluminum with copper, and because the aluminum ions penetrate relatively far into the substrate at the implantation energies available to us. Thus, an alloy layer of favorable thickness will be produced which has a relatively simple microalloy structure containing ion damage effects.

Highly perfect crystals were selected for x-ray studies in order that pre-existing dislocations would not interfere with ion-implantation effects. Bulk copper crystals were provided by F. W. Young of Oak Ridge National Laboratory. These crystals were grown by Bridgeman technique and then annealed for two weeks at a few degrees below the melting point. The crystals were radiation hardened with neutrons before final cutting to orientation. Chemical cutting techniques were used to shape the crystal.

The dislocation densities measured after final sample preparation, but prior to ion implanation, was less than 10^3 cm^{-2}.

Two crystals were prepared with 111 faces. Each was mounted in the ion accelerator with the (111) normal 6° from the ion beam direction. An Accelerators, Inc. Ion Implanter which can be run up to 200 Kev was used to implant the crystals at 25°C. Although the temperature rise was not measured, the crystals, which have a volume of approximately 2 cc, were considered to be a sufficient heat sink allowing less than a degree temperature rise during implantation. The implantations were made in three doses each varying in energy and duration for the purpose of producing a level aluminum distribution. The dose calculations were made on the basis of the LSS model (11) of ion penetration and the dose rates were as follows: $19.7X10^{13}$ ions cm^{-2} sec^{-1} at 200 Kev, $9.9X10^{12}$ ions cm^{-2} at 100 Kev and 2.4X10" ions cm^{-2} sec^{-1} at 50 Kev. The accumulated ion doses were $2X10^{16}$ ions cm^{-2}, $4X10^{15}$ ions cm^{-2} and $5.5X10^{15}$ ions cm^{-2} respectively. The results of Keinonen et al. (12) are used to correct the simple LSS predictions for ion ranges giving an Al concentration of 1.8 atomic per cent over a depth of 1200 Å. Estimates of the damage profile relative to the ion profile were made using the calculations of Winterbon (13,14). The estimated profiles are shown in Figure 1.

In the double-crystal diffraction method two crystals of nearly identical d-spacing are set in the anti-parallel reflection position that eliminates wavelength dispersion. Experiments were done at the Solid State Division of Oak Ridge National Laboratory. Copper radiation was reflected first from the 333 planes of a perfect Si crystal. The implanted copper crystal was set for the 222 reflection. The two d-spacings are closely matched. A 3 mm diameter area was implanted on the (111) Cu crystal surface so that both on implanted and unimplanted region could be investigated in the same crystal surface. The copper crystal is rotated through the diffraction peak position and the intensities are normalized to the incident beam which was measured by the detector through a calibrated filter. The scattering vector diagram in Figure 2 shows the arrangement where an open detector with no intervening collimation intercepts scattering from over an area of the Ewald scattering sphere. Scattering measurements were made on the implanted and unimplanted surface of each crystal. With the intention of exploring

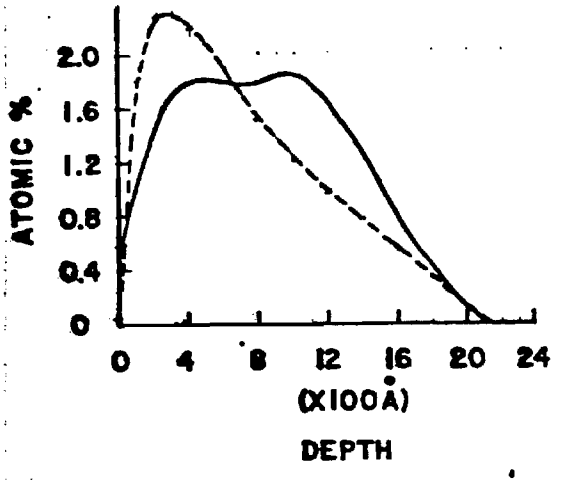

Fig. 1. Range and Damage Profiles.

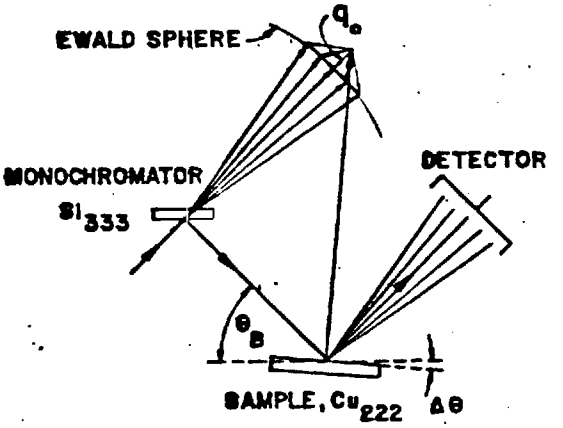

Fig. 2. Scattering Diagram.

the removal of damage, one of the crystals was annealed at 500°C for 30 minutes and the other crystal at 600°C for 30 minutes. X-ray measurements were repeated, then the first crystal was annealed at 900°C for 30 minutes.

Results

The scattering measurements made on the implanted crystal and the unimplanted crystal are shown in Figure 3 in which the logarithm of normalized intensity is plotted versus the rocking angle. Excess intensity in the tails of the rocking curve is on the order of a few percent and more intensity is found on the low rocking angle side. These scattering features arise from both microalloying of aluminum in copper and point defect clusters due to ion damage. Clusters of interstitial and vacancy collapse into sessile dislocation loops whose short-ranged strain fields of the loops yield diffuse x-ray scattering. The copper-aluminum alloy at the surface has a larger lattice parameter which in the absence of damage would give a small Bragg peak on the low angle side of the rocking curve. The aluminum ion distribution and the damage distribution overlap so that the two effects combine to produce an asymmetrical diffuse scattering as discussed below.

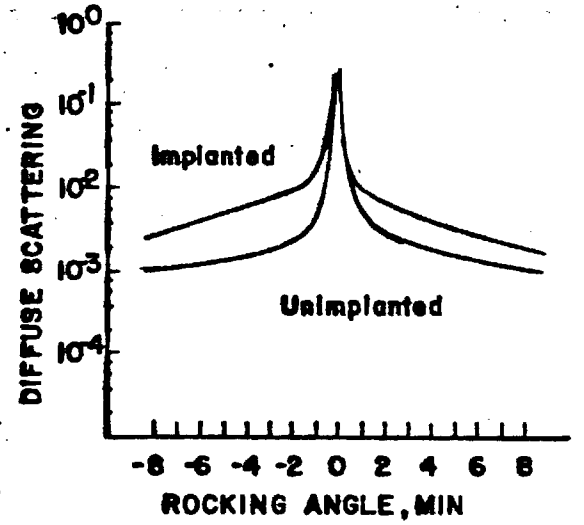

Fig. 3. Diffuse scattering from implanted and unimplanted crystals.

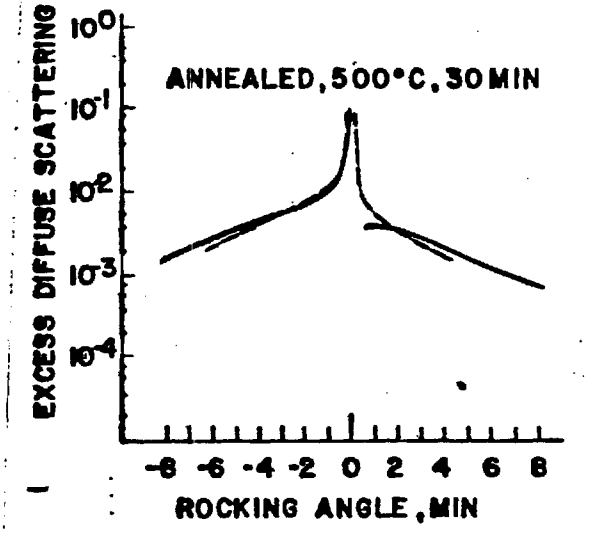

Fig. 4. Excess diffuse scattering changes with annealing at 500°C for 30 minutes.

Excess intensity curves are calculated from the difference between the unimplanted crystal rocking curve and the implanted as well as the implanted and annealed crystal rocking curves. In Figure 4, excess intensity curves are shown for the implanted and the implanted-500°C annealed cases. Annealing at 500°C for 30 minutes produces no appreciable intensity level or asymmetry change. In Figure 5, excess scattering curves show both a reduction in excess intensity as well as a loss of asymmetry in the scattering due to annealing at 600°C for 30 minutes. Not shown are the results of annealing in 900°C which restored the original condition of the copper crystal. A significant qualitative finding in these annealing observations is that the microalloying effect which gives asymmetry in excess scattering appears to be more readily annealed than dislocation loop effects.

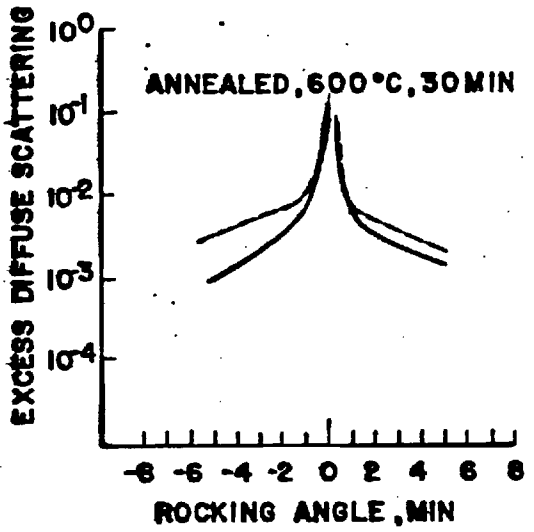

Fig. 5. Excess diffuse scattering changes with annealing at 600°C for 30 minutes.

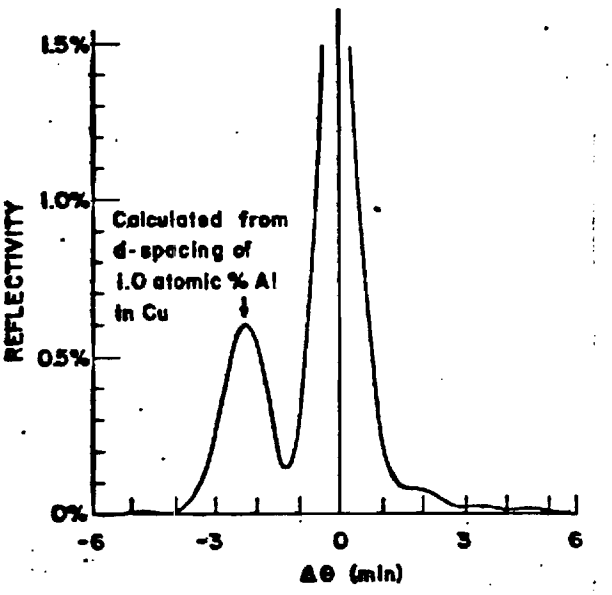

Fig. 6. Dynamical diffraction calculation of scattering from implanted copper.

Calculation of Scattering Effects

The scattering arises from a combination of microalloying and ion damage effects. These effects can be considered separately to provide a perspective on the observed scattering. Microalloying effects are modeled by assuming that the lattice parameter varies with depth according to aluminum content and that the alloyed layer is spacially coherent with the substrate. The resulting diffracted intensity can be calculated using an approach (10) based on an adaption of dynamical diffraction theory described by Klar and Rusticelli (15) for the description of elastic lattice distortion effects. Two coupled differential equations for the real and imaginary x-ray amplitudes are set up to incorporate lattice strain as a function of depth into the crystal. The equations are numerically integrated starting with boundary conditions on the real and imaginary scattering amplitudes at an external surface. Effects rising from the implanted microalloy are calculated by first determining the amplitude components at a depth well below the implanted alloy region. This is done by integrating from the reflecting surface into the crystal using the reflected amplitudes expected at the reflecting surface for an unimplanted crystal. The integration then procedes from the interior to the surface but now with alloying strain effects modifying the integration calculations. Figure 6 shows the calculated reflectivity for the case of a 1 atomic percent alloy at a depth of 1300 Å. A small Bragg peak appears on the low angle side whose position corresponds to a 1 atomic percent alloy and whose intensity is approximately 0.5%. Presuming that the intensity of this peak is in proportion to the ratio of alloy thickness (1300 Å) to penetration thickness ($1/\mu_{Cu}$), then the observed intensity should be 0.6%.

The analysis of scattering from radiation damage effects is complicated by the fact that the damaged region coincides with alloyed region created by implantation. The scattering is assumed to arise from the short range strain fields of the loops which give Huang scattering (16) near the Bragg peak

position. Since no distinct Bragg peak has been observed, quantitative analysis of observed scattering is not really valid and one must procede along qualitative directions given below. The analysis of scattering from point defect clusters including sessile dislocation loops of vacancy and interstitial type is concisely reviewed by Larson. (17) Huang scattering intensity around the Bragg peak gives detailed information on cluster density and type, but the scattering intensity is integrated over the Ewald sphere near the Bragg position so as to give an "integral diffuse scattering." The scattering averaged from above and below the Bragg peak is given by (18)

$$I^S(q_o) = \text{constant} \times C_L \left(\frac{b\pi R^2}{V_C}\right) \ln (q_L/q_o)$$

for $q_o \leq q_L$ where $q_o = h\cos\theta\Delta\theta$ with $h = d^{-1}_{hk\ell}$, θ is the Bragg angle and $d_{hk\ell}$ is the $hk\ell$ plane d-spacing. C_L is the density of dislocation loops of radius R with Burgers vector, b, V_C is the unit cell volume in q_L is approximately 1/R. This result can be used to obtain an average loop size, and a determination of loop size distribution and density is possible as well (18).

Analysis and Discussion

No distinct Bragg diffraction peak satellite associated with a implanted microalloy layer is observed. Since radiation damage is concentrated in the alloy layer, the degree of crystalline perfection within the layer is so poor that the dynamical diffraction calculation is simply not appropriate. The Scherrer formula estimate of the kinematic diffraction theory breadth for the implanted layer is approximately 5 times greater than the width calculated by dynamical theory. Thus, any distinct Bragg peak would be broadened into a small general scattering on the low angle side of the rocking curve as observed.

The analysis of the observed intensity in terms of dislocation loop scattering was persued using the approach outlined above. First, the angular position of defect scattering was measured relative to an assumed microalloy Bragg position. This position was calculated on the basis of the lattice parameter for a 1.8 atomic percent copper solid solution. The diffuse excess scattering is plotted versus $\ln(\Delta\theta)$ in Figure 7 and a straight line is seen. From the intercept of the line with the abscissa, q_L was obtained to give an average loop radius of 25 Å. This may be compared to a loop radius of 16 Å found in a similar analysis of neutron irradiated copper at room temperature.

A comparison of the magnitude of measured scattering intensity in the present experiments with a similar experiment (19) on nickel self-ion implantation shows that the observed scattering is within reasonable expected values. 4 Mev Ni ions where implanted into a nickel single crystal to a dose of $5X10^{13}$ ions/cm^2 at room temperature, although the dose is lower, a comparable point defect generation can be expected because of the higher ion energy. An estimate is made with a modified Kinchen-Pease model (20) for Frenkel pair production:

$$\nu = 0.8\, E_d/2E_D^{avg}$$

where E_d is the damage energy and E_D^{avg} is the average displacement energy. The ratio of defects produced in Cu by 200 Kev Al ions to the defects produced in Ni by 4 Mev Ni ions is 20 after dose differences are taken into account. Figure 8, which shows the excess scattering intensity, a scattering ratio of approximately 7 is observed. There are several factors which must be considered in comparing dislocation loop scattering intensities.

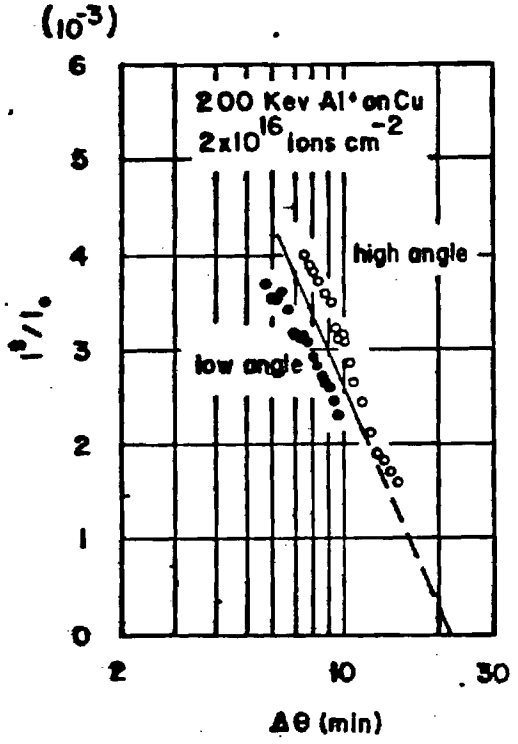

Fig. 7. Excess intensity vs. $\ln\Delta\theta$ is plotted to obtain an average loop radius of 25 Å in the implanted sample.

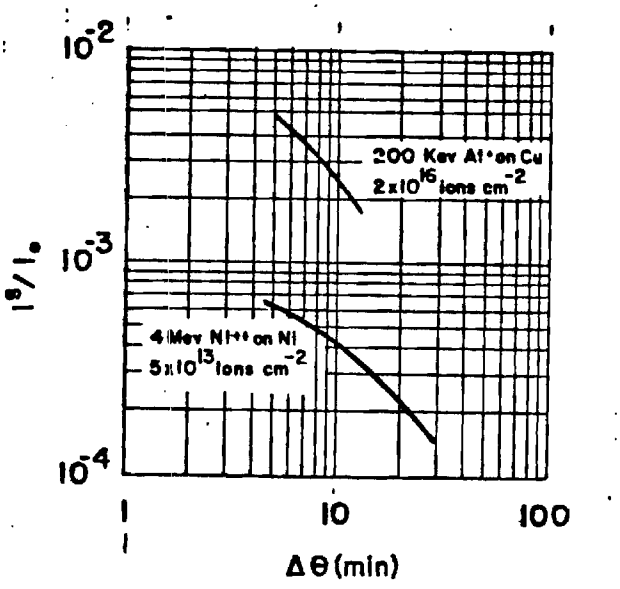

Fig. 8. Comparison of Ni self-ion implantation with Al ion implantation in Cu.

Since the intensity varies as R^4, differences in loop radius between the two cases will affect scattering levels considerably. Agreement between the two cases within a factor of ten is considered satisfactory.

The annealing response in aluminum implanted copper suggests that aluminum migrates into the interior at 600°C and leaves dislocation loops in place although reduced in density. Thus, the damaged state has a degree of stability making the dislocation loops a potentially useful barrier to slip at the surface. At 600°C one can expect removal of loops unless they are stablized by alloying interactions or entanglement. It is not yet possible to assess which factor might be most important.

Conclusions

X-ray diffraction analysis of intensities measured with the double-crystal arrangement has qualitatively shown that a microalloy layer which is heavily radiation damaged is produced by aluminum ion implantation into copper. With the current interpretation, we believe that an alloy layer having a larger lattice parameter will produce a compressive stress on the surface and a tensile stress on the interior as the alloy layer maintains coherency with the substrate. Upon annealing, the aluminum solute leaves the surface layer but radiation damage produced dislocation loops remain, possibly stablized by alloy effects or dislocation entanglement. The beneficial effects of such a surface structure on fatigue crack initiation in polycrystalline copper is discussed in a companion paper.

The diffraction effects seen in alloy implantations is dominated by radiation damage effects. The principal observation which can be used to

deduce surface stress state is assymmetry in the scattering about the substrate Bragg peak and such effects can be seen only in relatively perfect crystals.

Acknowledgments

The authors thank Dr. B. C. Larson and Mr. Jim Barhorst of the Solid State Division of Oak Ridge National Laboratory for their considerable help in collection of the data and many useful discussions. This research was sponsored by the Office of Naval Research under Contract N00014-78-C-0270, Dr. Philip A. Clarkin, Program Manager. The United States Government is authorized to reproduce and distribute reprints for Government purposes notwithstanding any copyright notation hereon.

References

1. E. Y. Chen and E. A. Starke, Jr., "Effects of Ion-Plating on the Low Cycle Fatigue Behavior of Copper Single Crystals," Mat. Sci. Eng., 24 (1976) pp. 209-221.

2. B. R. Livesay and E. A. Starke, Jr., "Interactions of Dislocations with Interfaces," Acta Met., 21 (1973) pp. 247-254.

3. P. D. Townsend, J. C. Kelly and N. E. W. Hartley, Ion Implantation, Sputtering and Their Application, Academic Press, New York, 1976.

4. G. Dearnaley et al. eds, Ion Implantation, North-Holland Publ. Co.; American Elsevier, New York, 1976.

5. S. Fujishiro, "Improved High Temperature Mechanical Properties of Titanium Alloys by Pt Ion Plating," presented at the Int. Conf. Metallurgical Coatings, San Francisco, April 1978.

6. B. D. Cullilty, "Elements of X-Ray Diffraction," 2nd ed., Chapter 16, Addison-Wesley Pub. Co., Inc., Reading, MA 1978.

7. B. E. Warren and B. L. Averbach, "The Effect of Cold-Work Distertion on X-Ray Patterns," J. Appl. Phys., 21 (1950) pp. 595-599.

8. J. E. Thomas, T. O. Baldwin and P. H. Dederichs, "Diffuse X-Ray Scattering in Fast-Neutron-Irradiated Copper Crystals," Phys. Rev. 3(4) (1971), pp 1167-1173.

9. B. C. Larson and W. Schmatz, "Huang Diffuse Scattering from Dislocation Loops and Cobalt Precipitates in Copper," Phys. Rev. B 10(B) (1974), pp. 2307-2314.

10. B. C. Larson, C. W. White and B. R. Appleton, "Unidirectional Contraction in Boron-Implanted Laser-Annealed Silicon," Appl. Phys. Lett., 32 (12) (1978), pp. 801-803.

11. J. Lindhard, M. Scharff and H. E. Schiott, "Range Concepts and Heavy Ion Ranges," Kgl. Danske Videnskab, Mat.-Fys. Medd. 33 (14) 1963, pp. 1-42.

12. J. Keinonen, M. Hautala, M. Luomajarvi, A. Anttila and M. Bister, "Ranges of $^{27}Al^{+}$ Ions in Nine Metals Measured by (p,γ) Resonance Broadening," Rad. Eff., 39 (1978), pp. 189-193.

13. K. B. Winterbon, P. Sigmund and J. B. Sanders, "Spatial Distribution of Energy Deposited by Atomic Particles in Elastic Collisions," Kgl. Danske Videnskab. Selskab, Mat.-Fys. Medd., 37 (14) (1970), pp. 1-73.

14. K. B. Winterbon, Ion Implantation Range and Energy Depositon Distributions, Vol. 2, Low Incident Ion Energies. IFI/Plenum Press, New York, 1975.

15. B. Klar and Rusticelli, "Dynamical Neutron Diffraction by Ideally Curved Crystals," Nuovo Cimento, 13B (1973) pp. 249-270.

16. P. H. Dederichs, "Diffuse Scattering from Defect Clusters Near Bragg Reflections," Phys. Rev. B, 4 (4) (1971) pp. 1041-1050.

17. B. C. Larsen, "X-Ray Studies of Defect Clusters in Copper," J. Appl. Cryst., 8 (1975), pp. 150-160.

18. B. C. Larson and F. W. Young, Jr., "A Comparison of Diffuse Scattering by Defects Measured in Anomalous Transmission and Near Bragg Reflections," Phys. Rev., B4 (1971) pp. 1709-1713.

19. J. Narayan and B. C. Larsen, "Defect Clusters and Annealing in Self-Ion-Irradiated Nickel," J. Appl. Phys., 48 (11) (1977) pp. 4536-4539.

20. K. L. Merkle, "Defect Production by Energetic Particle Bombardment," pp. 58-94 in Radiation Damage in Metals, N. L. Peterson and S. D. Harkness eds, ASM, Metals Park, Ohio, 1976.

APPENDIX B

X-RAY SCATTERING INVESTIGATION OF MICROALLOYING AND DEFECT STRUCTURE IN ION IMPLANTED COPPER

By

S. Spooner

Presented at the AIME Symposium on Advanced Techniques for the Characterization of Microstructures, Los Vegas, Nevada, February 24-28, 1980. To be published in the Proceedings of the Symposium.

X-RAY SCATTERING INVESTIGATION OF MICROALLOYING AND DEFECT STRUCTURE IN ION IMPLANTED COPPER

S. Spooner

Fracture and Fatique Research Laboratory
Georgia Institute of Technology
Atlanta, Georgia 30332

The double-crystal method for x-ray scattering analysis of radiation described by B. C. Larson (1) has been applied to the investigation of aluminum implanted copper. The interpretation of x-ray observations is based on effects of lattice strain in the surface microalloy and the presence of dislocation loops which originate from implantation damage. The copper crystal with a dislocation density less than 10^3 cm/cm^3 was implanted with aluminum to a dose of 2×10^{16} ions/cm^2 with energies up to 200 keV. The response of the implanted crystal to annealing at 500 and 600°C was determined. The quantitative use of the x-ray technique to assess implantation effects and limitations of the technique are discussed.

Introduction

X-ray diffraction is an effective method for analyzing radiation damage particularly for quantitative measurement of lattice strain effects associated with defect clusters (1). In recent years there have been a variety of x-ray diffraction investigations of ion implantation damage produced in single crystals based on double-crystal measurements. Komenou et al (2) observed x-ray scattering resembling Pendellosung interference in rocking curves from Ne^+ -implanted garnet films which Speriosu (3) interpreted according to a kinematic diffraction theory encorporating strain and damage distributions as a function of depth. A fanasev et al (4) have used dynamical theory for calculating the scattering from a silicon crystal with disturbed layers. Yamagishi and Nittono (5) studied Ar^+ ion-implanted copper whiskers with both x-ray topography and a triple-crystal diffraction method to assess lattice strain response with dose and annealing. In the foregoing studies (2-5) no absolute intensity measurements were made so that analysis of structural changes depended mostly upon scattering distribution shape. In the present study, absolute reflectivity measurements are used to study the effects of AL^+ -ion damage in copper due to low energy (200 kev) and high dose ($2X10^{16}$ ions/cm^2) with a double-crystal diffraction method. Both surface alloying and implantation damage are under consideration for their important influence on fatigue crack initation (6). Because radiation damage production of point defect clusters enters our work in a fundamental way, this paper offers an example of the utility of x-ray scattering techniques in radiation damage research.

The principal challenge is this x-ray study was to find an effective x-ray method for investigating the damage and surface alloying effect in an implanted layer which is much thinner than the sampling depth of x-rays. In addition, there was the consideration of which theoretical analysis of scattering intensity would be most appropriate to describe the combined damage and surface alloying scattering effects. This question was approached from two perspectives; (a) use of dynamical theory of diffraction for the analysis of lattice strain due to surface alloying (7,8) and (b) use of kinematic theory for the description if scattering from defect clusters (1). It is shown that the scattering data is dominated by implantation damage defect clusters and that the kinematic theory is most appropriate for the description of scattering in the case at hand. Furthermore, it is shown that a quantitative evaluation of implantation damage can be obtained from the absolute reflectivity measurements made in the double-crystal method.

X-Ray Scattering Models

The implanted region structure is modeled by the superposition of damage produced clusters within a surface alloy layer which has a lattice parameter that is different from the unimplanted substrate. As yet, no single formulation for scattering intensity gives a calculatin of the scattering for the combined defect cluster and lattice distortion effects. Instead, we make a calculation for the case of scattering from a defect-free surface alloy on one hand and a calculation for the scattering from defect clusters in a pure matrix on the other hand. The measured x-ray scattering effects are then used to determine the manner in which the two calculations might be applied to represent the scattering from the implanted layer.

For a surface alloy layer free of defects, dynamical theory of x-ray scattering can be used to calculate the reflectivity of x-rays as a function of crystal rotation in a double-crystal rocking curve. In a two-crystal arrangement, the first crystal which is alloy-free is set to maximum reflectivity. The second crystal is rotated about an axis perpendicular to the scattering plane (defined by the incident and reflected x-ray beams). The resulting reflectivity curve is the convolution to the reflection

characteristic of the first crystal with the reflectivity of the second crystal. Larson (7,8) has adapted for this surface alloy problem a method of calculation used by Klar and Rustichelli (9) for neutron scattering from elastically bent crystals. The reflectivity from a crystal is obtained by the computation of the real amd imaginary components of the complex scattering amplitude of the reflected radiation. Two coupled differential equations - one for real and one for imaginary component - are integrated numerically. The integration is dependent upon initial values of the amplitude components and the variation in the Bragg angle for the crystalline sublayers due to the elastic lattice distortion arising from bending or composition change. Full algebraic development of the theory can be found in papers by Larson and Borhorst (8) and Klar and Rustichelli (9). The equations requiring integration express the derivatives of the real (X_1) and imaginary (X_2) scattering amplitude components with respect to a variable A which is proportional to depth measured relative to the external surface:

$$\frac{dX_1}{dA} = k\,(X_1^2 - X_2^2 + 1) + 2X_2(X_1 - y) - 2gX_1 \qquad (1)$$

$$\frac{dX_2}{dA} = -(X_1^2 - X_2^2 + 1) + 2X_1(X_2 k + y) - 2gX_2 \qquad (2)$$

where k and g are constants which depend on x-ray absorption and the parameter y contains the misset angle, $\Delta\theta$, for the rocking curve as follows:

$$y = C_1\,\Delta\theta - C_2 \qquad (3)$$

where C_1 and C_2 are constants dependent on x-ray scattering parameters that are fixed for the Bragg diffraction peak under examination. It is shown (8) that the parameter y can be reexpressed for the case where the lattice parameter varies with A as follows:

$$y = C_1(\Delta\theta + \varepsilon(A)\,\tan\theta_B) - C_2 \qquad (4)$$

where the variation of the lattice parameter with depth is contained in the strain function $\varepsilon(A)$. In the case at hand, $\varepsilon(A)$ is determined by the compostion of the surface alloy as a function of implantation depth.

The method by which the change in reflectivity due to surface alloying is calculated does not require integration over the entire crystal thickness. Instead, one uses the well known results (10,11) for the reflectivity from a perfect crystal as a starting point. The real and complex components of the scattering amplitude at a set rocking angle are used as initial values for the integration into the interior of the perfect crystal($\varepsilon(A) = 0$) to a depth below the implanted ions. Then, the amplitude components at that depth are used as initial values for the integration back to the surface but with the effects of surface alloying, $\varepsilon(A)$, now allowed to affect the computation of scattering amplitude. A set of these calculations is done for a range of rocking angles where the reflectivity is calculated from,

$$R(\Delta\theta) = X_1^2 + X_2^2 \qquad (5)$$

where the amplitude components, X_1 and X_2 are evaluated at the reflecting crystal surface. Note that the result is an absolute reflectivity.

Figure 1 shows the results of calculation we have obtained for the case in which a 1 atomic per cent aluminum is implanted in copper to a depth of approximately 1100A°. The lattice parameter expansion used in this calculation was calculated from the data given on linear lattice strain by

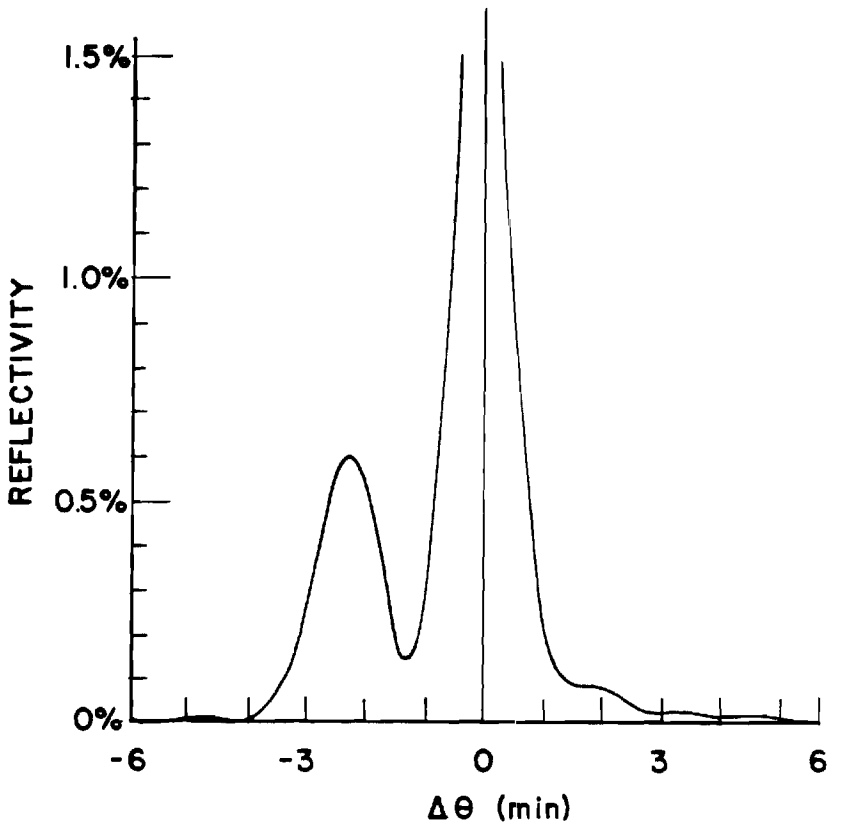

Fig. 1 - Calculated reflectivity from a 1100 Å surface alloy of 1 atomic percent of aluminum in copper. The subsidiary peak appears at an angle appropriate for the lattice parameter of this composition.

Fig. 3

Scattering geometry for the double-crystal method used in this experiment. Upon rocking the crystal the Ewald scattering sphere is swept through the Bragg point. At a fixed crystal setting the diffuse scattering is integrated over a portion of the scattering sphere near the Bragg point.

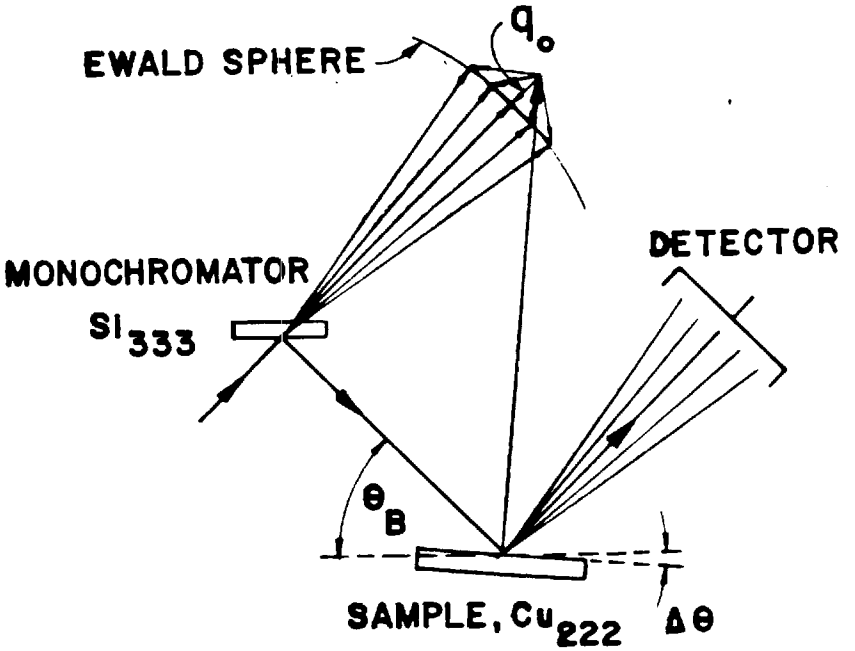

King (12) equal to +0.0026 per atomic percent of aluminum in copper. A sharp subsidiary peak of 0.5% reflectivity is seen at a Bragg angle displaced to a lower angle corresponding to the expanded lattice parameter. The small peak width is approximately 1 minute of arc. The reflectivity very nearly equals the ratio of implanted layer thickness to x-ray penetration thickness, $1/\mu_o$, where μ_o is the linear absorption parameter.

Consider now the calculation of the scattering from defect clusters in a crystal of uniform lattice parameter. In this case, Kinematic diffraction theory is used to calculate the scattering intensity from an isolated defect cluster. The scattering resulting from a collection of defects is the sum of these intensities. This implies that no scattering interference occurs between scattering amplitudes coming from each defect. Larson (1) summarizes the calculation of the scattering intensity from defect clusters. The experimental geometry used in our experiments is shown in Figure 2 where the scattered x-rays are recieved into a large detector and to each of the scattering vectors is associated a scattering space vector q going from the Bragg spot (at the top) to the surface of the Ewald scattering sphere. In such an experiment, the intensity is averaged over the scattering space vectors, q. q_o is the shortest vector between the Bragg position and the Ewald sphere at a given crystal setting. The measured intensity is called the integral diffuse scattering. The intensity is measured as a function of rocking angle of the crystal in the same geometry used for measurement of dynamical diffraction effects described above.

The diffuse scattering from dislocation loops measured close to the Bragg peak is attributed to long range strain fields around the loop and is called Huang scattering. Scattering measured farther away from the Bragg peak is attributed to short range strain fields and is termed Stokes-Wilson scattering. The diffuse scattering is distributed about the Bragg position in a way dependent on the precise strain field distribution (1,13). The calculation of integral diffuse scattering requires an averaging of the diffuse scattering over the portion of the Ewald scattering sphere which is close to the Bragg position. (14) For the scattering from loops of radius R, the Huang scattering smoothly joins the Stokes-Wilson scattering at a scattering parameter $q_o = q_2 = 1/R$ where $q_o = h\Delta\theta \cos\theta_B$ with $h = 2\pi/d_{hkl}$, θ_B the Bragg angle for reflection from hkl planes and $\Delta\theta$ the mis-set angle of the rocking curve. A symmetric diffuse scattering cross section is defined

$$\sigma_h^s(q_o) = \tfrac{1}{2}\left(\sigma_h^s(-q_o) + \sigma_h^s(q_o)\right) \qquad (6)$$

which is obtained by the average of intensities measured symmetrically above and below the Bragg position ($q_o = 0$). The symmetric diffuse cross sections for Huang and Stokes-Wilson scattering are given by,

$$\text{(Huang)} \qquad \sigma_h^s(q_o) = (r_e f_h e^{-M})^2 (h/K)^2 2\pi\tau (b\pi R^2/V_c)^2 \ln(e^{\frac{1}{2}} q_L/q_o) \qquad (7)$$

for $q_o < q_1$, and,

$$\text{(stokes-Wilson)} \qquad \sigma_h^s(q_o) = (r_e f_h e^{-M})^2 (h/K)^2 2\pi\tau (b\pi R^2/V_c)^2 q_L^2/2q_o^2 \qquad (8)$$

for $q_o > q_1$. r_e is the Thompson electron radius (2.82×10^{-13} cm), f_h atomic scattering factor, e^{-m} is the Debye-Waller factor, $k = 2\pi\lambda$, λ = wavelength, τ is a constant of order 1 which depends on averaging of loop orientations, b Burgers vector, V_c atomic volume. The scattering intensity relative to the incident intensity is given,

In summary of the two calculations, the dynamical theory predicts a subsidiary peak which appears at an angle determined by the lattice strain due to alloying. The kinematic theory predicts a diffuse scattering which is proportional to the number and size of loops. Both calculations give the absolute reflectivity with no adjustable parameters other than those describingthe structure. The dynamical thoery calculation depends on the assumption that the surface alloy is crystallographically coherent with the unalloyed crystal. The limit to the kinematic theory is likely to be found with very high defect cluster densities where interference between diffuse scattering amplitudes may occur.

Experimental

The calculated strain scattering effects must be measured at small angles near the Bragg diffraction peak of the unaffected crystal. The implant affected region is less than 1 micron and the pentration depth is approximately $1/\mu o$ = 22 microns. It is required that the bulk of the crystal be perfect (mosaic spread less than 1 minute) in order that the small scattering effects can be measured near the Bragg peak. Furthermore, it is required to subtract a sigificant background due to the tails of the bulk crystal Bragg peak in order to determine the diffuse scatterin intensity due to surface alloying and defect clusters. A convenient approach to this measurement is to translate the crystal between an implanted and unimplated area on the sample crystal. Crystals used in these studies were provided by F. W. Young of ORNL. The crystals were grown by Bridgman technique, wt to orientation, then annealed at a few degrees below the melting point for two weeks. The crystal pieces were hardened by neutron irradiation and then further cut and shaped by chemical cutting methods.(15) The dislocation density measured by etch pit techniques was less than 10^3 cm^{-2} after shaping processes were complete.

The two-crystal arrangement consisted of a silicon crystal fixed to diffract the Cu K_{α_0} radiation onto the implanted copper crystal. The (333) d-spacing (1.0451Å) of silicon happens to match the (222) d-spacing (1.0436Å) of copper very well so that the system is well focussed to give a narrow rocking curve width. The copper crystal is initially aligned to give a sharp maximum in the rocking curve by adjusting the (111) normal about an axis in the scattering plane (defined by the incident and scattered beams). When properly adjusted, the full width at half-maximum (FWHM) of the copper rocking curve is 12.5 arc-sec. The crystal is mounted on a goniostat which can be translated in the plane of the crystal surface so that rocking curves can be made from the implanted area and masked unimplanted areas. In a typical run, the copper crystal is rocked about an axis perpendicular to the scattering plane at a rate of 5 to 20 arc-sec per minute while x-ray intensities are recorded continuously at 10 second intervals. The x-ray detector has an active receiving area of 5 cm^2 at a distance of 8 cm so that the subtended soild angle (0.08 steradians) intergrates the scattering over a large portion of the Ewald scattering sphere in the vicinity of the 222 Bragg peak of copper.

The implantation of aluminum into copper was chosen for these experiments because the ion penetration was favorable and the microalloy concentration

of implantation are given elsewhere. (6) The implanted layer was 1200 Å (16) thick with a composition of 1.8 atomic per cent. The distribution of damage over the alloy thickness was estimated on the basis of calculations by Fritzsche (17) and Winterbon. (8) The alloy distribution (solid line) and the damage profile (dashed line) are shown in Figure 3.

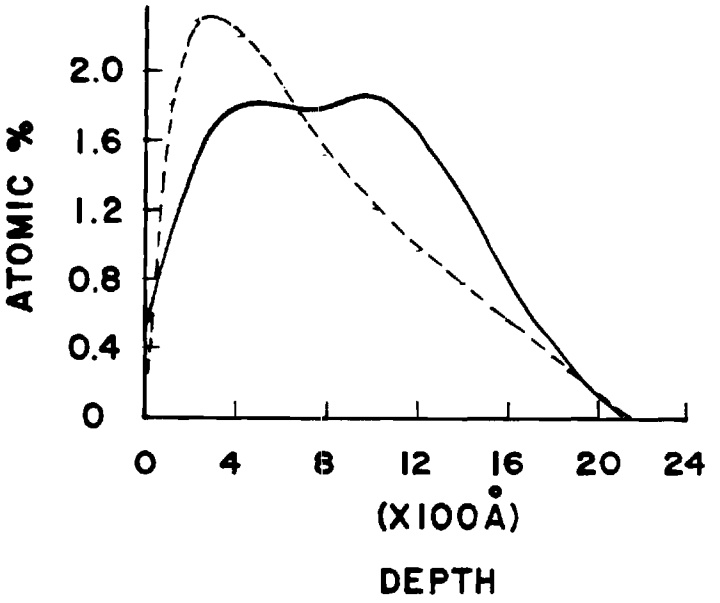

Fig. 3

Distribution of implanted Al^+ ions (solid) and the energy deposition (dashed) for the implantation of $2x10^{16}$ion/cm^2 with energies upto 200 keV. Note that damage is concentrated toward the surface.

Annealing of the specimens was performed as a means to differentiate the sources of scattering in the implanted layers. The crystals were placed in a vacuum of 10^{-8} Torr at 500°C, at 600°C, and 900°C for 30 minutes. Annealing at 900°C restored the original structure as seen in the rocking curves.

Results and Discussion

The rocking curves for unimplanted copper and for aluminum implanted copper were measured on the same crystal. These cruves are shown in Figure 4.

Fig. 4

Rocking curves are shown for the implanted (upper) and unimplanted(lower) crystal. The scattering is expressed as a fraction of the incidnet beam intensity. Note the larger scattering at low angles.

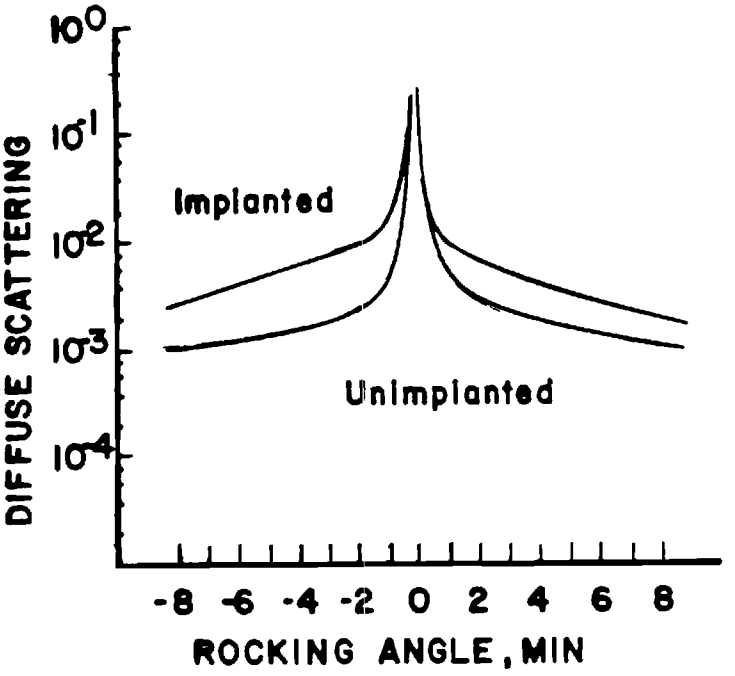

The diffuse scattering from the implanted crystal is more intense on the low angle side of the Bragg peak position. The excess diffuse scattering is calculated by subtraction of the unimplated rocking curve intensity from the corresponding intensity in the implanted crystal. The excess diffuse scattering for the implanted crystal is shown in Figures 5 and 6 as a dashed line. The effect of 30 minute anneals on the excess diffuse intensity is shown in Figure 5 for annealing at 500°C and in Figure 6 for annealing at 600°C.

Fig. 5

Excess diffuse scattering intensity for the sample before annealing (dashed) and after annealing (solid) at 500°C is shown. Note that little change in the general level and distribution of the excess intensity occurs upon annealing.

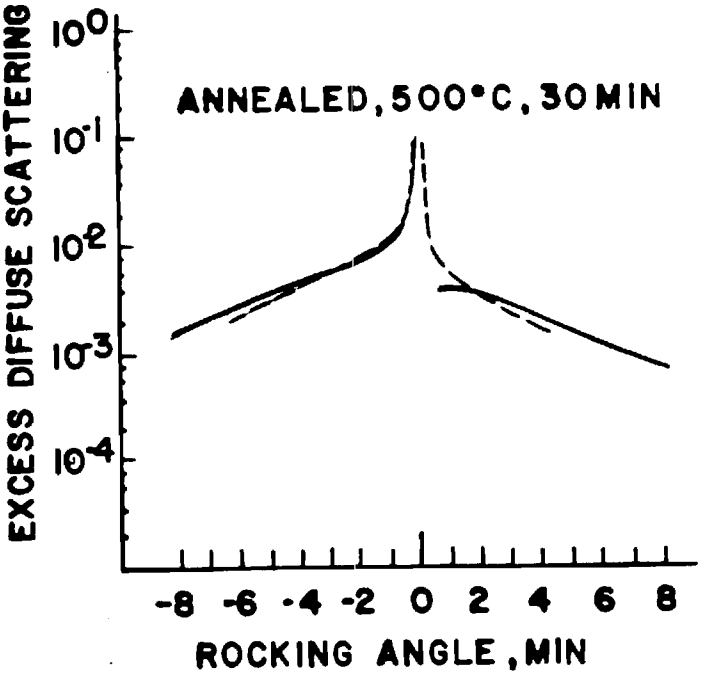

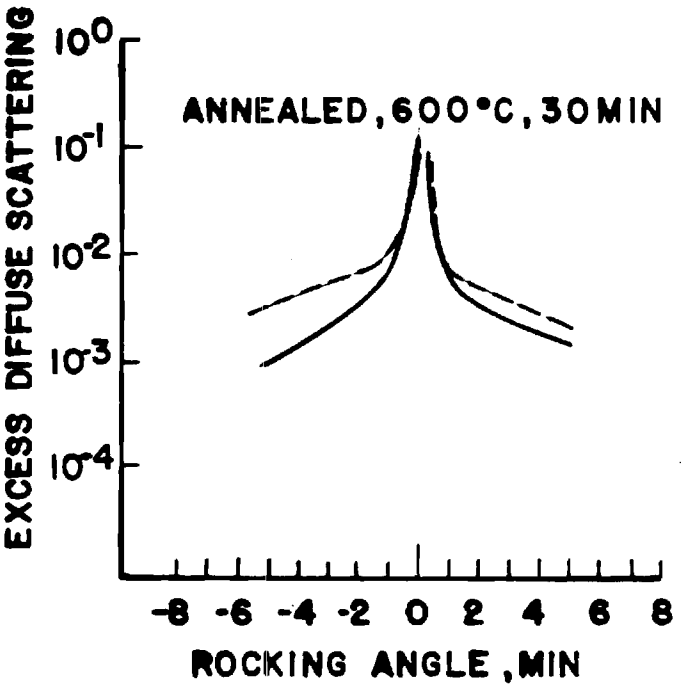

Fig. 6.

Excess diffuse scattering intensity for the sample before annealing (dashed) and after annealing (solid) at 600°C. The level and the distribution of the excess intensity has changes as a result of the annealing at this temperature.

No large change due to annealing occurs at 500°C while for annealing at 600°C, there is a reduction of scattering and the scattering becomes more symmetric with respect to the Bragg peak position.

The observation of a higher diffuse scattering at low rocking curve angles can be attributed to the fact that implanted aluminum expands the copper lattice so that Bragg scattering from the implanted region occurs at a lower angle than that for the unimplanted material. The composition of the implanted layer was estimated to be 1.8 atomic per cent. The resulting Bragg position would be displaced to lower angle by 4.2 minutes for the 222 reflection from the copper alloy layer.

No subsidiary peak is seen in the rocking cruve data which indicates that conditions for the dynamical diffraction from the surface alloy do not apply. Kinematic theory for Bragg scattering from an incoherent microalloy layer of 1100 Å predicts a rocking curve width about 9 minutes (compare for example the Scherrer width (19)). The kinematic intensity relative to the dynamical subsidiary peak would be reduced in proportion to the ratio between the two peak widths. This suggests that if the implanted layer loses strict coherence with the unimplanted material, the Bragg diffraction intensity from the layer would be relative small and spread out on the scale of these rocking curve measurements.

The diffuse scattering seen on both sides of the main Bragg position can be compared to calculations of the scattering from dislocation loops. Figure 7 the excess diffuse scattering is plotted versus the log of the rocking angle according to Egn. (7) for Huang loop scattering. The rocking angle was measured relative to the supposed Bragg position for the alloy. Although there is a displacement between the two sets of points, the average of the high angle and low angle intensity is close to a straight line which yields an estimated loop diameter of 25Å.

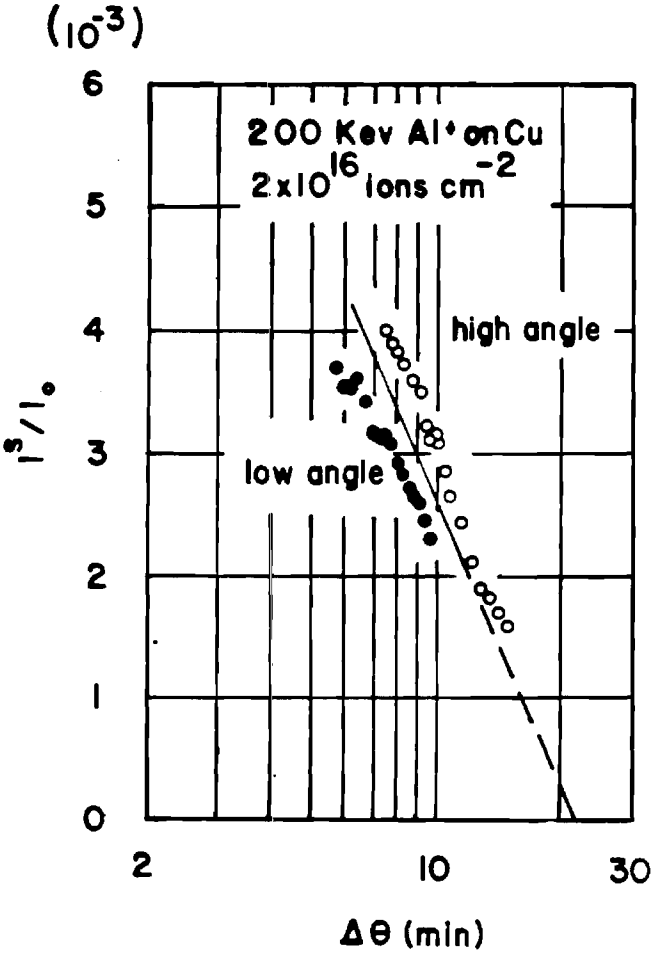

Fig. 7

The excess diffuse scattering from the implanted crystal is plotted versus $\ln(\Delta\theta)$ for the intensity above and below the Bragg position assumed to apply for the implanted region of the crystal.

An estimate of the density of loops can be made by comparing measured reflectivity with Egn. (9). We use a loop radius of 30Å and a reflectivity of 1% at $\Delta\theta$ = 2 minutes. Substitution of appropriate constants into Egn. 9 for a 30Å loop size gives

$$I^S(qo)/I_o = 6.1 \times 10^{-21} \frac{C}{V_v} \ln (44/\Delta\theta \text{ (min)})$$

from which a value of C/V_v is 5.3×10^{17} loops/cc. (The loops are concentrated by a factor of 200 in the implanted layer since the above calculation assumes the loops to be uniformly distributed).

The failure to observe a sharp Bragg peak associated with the implanted aluminum and the general agreement with scattering levels calculated for loop scattering point to the conclusion that the kinematic theory for diffraction from an implanted crystal is most appropriate. The annealing at 600°C produces symmetrical scattering which suggests that most of the aluminum is removed from the region where loops persist. Thereby, the loop scattering now originates in essentially pure copper. The role of aluminum is seen as simply expanding the lattice in a region which, by virture of severe damage, is no longer strictly coherent with the unimplanted crystal.

Analysis of x-ray diffraction in aluminum ion implanted copper suggests that defect cluster scattering dominates the observed rocking curve intensity. Alloying in the implanted layer contributes through a shifting of the diffuse scattering to lower angles due to the fact that the defect clusters are formed in a region of aluminum-expanded lattice. The formation of a distinct peak predicted by dynamical diffraction theory does not occur probably because spatial coherency between the alloy layer and the substrate is lacking due to severe lattice damage. Problems in the analysis of scattering remain in the area of (1) formulating a model of combined alloying and defect cluster scattering and (2) description of very high defect cluster scattering. Nevertheless the simplistic interpretation of x-ray scattering observation provides useful insights into the type and quantity of damage as well as the annealing response of the implanted structure.

Acknowledgements

The author thank Dr. B. C. Larson and Mr. Jim Barhorst of the Solid State Division of Oak Ridge National Laboratory for their considerable help in collection of the data and many useful discussions. This research was sponsored by the Office of Naval Research under Contract N00014-78-C-0270, Dr. Philip A. Clarkin, Program Manager. The United States Government is authorized to reproduce and distribute reprints for Government purposes notwithstanding any copyright notation hereon.

References

1. B. C. Larson, "X-ray Studies of Defect Clusters in Copper", J. Appl. Cryst 8. pp. 150-160 (1975).

2. K. Komenou, I. Hirai, K. Asama and M. Sakai, "Crystalline and Magnetic Properties of an Ion-Implanted Layer in Bubble Garnet Films", J. Appl. Phys 49 pp. 5816-5822 (1978).

3. V. S. Speriousu, H.L. Glass and T. Kobayashi, "X-ray Determination of Strain and Damage Distributions in Ion-Implanted Layers", Appl. Phys. Lett. 34, pp. 539-542 (1979).

4. A. M. Afanasev, M. V. Kovalchuk, E. K. Kovev and V. G. Kohn, "X-ray Diffraction in a Perfect Crystal with Disturbed Surface Layer", Phys. Stat. Sol. (a) 42, pp. 415-422 (1977).

5. H. Yamagishi and O. Nittono, "X-ray Study on Lattice Defects in Ar^+ Ion Implanted Copper Whiskers", Nippon Kinzokv Gakkaishi 43, pp. 689-695 (1979) (Abstract in English).

6. S. Spooner and K. Legg, "X-ray Diffraction Characterization of Aluminum Ion Implanted Copper Crystals" paper presented at Materials Research Society Meeting, Cambridge, Mass., Nov. 1978.

7. B. C. Larson, C. W. Shite and B. R. Appleton, "Unidirectional Contraction in Boron-Implanted Laser-Annealed Silicon", Appl. Phys. Lett. 32 (1978) pp. 801-803.

8. B. C. Larson and J. F. Barhorst, "X-ray Study of Lattice Strain in Boron Implanted Laser Annealed Silicon", submitted for publication, (October, 1979).

9. B. Klar and F. Rusticheili, "Dynamical Neutron Diffraction by Ideally Curved Crystals", Nuovo Cimento, 13B (1973) pp. 249-270.

10. B. E. Warren, "X-ray Diffraction", Chapter 14, pp. 315-354, Addison-Wesley, Reading, Mass. (1969).

11. W. H. Zachariasen, "Theory of X-ray Diffraction in Crystals", Chapter 3, pp. 83-155 (esp. 140-147), Dover Publications, New York (1967).

12. H. W. King, "Quantitative Size-Factors for Metallic Solid Solutions", J. Mat. Sci 1 (1966) pp. 79-90.

13. B. C. Larson and W. Schmatz, "Huang-Diffuse Scattering from Dislocation Loops and Cobalt Precipitates in Copper", Phys. Rev. B 10, (1974) pp. 2307-2314.

14. B.C. Larson and F. W. Young, Jr., "A Comparison of Diffuse Scattering by Defects Measured in Anomalous Transmission and Near Bragg Reflections", Z. Naturtorsch 28a (1973) pp. 626-632.

15. F. W. Young, Jr., "Etch Pit Studies of Dislocations in Copper Crystals Deformed by Bending. I. Annealed Crystals. II. Irradiated Crystals", J. Appl. Phys. 33 (1962) pp. 3553-64.

16. J. Keinonen, M. Hautala, M. Luomajari, A. Anttila and M. Bister, "Ranges of $^{27}AL^{+}$ Ions in Nine Metals Measured by (p,γ) Resonance Broadening", Rad. Eff. 39 (1978) pp. 189-193.

17. C. R. Fritzche, "A Simple Method for the Calculation of Energy Deposition Profiles from Range Data of Implanted Ions", Appl. Phys 12 (1977) pp. 347-353.

18. K. B. Winterbon, "Ion Implantation Range and Energy Deposition Distributions, Vol. 2, Low Incident Ion Energies, IFI/Plenum Press, New York (1975).

19. B. D. Cullity, "Elements of X-ray Diffraction", 2nd ed., Chapter 16, Addision-Wesley Pub Co., Inc. Reading, MA (1978).

APPENDIX C

THE EFFECT OF ALUMINUM ION IMPLANATION ON THE FATIGUE CRACK INITIATION OF POLYCRYSTALLINE COPPER

By

A. Kujore
S.B. Chakraborty
E.A. Starke, Jr.
and
K. O. Legg

Presented at the Materials Research Society's Symposium on Surface Modification of Materials by Ion Implantation, Cambridge, MA, November 30, 1979. To be published in the Proceedings of the Symposium.

THE EFFECT OF ALUMINUM ION IMPLANTATION ON THE FATIGUE CRACK INITIATION OF POLYCRYSTALLINE COPPER[+]

A. Kujore, S.B. Chakrabortty, E.A. Starke, Jr.
Fracture and Fatigue Research Laboratory
and
K.O. Legg
School of Physics
Georgia Institute of Technology
Atlanta, Georgia 30332

The effect of Al ion implantation on the low cycle and high cycle
gue behavior of polycrystalline copper has been investigated. The
ic stress strain response, stress-life relationship and fatigue crack
leation behavior of implanted copper are compared with unimplated copper.

The ion implantation did not seem to effect the monotonic yield stress,
did decrease the extent of work hardening in the low strain range.
milar decrease was observed in the cyclic hardening behavior. Al ion
antation produced a significant improvement in fatigue life for both
in and stress controlled tests. This improvement is associated with
fications of the deformation behavior in the surface and near-surface
ons of the implanted copper, and its subsequent effect on fatigue
k initiation.

s research was sponsored by the Office of Naval Research under Contract
14-78-C-0270, Dr. Philip A. Clarkin, Program Manager. The United
es Government is authorized to reproduce and distribute reprints for
rnment purposes notwithstanding any copyright notation hereon.

Introduction

The fatigue process may be divided into two stages, crack initiation
l subsequent crack propagation. Microcracks usually form at the surface
a material due to cyclic straining, and link-up and growth of these
:rocracks into a major fatal crack may be termed the initiation stage.
najor factor in the initiation of fatigue cracks concerns slip processes
the surface and these are considerably influenced by the surface
ıdition. It is well known that gross surface alterations like shot
:ning and case hardening can improve fatigue life, and recent results
/e shown that small surface alterations can also have a considerable
fect on fatigue behavior. Chen and Starke (1) studied the effect of
ı-plated coatings of copper, nickel, and silver on the low cycle fatigue
)perties of copper single crystals. They concluded that the ion-plating
)cess itself does not significantly change the cyclic flow stress, but
: stacking fault energy of the coating material effects crack initiation
influencing the topography of the slip bands on the surface.

It is unclear whether similar small surface modifications of poly-
/stalline samples will produce a change in cyclic life similar to that
;erved for single crystals. Changes in the deformation behavior of
rface grains may be produced by minor surface alterations; however,
:igue cracking of polycrystalline materials may be totally controlled
grain boundary events. The current research was undertaken to
ıcidate these points. This paper concerns a study of the effect of
ıminum ion implantation on the low cycle and high cycle fatigue
)perties of polycrystalline copper.

Experimental

Cold drawn polycrystalline rods, having 0.03 wt.% oxygen as the major
)urity were supplied by the Southwire Company, Carrollton, Georgia.
v and high cycle fatigue specimens were machined from the rods and
)sequently annealed for one hour in vacuum at 810°K, ground and hand
lished with billiard cloths impregnated with 0.3 μm alumina, and finally
:ctropolished in a nitric-methonal solution. The cylindrical low cycle
:igue samples had a gage section approximately 10 mm long by 3.8 mm
ımeter, and the hour-glass-shaped high cycle fatigue samples had a
ıimum diameter of 3.5 mm. Some specimens were sputter cleaned by
gon ions at 2.0 KV. Others were implanted with 100 KeV Al^+ ions to
dose of $5X10^{19}$ ions/m^2. To insure uniformity of implantation, the
:cimens were rotated in the beam which was scanned across an aperature
ıanning the gage length. Fatigue tests of Al^+ ion implanted and un-
)lanted samples were conducted on a servohydraulic closed-loop testing
:hine, in laboratory air, at 298°K. Low cycle fatigue measurements were
le using constant total strain control with a saw-tooth wave form at a
rain rate of $5X10^{-4}$/sec. Stress control, high cycle fatigue tests were
le using a frequency of 10 Hz. Optical and electron microscopy were
ed to characterize the deformation behavior.

Results

Stress/Strain Response: Al^+ ion implantation did not change the mono-
nic yield stress of polycrystalline copper. However, a small but
atistically significant difference between monotonic hardening in the
w strain range was observed with the ion-implanted material showing a
wer degree of hardening. The monotonic stress-strain curve can be
scribed mathematically by the Lüdwik relationship, $\sigma = \sigma_o + K \varepsilon_p^n$, where
is the yield stress, ε_p the plastic strain, n the strain hardening
ponent and K the stress increament at $\varepsilon_p = 1$. Figure 1, which is a

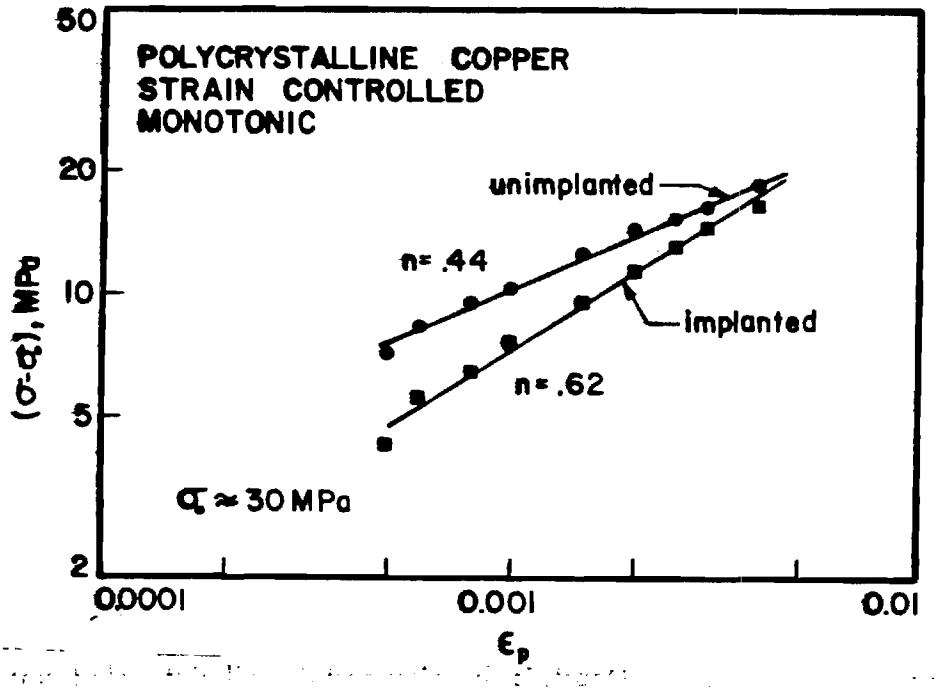

Figure 1. Monotonic stress-strain curves for Al-ion implanted and unimplanted polycrystalline copper

t of ln $(\sigma-\sigma_o)$ versus ln ε_p, illustrates the difference in monotonic dening behavior as a function of plastic strain.

Considerable cyclic hardening was observed for both implanted and mplanted samples at all strain amplitudes, Figure 2. "Waistometer-type dening" (2) was recorded subsequent to the saturation state. However, ce this is an effect of the testing procedure and not a material racteristic, this portion was deleted and replaced by dotted lines. h unimplanted and implanted copper showed cyclic hardening behavior ical of annealed fcc materials: initial rapid hardening followed by a uration stage. The relationship between cyclic stress and plastic strain be described mathematically by a power function similar to Lüdwik ationship, (3) i.e., $\sigma_a - \sigma_o = \sigma_k' (\Delta\varepsilon_p/2)^{n'}$, where σ_o is the stress for $/2 = 0$, σ_a is the stable stress amplitude, $\Delta\varepsilon p/2$ is the plastic strain litude, n' is the cyclic strain hardening exponent, and σ_k' is the cyclic ength coefficient. Figure 3, which is a plot of ln $(\sigma_a - \sigma_o)$ versus ln $p/2)$ shows that, analogous to the monotonic behavior, the implanted erial cyclically hardens less than the unimplated material.

Strain-Life Curves (LCF): Figure 4 compares the strain-life curves ffin-Manson plots) for the implanted and unimplanted polycrystalline per. Coffin (4) and Manson (5) independently proposed a relationship ween the plastic-strain amplitude and the cycles to failure of the form: $/2 = \varepsilon_f' (2N_f)^c$ where ε_f' is the fatigue-ductility coefficient, $2N_f$ is number of reversals to failure, and c is the fatigue ductility onent. Al^+ ion implantation significantly improves the cyclic ductility, noted by an increase in ε_f', but also increases the absolute value of cyclic ductility exponent.

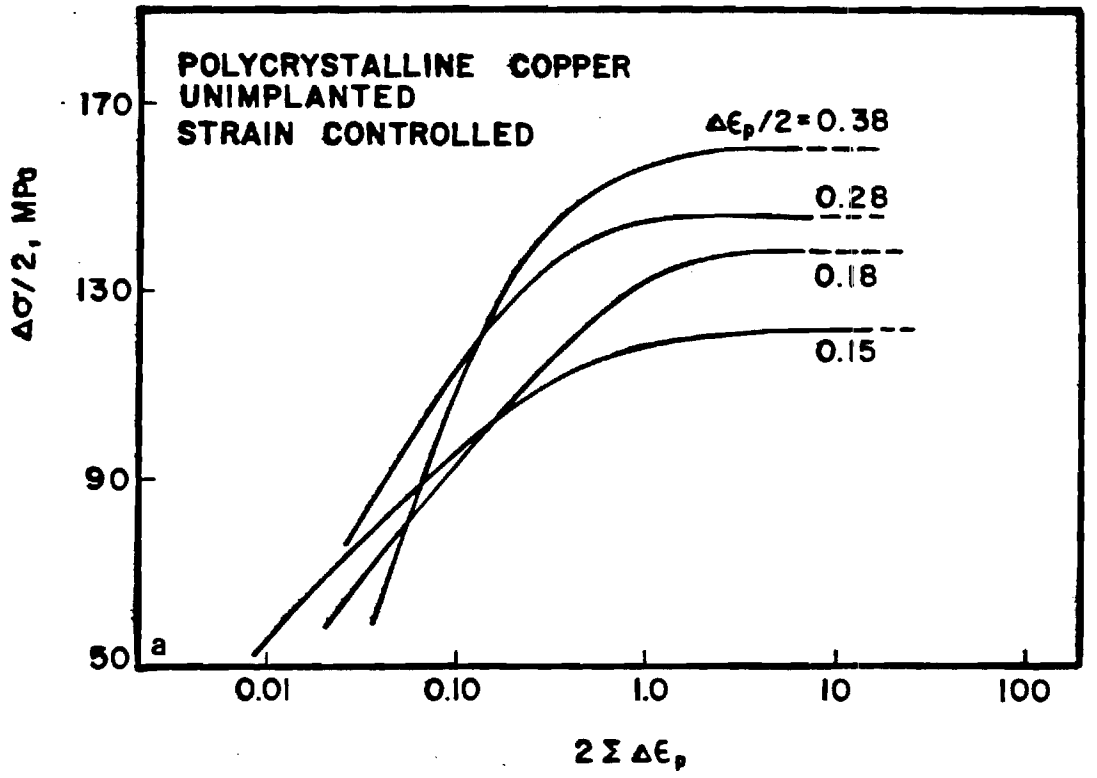

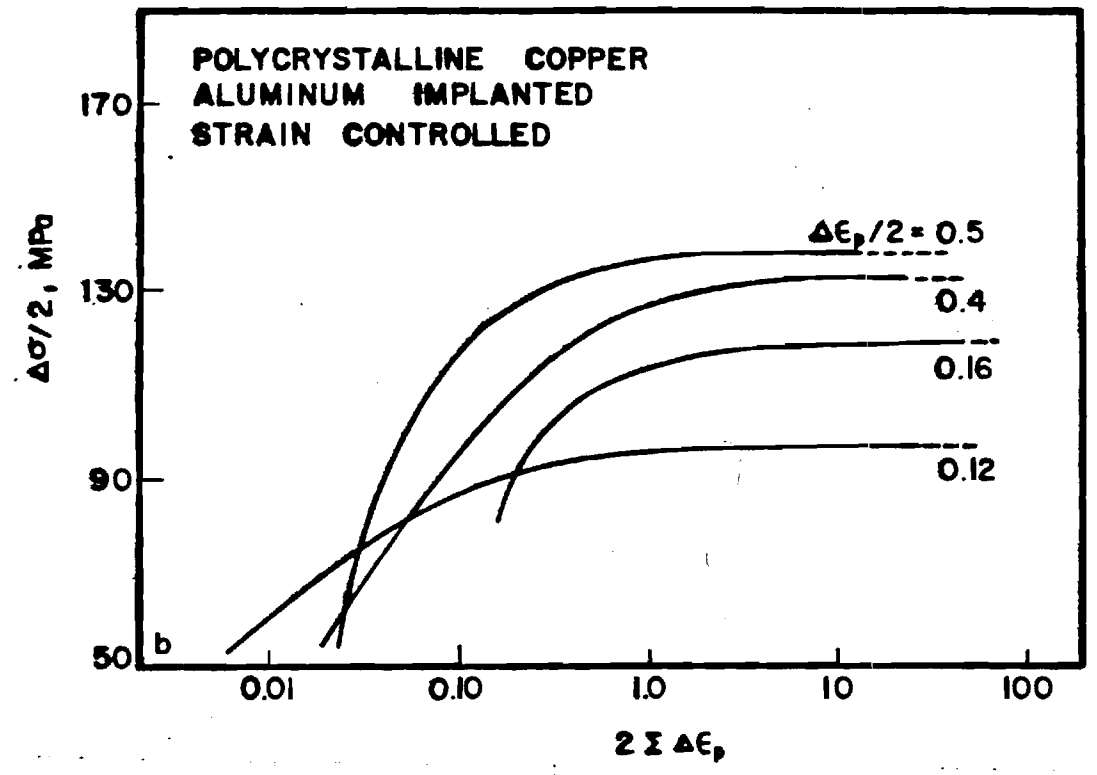

Figure 2. Cyclic-stress response curves obtained during strain controlled LCF testing.

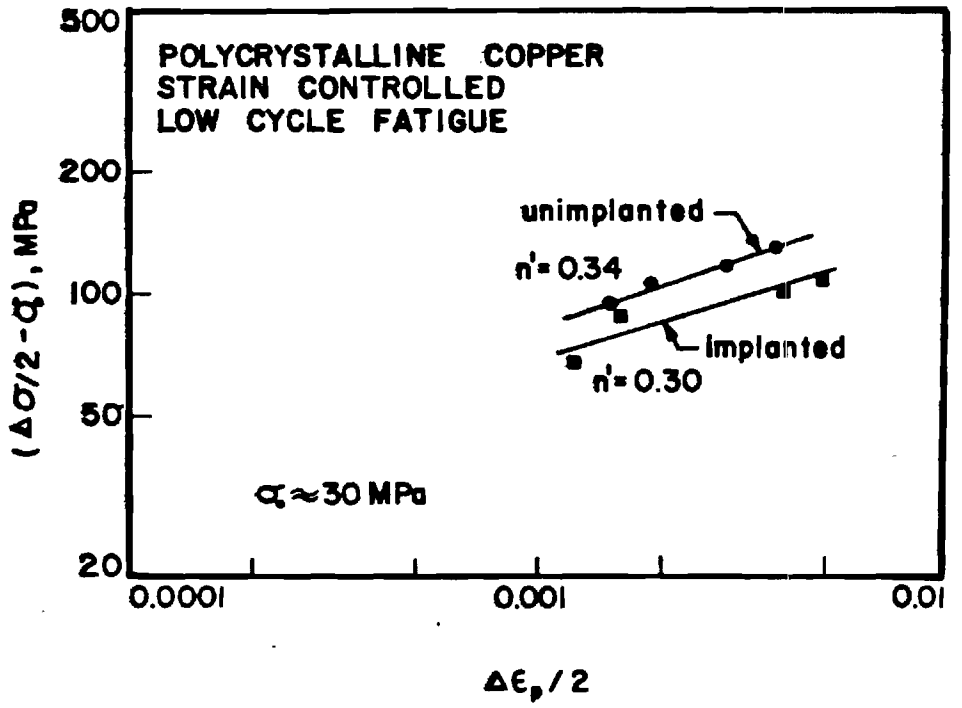

Figure 3. Cyclic-stress-strain curves for Al-ion implanted and unimplanted polycrystalline copper.

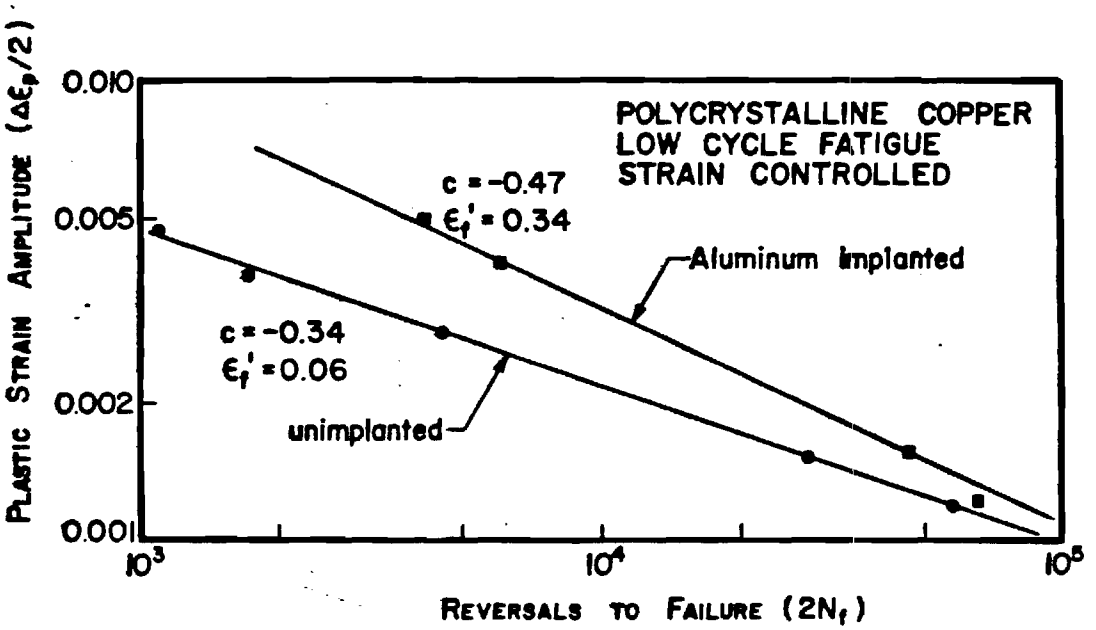

Figure 4. Strain-life curves for Al-ion implanted and unimplanted polycrystalline copper.

THE METALLURGICAL SOCIETY

DO NOT WRITE IN BOX

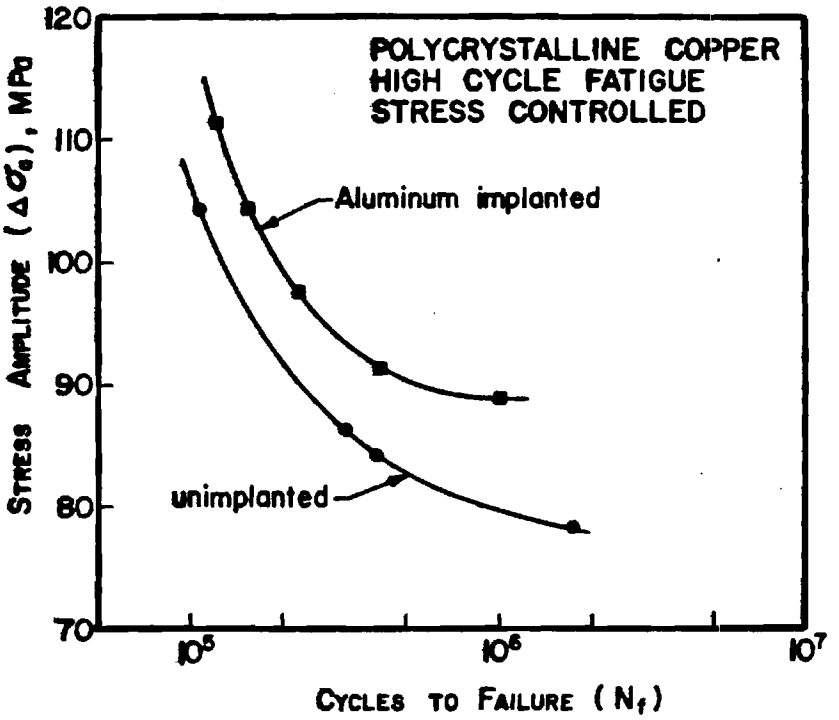

Figure 5. Stress-life curves for Al-ion implanted and unimplanted polycrystalline copper.

Stress-Life Curves (HCF): Figure 5 shows the effect of Al^+ ion lantation on the high cycle fatigue behavior of polycrystalline copper. nificant improvement in the high cycle fatigue life is observed, and improvement is greatest at the lower stresses.

Cyclic Surface-Deformation: Figure 6 compares the surface slip kings of Al^+ ion implanted and unimplanted LCF specimens. It appears t coarse persistent slip bands (PSB) with associated intrusion/ rusions form in both cases. However, the propensity of coarse PSB mation is higher for the unimplanted copper, and somewhat finer, more ogeneous slip appears to be favorable for the implanted material. This ults in more PSB cracking for the unimplanted copper, although extensive in boundary cracking is present in both materials. The grain boundary cking is associated with surface rumpling resulting from incompatibility coarse deformation in neighboring grains. The surface rumpling and ociated grain boundary cracking is more evident in the unimplanted per. Surface studies showed that microcrack link-up is also easier in unimplanted material due to the higher frequency of microcracks in grain interiors.

Figure 7 shows areas of intense slip markings on the high cycle fatigue ples. It appears that the propensity of PSB formation is quite high in surface grains having heavy deformation. Cracking associated with these 's is also evident. No distinction could be made between the surface markings of the two materials. Unlike the LCF surface analysis, face studies of the HCF samples were made after fatigue failure had urred. Because of life differences the implanted material had undergone onsiderably larger extent of fatigue cycling for the constant ess-amplitude tests.

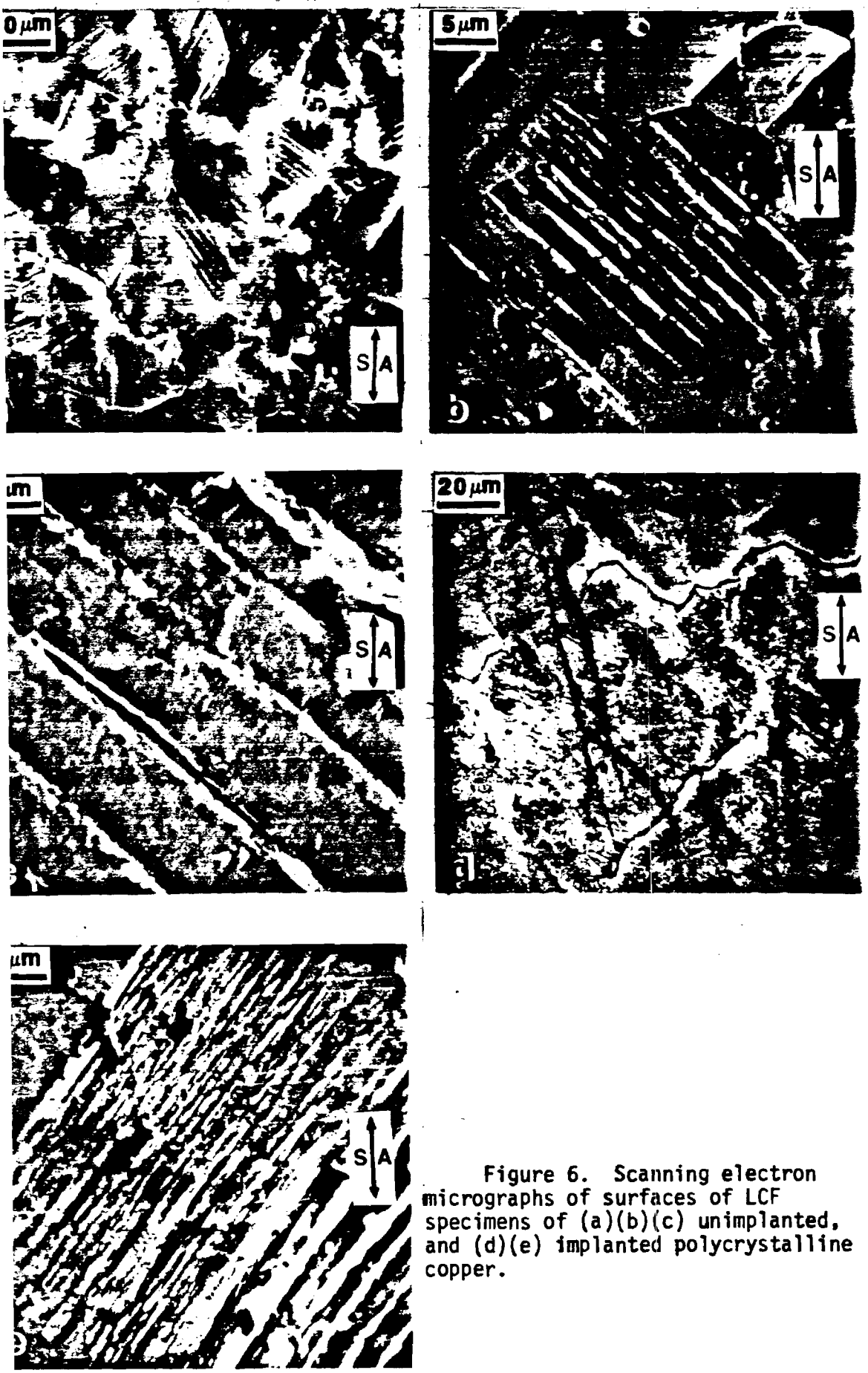

Figure 6. Scanning electron micrographs of surfaces of LCF specimens of (a)(b)(c) unimplanted, and (d)(e) implanted polycrystalline copper.

THE AMERICAN SOCIETY OF MECHANICAL ENGINEERS AIME

DO NOT WRITE IN BOX

THE METALLURGICAL SOCIETY AIME

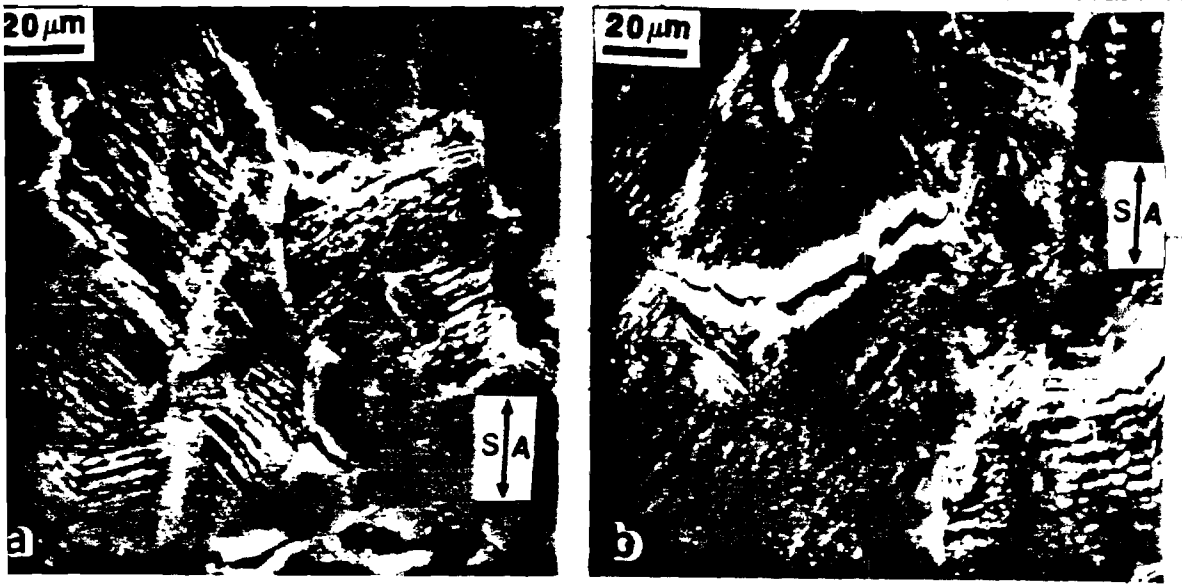

Figure 7. Scanning electron micrographs of surfaces of HCF specimens of (a) unimplanted and (b) implanted polycrystalline copper.

Discussion

The observations made here are results of our preliminary estigations. In depth studies are underway to elucidate some of the nts discussed here and will be presented in future publications.

X-ray diffuse measurements by Spooner and Legg (6) and theoretical siderations may be used to estimate the surface modification made by -implantation. In our case, the ion beam is broader than the diameter the fatigue specimens which are rotating cylinders. This is expected to duce an aluminum concentration profile with a peak of 0.7 wt. % at a th of 55 nm with a full width at half maximum of 85 nm as against 70 nm both parameters in normal incidence implantation (6) . The resulting age profile (6) is expected to be similar but may be slightly displaced h respect to the concentration profile. Sputter cleaning of the mplanted samples may have also created some damage in the surface layer. ever, since the helium ions used for this purpose were of very low rgy, it is assumed that damage was minimal. The sputter cleaning was e to keep the surface topography of the implanted and unimplanted cimens as similar as possible.

The aluminum concentration will lower the stacking fault energy of the face layer. The effect will be a reduction in the propensity of cross p. Normally, such a reduction reduces the work hardening rate at low ains since it decreases dislocation multiplication and dislocation-location interactions. However, for a monotonic test on implanted ples the effect will be small and only noticeable at very small strains ce here the plastic strain in the surface grains make up a significant tion of the total plastic strain of the sample. This explains the ference in flow stress at small strains and the convergence of flow ess with increasing strain as noted in Figure 1.

Since Al ions are larger than Cu ions residual compressive stresses l be generated in the damaged layer (with the corresponding residual sile stresses in the interior). This compressive residual stress will ose any applied tensile stress. In stress controlled fatigue this l reduce the effective tensile stress on the surface of the material and er the plastic strain at the surface. The reduction of SFE and

propensity of cross slip in the surface layer of the Al implanted samples also reduces the tendency of PSB formation, increases the reversibility of cyclic deformation, and reduces cyclic hardening (7). The sessile vacancy loops formed by the ion implantation (6) act as a barrier to slip and reduce slip distances which tends to homogenize slip in the surface region. The slip homogeneity will be further improved by the presence of dislocations which may be able to accommodate small cyclic slip without any generation of additional dislocations.

The implantation shows a tendency to change the surface deformation mode from coarse slip bands to more finer planar slip. This type of homogeneity of deformation should reduce the extent of cyclic deformation in each slip band. Since chances of slip reversibility improve with a decrease in cyclic plastic strain, the deformation at the surface of the implanted material should be more reversible. Consequently the implanted material should show less cyclic hardening than the unimplanted material, as observed in Figure 3.

Fatigue crack initiation in polycrystalline copper has been observed to occur along grain boundaries at high strains (8) and along PSB's at low strains (9, 10). In either case irreversibility of deformation of the surface region is what leads to the cracking. In our results we have seen that at moderate strains (regime of our LCF studies) both grain boundary and PSB cracks are present (Figure 6). However, the propensity of PSB crack formation is reduced for the ion implanted material. This is expected, since as discussed earlier, implantation should decrease the propensity of PSB formation. Our results also show that LCF fatigue life for implanted specimens is much improved. This again agrees with our interpretation. When deformation is made both more homogeneous and more reversible due to implantation the incompatibility of cyclic slip in neighboring grains is reduced and grain boundary offsets are reduced or it takes a larger number of cycles to form a grain boundary offet of the same size.

The slope of the Coffin-Manson plot (the cyclic ductility exponent) is larger for the implanted material. In other words the number of reversals to failure of the implanted and unimplanted materials appears to converge at lower strains. There are possibly two reasons for this. Firstly, the plot is logarithmic and even though there is a large difference between fatigue lives of the two materials at low strains the number of cycles appear closer in logarithmic scale. Secondly, when the imposed strain is low the deformation is more localized and this perhaps has a stronger control over fatigue life than the surface coating.

At the life range of $\sim 10^5$ the improvement in life due to implantation appears to be the same for both low cycle and high cycle fatigue samples. Since the difference in cyclic flow stress of the materials is small the slip homogeneity and reversibility effect in LCF should also be reflected in the HCF data. When the stress is further reduced, slip becomes completely reversible for the implanted material and a drastic improvement in life is observed. For the implanted material a reduction of surface deformation and an increase in deformation homogeneity and reversibility may have produced much better fatigue behavior in this range. As mentioned previously, the compressive residual stress on the surface of the implanted material will oppose the applied tensile stress and reduce the plastic stress at the surface. Consequently, the fatigue life for a given applied stress is longer for the copper that had been implanted with aluminum ions.

THE METALLURGICAL SOCIETY OF AIME

Author's name Kujore

No significant change in monotonic yield stress due to Al ion implantation on copper was measured. However, Al ion implantation results in a small decrease in monotonic hardening at low strains.

Al ion implanted polycrystalline copper shows significantly less fatigue hardening than unimplanted copper.

An improvement in low cycle and high cycle fatigue life is observed due to Al ion implantation on polycrystalline copper. The most significant improvement appears to be the higher fatigue limit for the implanted material.

References

E.Y. Chen and E.A. Starke, Jr., "Effects of Ion-Plating on the Low Cycle Fatigue Behavior of Copper Single Crystals", Materials Science and Engineering, 24 (1976) pp. 209-221.

Shirikant P. Bhat and Campbell Laird, "High Temperature Cyclic Deformation of Nickel", Fatigue of Engineering Materials and Structures, 1 (1979) pp. 59-77.

Edgar A. Starke, Jr. and Gerd Lütjering, "Cyclic Plastic Deformation and Microstructure", pp. 205-243 in Fatigue and Microstructure, M. Meshii, ed.; ASM, Metals Park, Ohio, 1978.

L.F. Coffin, "A Study of the Effects of Cyclic Thermal Stresses on a Ductile Metal", Transactions of the ASME, 76 (1954) pp. 931-950.

S.S. Manson, NACA, Technical Note 2933 (1954).

S. Spooner and K.O. Keith,"X-Ray Diffraction Characterization of Aluminum Ion Implanted Copper Crystals:, this Symposium.

M. Wilhelm and P. Everwin, "Cyclic Deformation Behaviour of α-Copper and Underaged Copper-Cobalt Alloy Single Crystal", paper presented at the 5th International Conference on the Strength of Metals and Alloys in Aachen, August, 1979.

C. Laird and D.J. Duquette, "Mechanisms of Fatigue Crack Nucleation", pp. 88-117 in Corrosion Fatigue, Chemistry Mechanisms and Microstructure, A.J. McEvily and R.W. Staehle, eds., NACE, Houston, Texas, 1972.

W.H. Kim and C. Laird, "Crack Nucleation and Stage I Propagation in High Strain Fatigue-I. Microscopic and Interferometric Observations", Acta Metallurgica, 26 (1978) pp. 77-787.

W.H. Kim and C. Laird, "Crack Nucleation and Stage I Propagation in High Stress Fatigue-II Mechanism", Acta Metallurgica, 26 (1978) pp. 789-799.

SECURITY CLASSIFICATION OF THIS PAGE *(When Data Entered)*

REPORT DOCUMENTATION PAGE		READ INSTRUCTIONS BEFORE COMPLETING FORM
1. REPORT NUMBER	2. GOVT ACCESSION NO.	3. RECIPIENT'S CATALOG NUMBER
4. TITLE *(and Subtitle)* The Effect of Ion Plating and Ion Implantation on the Cyclic Response and Fatigue Crack Initiation of Metals and Alloys		5. TYPE OF REPORT & PERIOD COVERED Technical Report 79-2 1 March 1979 - 29 Feb 1980 6. PERFORMING ORG. REPORT NUMBER
7. AUTHOR*(s)* S. B. Chakrabortty, S. Spooner, and E. A. Starke, Jr.		8. CONTRACT OR GRANT NUMBER*(s)* N00014-78-C-0270
9. PERFORMING ORGANIZATION NAME AND ADDRESS Fracture and Fatigue Research Laboratory Georgia Institute of Technology Atlanta, GA 30332		10. PROGRAM ELEMENT, PROJECT, TASK AREA & WORK UNIT NUMBERS
11. CONTROLLING OFFICE NAME AND ADDRESS Metallurgy Program, Material Sciences Div. Office of Naval Research 800 N. Quincy St., Arlington, VA 22217		12. REPORT DATE April 9, 1980 13. NUMBER OF PAGES 56
14. MONITORING AGENCY NAME & ADDRESS*(if different from Controlling Office)*		15. SECURITY CLASS. *(of this report)* Unclassified 15a. DECLASSIFICATION/DOWNGRADING SCHEDULE

16. DISTRIBUTION STATEMENT *(of this Report)*

unlimited

17. DISTRIBUTION STATEMENT *(of the abstract entered in Block 20, if different from Report)*

18. SUPPLEMENTARY NOTES

19. KEY WORDS *(Continue on reverse side if necessary and identify by block number)*

ion plating, ion implantation, fatigue

20. ABSTRACT *(Continue on reverse side if necessary and identify by block number)*

Fatigue crack initiation can be affected by surface phenomena and the possibility exists for improving the fatigue performance by altering the state of the surface without greatly changing bulk properties. This program was initiated on 1 March 1978, with the objective of determining the effect of ion implantation and ion plating on the cyclic stress-strain response and fatigue crack nucleation of a metal substrate. To meet this objective, we have selected surface film-substrate combinations designed to separate the various parameters, e.g., crystal structure, SFE, shear modulus, misfit, residual stress, etc., which

DD FORM 1 JAN 73 1473

SECURITY CLASSIFICATION OF THIS PAGE *(When Data Entered)*

INTERIM TECHNICAL REPORT

FOR THE PERIOD

1 MARCH 1980 - 28 FEBRUARY 1981

THE EFFECT OF ION PLATING AND ION IMPLANTATION ON THE CYCLIC RESPONSE AND FATIGUE CRACK INITIATION OF METALS AND ALLOYS

BY

S. B. CHAKRABORTTY AND E. A. STARKE, JR.
FRACTURE AND FATIGUE RESEARCH LABORATORY

RESEARCH REPORT
CONTRACT N00014-78-C-0270

PREPARED FOR
OFFICE OF NAVAL RESEARCH
DEPARTMENT OF THE NAVY

APPROVED FOR PUBLIC RELEASE:
DISTRIBUTION UNLIMITED

PERMISSION IS GRANTED THE U.S. GOVERNMENT
TO REPRODUCE THIS REPORT IN WHOLE OR IN PART.

GEORGIA INSTITUTE OF TECHNOLOGY
ATLANTA, GEORGIA 30332

ABSTRACT

The effect of ion implantation on the strain and stress controlled fatigue behavior of polycrystalline copper has been investigated. The cyclic stress-strain response, strain-life and stress-life relationships and fatigue crack nucleation behavior have been studied. The results from the non-implanted materials have been compared with those from the implanted materials. Four implant species, one with a positive misfit, one with a negative misfit, one with a zero misfit, and one insoluble under equilibrium conditions have been used. Most of the fatigue tests were performed in laboratory air. Ion implantation changes the surface deformation behavior for both monotonic and cyclic loading with a corresponding change in hardening rate. Larger changes are observed for the cyclic loading. Implantations which lead to a more homogeneous deformation (fine slip) near the surface, improves the resistance to fatigue crack initiation. Surface compressive residual stresses, induced from implanting a positive misfit species, have a major influence on crack initiation in the stress-life regime.

I. INTRODUCTION

Viable structural materials should have an optimum combination of properties like fabricability, strength, fracture toughness, corrosion and fatigue resistance. Often it is difficult to design an alloy which will satisfy the critical demand of its application with respect to all of these properties. Therefore, it will be advantageous to have a technique available which may improve some of the properties of a given alloy without any measurable loss in other properties. Surface treatment in general is such a technique and may lead to substantial improvement in surface sensitive properties like corrosion, wear, and fatigue crack initiation resistance.

Metallic coatings have been widely used in industry for controlling corrosion and erosion. However, some of the earlier techniques produced poor coatings (poor adherence and poor deposit structures) or sometimes altered the bulk properties. The more recent ion plating and ion implantation techniques produce an altered surface chemistry without a noticeable degradation in the bulk properties. Ion plating creates a clean strongly adherent interface and ion implantation usually does not create any well defined interface. Under this contract we are studying the effects of implantation and plating of various selected species on the fatigue behavior of some metals and alloys. As discussed below, results of our investigation show that significant changes can be made by ion implantation and plating.

II. CURRENT PROGRESS

X-Ray Diffraction Analysis of Implanted Copper Single Crystals

Some results of this aspect of our research have been published.[1,2] The main features of this type of analysis are summarized below.

The state of stress at the surface of the implanted crystal can be inferred from the lattice strain which in turn is measured by a shift in the Bragg angle.

Implantation not only modifies the lattice parameter by microalloying but can severely damage the surface with the production of point defects which can also shift the lattice parameter and give a large diffuse scattering. All these effects are confined to depths much less than a micron. Non-destructive methods of implantation characterization with x-rays must employ special approaches to obtain the structural information. X-rays would not normally be useful for analysis of implantation since the sampling depths is many times the depth of the implantation-affected volume. In order to avoid obscuring the scattering effects from the implanted layer, a perfect crystal substrate is used in a double-crystal diffraction arrangement. When a perfect crystal and an implanted crystal are arranged so that maximum intensity is obtained by the second reflection, the angular resolution in diffuse scattering measurements and peak shifts is measured in seconds of arc. In this way, both Bragg peak shifts and diffuse scattering from defects associated with the implanted layers can easily be measured.

The two principal sources of extra scattering from an implanted single crystal are (1) the scattering from the implanted layer whose Bragg angle is changed by alloying and (2) the scattering from point defect clusters (interstitial and vacancy loops). Analysis of the scattering attributed to lattice strain due to alloying has been done in several cases where point defect scattering was not present.[3] A modification of dynamical diffraction theory can be used to analyze x-ray scattering in terms of strain distribution to get a detailed description of alloy distribution.

The second source of scattering dominates the measured scattering in the implanted metals under investigation in this program. One result is that alloy distribution and strain effects are somewhat obscured. Nevertheless quantitative analysis of the damaged state of the implanted layer can be done. Scattering theory (kinematic) for scattering from dislocation loops and spherical precipitates

has been worked out.[4] Diffuse scattering measurements in a double-crystal experiment may be used to determine loop size distribution, to obtain the total point defects per volume, and to distinguish between vacancy and interstitial loops.

The results of the x-ray analysis on implanted copper single crystals show that aluminum implantation produces compressive residual stresses while boron implantation creates tensile residual stresses. Analysis of observed x-ray intensity also shows dislocation loop scattering. Aluminum implanted samples have a loop radius of approximately 25A while the loop radius for boron implanted samples is 80A.

The Effect of Ion Implantation on the Fatigue Behavior of Polycrystalline Copper

Results of this aspect of our investigation have been reported in some of our recent publications.[5-9] The most important features of our results are summarized below.

Four different species, aluminum, boron, chromium, and copper have been used to implant polycrystalline copper. It is expected that all four elements will introduce a similar defect structure, but of varying degrees of intensity. Also, boron atoms, because of their small size with respect to copper, introduce tensile residual surface stresses, and aluminum atoms, because of their larger size, introduce compressive stresses. Self-implanted copper should have little or no surface residual stresses. X-ray diffraction results[1,2,5] of aluminum and boron implanted copper single crystals have confirmed the predicted effect. Solute elements also effect the stacking fault energy, the propensity of cross slip, and thus the reversibility of deformation. Chromium, being insoluble in copper under equilibrium conditions may precipitate during cyclic loading of the Cr-implanted samples. The use of these four elements for implantation allows examination of the effects of residual stresses, the homogeneity and reversibility

of deformation, cyclic deformation, and fatigue crack initiation behavior of polycrystalline copper. Details of the experimental procedures have been described elsewhere.[6]

We attempted to measure the damage in the ion implanted surface region by comparing its back scattered electron channeling pattern[10] (ECP) with that of a non-implanted surface. As expected from the TEM results,[6] the ECP's show that the damage is most severe for the copper implanted surface; least severe for the boron implanted surface.[9] The aluminum implanted surface is intermediate between these two. We are now attempting to evaluate these figures to quantitatively assess the the degree of damage.

In addition to producing a defect structure and residual surface stresses, the alloying of the surface material is expected to lower the stacking fault energy (SFE) of this region. Of course no modification in SFE would result from self-implantation. It is likely that precipitation of chromium will occur in the chromium implanted samples during fatigue cycling. The effect of lowering the SFE will be lost at that stage and the presence of chromium has to be considered instead.

The implantation of Al, B, or Cr ions lowers the yield stress and the degree of monotonic and cyclic hardening. The reduction in yield stress and monotonic hardening at low strains is perhaps due to the availability of free dislocations on the surface which tends to promote slip at lower stresses. Aluminum implantation, which produces a larger degree of surface defects, consequently shows a larger reduction of monotonic flow stress.

The reduction of cyclic hardening may be explained in terms of the lowering of the SFE and the presence of dislocation loops and arrays due to ion-implantation. Lowering the SFE leads to a reduction in the tendency for cross slip. This improves the reversibility of cyclic deformation and reduces cyclic hardening.

Dislocation loops are barriers to slip and tend to homogenize deformation by reducing the slip distance. Improved homogeneity of slip due to implantation aids in reducing the resistance to cyclic deformation. Aluminum implanted samples have a higher degree of surface defects, the greatest reduction in hardening, and therefore the lowest cyclic flow stresses. The chromium implanted samples have a similar defect structure. However, it appears that chromium precipitation during cycling increases cyclic hardening somewhat by tying up slip dislocations.

Since fatigue damage is caused by cyclic plastic strain, the fatigue life should be related to the plastic strain amplitude. Consequently, many recent studies have relied on strain-controlled low cycle fatigue (LCF) of smooth samples. Since the strain amplitude of these tests exceeds the macroscopic elastic limit, the effect of surface residual stresses is minimal. The data are normally presented as strain-life curves, where the log of the plastic strain amplitude is plotted versus the log of the reversals to failure. The strain-life results of this study will be discussed with respect to the microstructural and deformation behavior described in the previous paragraphs.

The strain-life relationships for the nonimplanted and implanted polycrystalline copper are presented in Figure 1. The defect structure produced by ion implantation improves the homogeneity of deformation, and in general this leads to improvement in the low cycle fatigue life, regardless of the exact mechanism of cracking. Fatigue crack initiation in polycrystalline copper has been previously shown to occur along surface grain boundaries at high strains[11,12] and along PSB's[13,14] emerging on the surface at low strains. Our results are consistent with these observations. However, for our studies both types of cracking are observed because of the intermediate strain range used. Microcrack formation by either mechanism becomes more difficult when the slip is more reversible and more homogeneous. The difference between the FCI resistance of

boron and aluminum implanted samples is again due to the difference in defect structure. Aluminum implantation produces the most significant effect because it gives rise to a more severe defect structure. Even though chromium implantation results in a defect structure similar to aluminum, the expected intervention of chromium precipitation decreases the resistance to FCI under what is expected from its defect structure.

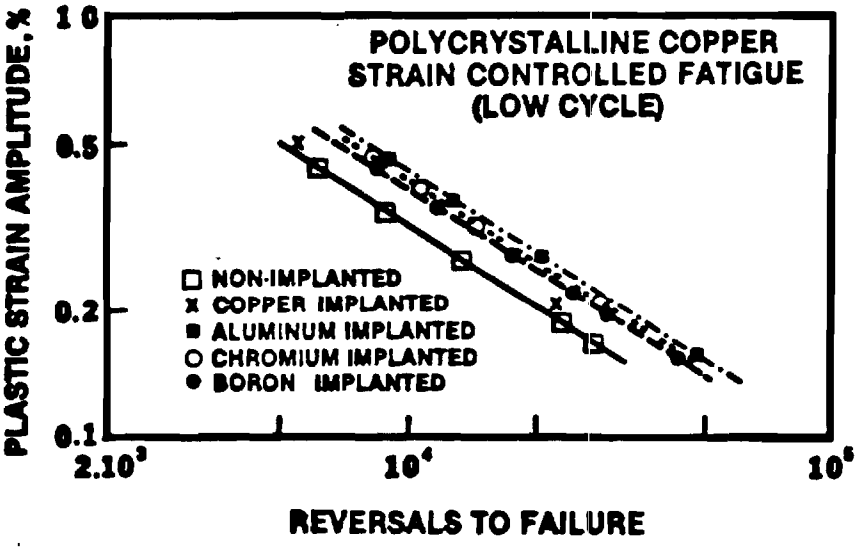

Figure 1. The effect of ion implantation on the cyclic strain-life behavior of polycrystalline copper.

Since residual stresses have a minimal effect on strain-life results, the primary feature to be considered here is the deformation behavior of the near surface region. The defect structure increases the homogeneity of deformation and the surface alloying lowers the SFE and thus increases the reversibility of deformation. In order to isolate the effect of damage only, we are now conducting some tests on self-implanted copper. The preliminary results, Figure 1, indicate that self-implantation has a limited beneficial effect on strain-life response even though it shows the largest extent of damage. It seems that for the conditions and materials used in this study, reversibility, as controlled by surface alloying and SFE modification, is more important than a severely damaged surface layer.

Under stress control the ion implanted samples are expected to show improvement in fatigue life due to better slip homogeneity and reversibility. However, since the stress amplitudes used are lower than the macroscopic yield strength, surface residual stresses may also play an important role in determining the fatigue life. The residual stresses may control the flow stress, and therefore the plastic strain of the surface region. The magnitude and distribution of plastic strain controls the fatigue crack initiation behavior.

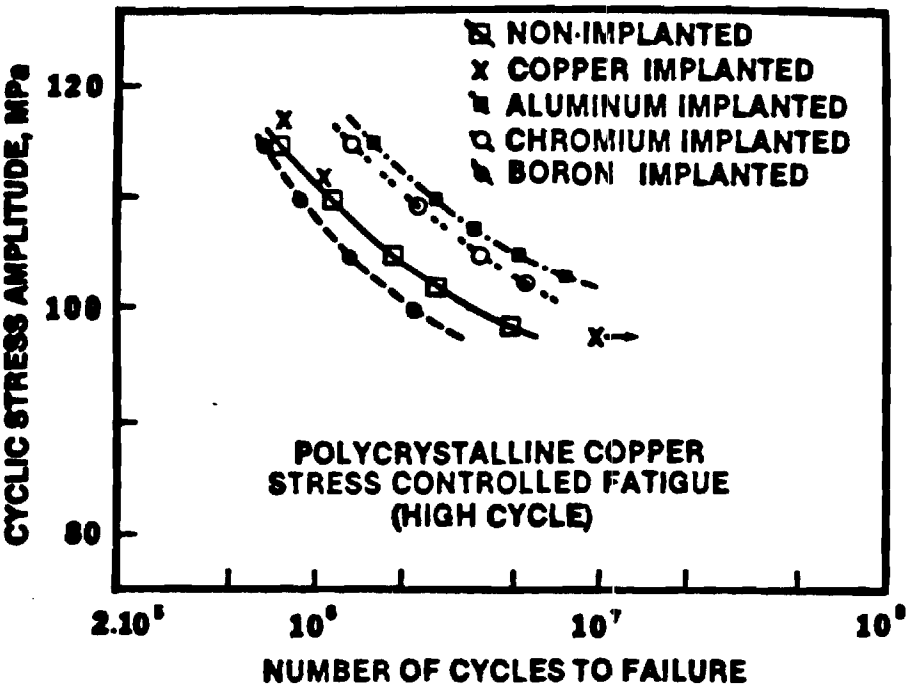

Figure 2. The effect of ion implantation on the cyclic stress-life behavior of polycrystalline copper.

Aluminum implanted samples have a beneficial compressive surface stress. The compressive stress tends to reduce the more damaging (i.e., tensile) component of the cyclic stress and hence improves the fatigue life, Figure 2. The tensile residual surface stress produced by boron implantation decreases the resistance to stress cycling. The beneficial effects of surface defects due to implantation are overcompensated by the detrimental effects of the residual tensile surface stresses, Figure 2. Our preliminary results show

that self-implantation, although producing a more severe defect, modifies the stress-life less than either aluminum or chromium implantation, Figure 2. Consequently, surface residual stresses appear to have the dominant effect on the fatigue life for the experimental conditions used here.

The results of this study have shown that ion implantation can have beneficial effects on the fatigue life of materials. For an exact determination of the influence of a particular implanted species, it is necessary to characterize the defect structure and surface residual stresses produced. We have shown that tests under both strain and stress control are necessary in order to separate metallurgical effects from residual stress effects.

The Effect of Ion Plating on Fatigue Properties of Copper

In this part of our investigation copper was ion plated with silver and nickel. These plating species were chosen because they have substantially different stacking fault energies compared to the copper substrate. It may be expected that a low SFE coating (e.g., Ag) will improve slip reversibility and may lead to an improvement of FCI resistance of the substrate metal (i.e., copper).

Our results show that ion plating of both silver and nickel reduces yield stress and the degree of monotonic and cyclic hardening. Ion plating also appears to increase fatigue life under both strain and stress control. We have observed that silver plating improves the homogeneity and reversibility of cyclic deformation and thereby improves the FCI resistance. This has been attributed to the lower SFE of the silver coating.[15] We have observed that nickel plating reduces the degree of cyclic deformation on the surface. This apparently has an offsetting effect on the expected reduction in homogeneity and reversibility of slip due to high SFE of the nickel coating. Therefore, a slight improvement in FCI results.

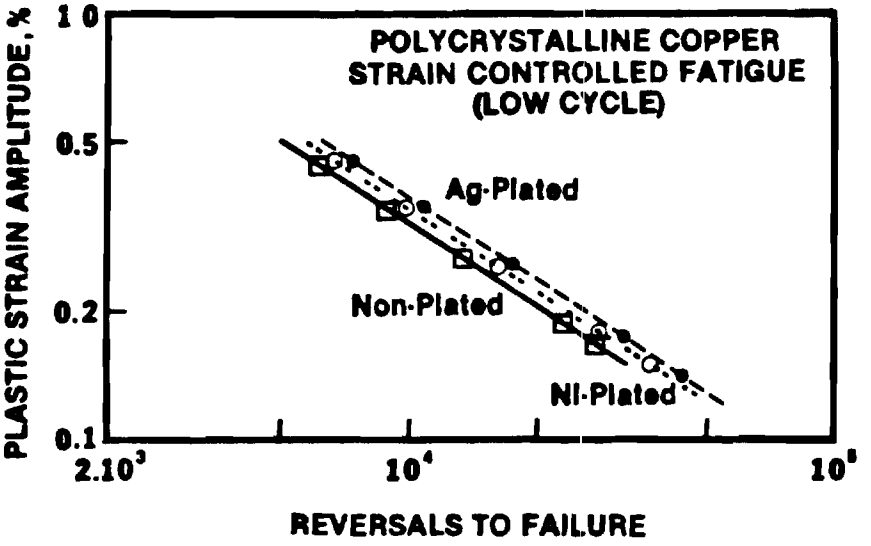

Figure 3a. The effect of ion plating on the cyclic stress-life response of polycrystalline copper

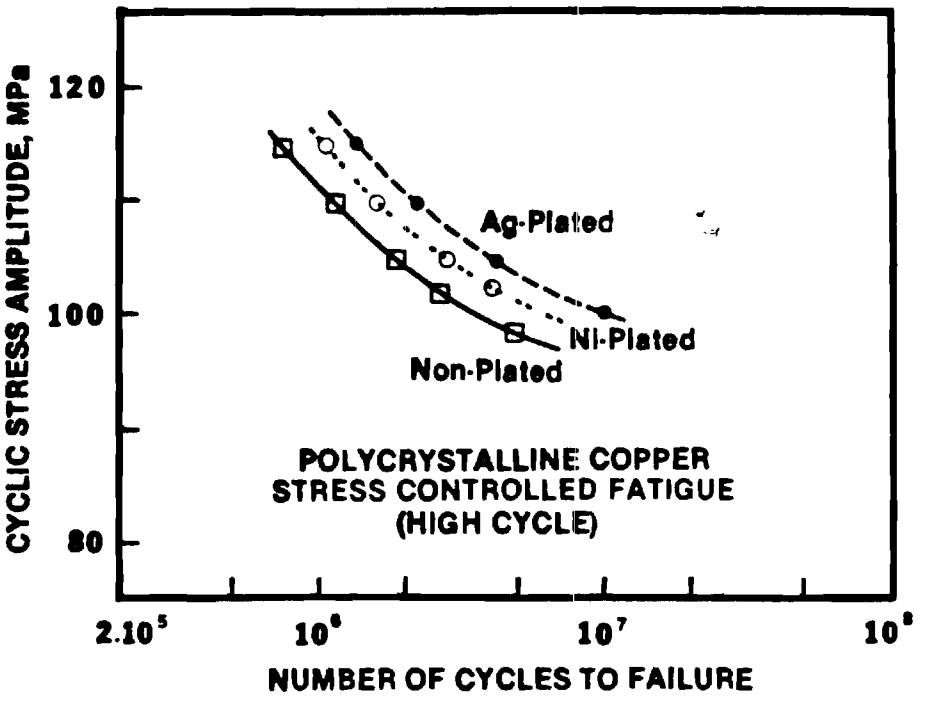

Figure 3b. The effect of ion plating on the cyclic stress-life response of polycrystalline copper.

III. CONCLUSIONS

The results of this study have shown that ion implantation can have beneficial effects on the fatigue life of materials. For an exact determination of the influence of a particular implanted species, it is necessary to characterize the defect structure and surface residual stresses produced. We have shown that tests under both strain and stress control are necessary in order to separate metallurgical effects from residual effects.

REFERENCES

1. S. Spooner and K. O. Legg, in Ion Implantation Metallurgy, ed. C. M. Preece and J. K. Hirvonen, TMS-AIME, New York, 1980.

2. S. Spooner, "X-Ray Scattering Investigation of Microalloying and Defect Structure in Ion Implanted Copper," presented at the AIME Symposium on Advanced Techniques for the Characterization of Microstructures, Las Vegas, Nevada, February 1980. To be published in the Proceedings of the Symposium.

3. B. C. Larson, C. W. White and B. R. Appleton, "Unidirectional Contraction in Boron-Implanted Laser Annealed Silicon," Appl. Phys. Lett., 32, pp. 801-803 (1978).

4. B. C. Larson and W. Schmatz, "Huang Diffuse Scattering from Dislocation Loops and Cobalt Precipitates in Copper," Phys. Rev. B 10(b), pp. 2307-2314 (1974).

5. S. B. Chakrabortty, S. Spooner, and E. A. Starke, Jr., "The Effect of Ion Plating and Ion Implantation on the Cyclic Response and Fatigue Crack Initiation of Metals and Alloys," Technical Report 79-2, Office of Naval Research, Contract No. N00014-78-C-0270, April 1980.

6. A. Kujore, S. B. Chakrabortty, E. A. Starke, Jr. and K. O. Legg, "The Effect of Ion Implantation on the Fatigue Properties of Polycrystalline Copper," presented at the Conference on Ion Beam Modification of Materials, Albany, New York, July 1980. To be published in Proceedings of the Symposium.

7. A. Kujore, S. B. Chakrabortty, and E. A. Starke, Jr., in Ion Implantation Metallurgy, eds., C. M. Preece and J. K. Hirvonen, TMS-AIME, New York, 1980.

8. S. B. Chakrabortty, A. Kujore and E. A. Starke, Jr., "The Effect of Ion Implantation on Cyclic Stress-Stress Response of Polycrystalline Copper," Thin Solid Films, 73, (1980).

9. S. G. Chakrabortty, A. Kujore, E. A. Starke, Jr. and K. O. Legg, "The Effect of Ion Implantation on the Fatigue Behavior of Metals and Alloys," Trans. on Nuclear Sci., 28, 1812 (1981).

10. D. C. Joy, Quantitative Scanning Electron Microscopy," ed. D. B. Holt, Academic Press, London, p. 131 (1974).

11. W. H. Kim and C. Laird, Acta Met., 26, 777 (1978).

12. W. H. Kim and C. Laird, Acta Met., 26, 789 (1978).

13. M. L. Eben and W. A. Backofen, Trans. AIME, 215, 510 (1959).

14. C. Laird and D. J. Duquette, in Corrosion Fatigue: Chemistry, Mechanisms and Microstructure, eds. A. J. McEvily and R. W. Staehle, NACE, Houston (1972).

15. E. Y. Chen and E. A. Starke, Jr., "The Effects of Ion-Plating on the Low Cycle Fatigue Behavior of Copper Single Crystals," Materials Science and Engineering, 24, 209 (1976).

UNCLASSIFIED

SECURITY CLASSIFICATION OF THIS PAGE (When Data Entered)

REPORT DOCUMENTATION PAGE		READ INSTRUCTIONS BEFORE COMPLETING FORM
1. REPORT NUMBER	2. GOVT ACCESSION NO.	3. RECIPIENT'S CATALOG NUMBER
4. TITLE (and Subtitle) THE EFFECT OF ION IMPLANTATION ON THE FATIGUE PROPERTIES OF POLYCRYSTALLINE COPPER		5. TYPE OF REPORT & PERIOD COVERED Progress Report Feb 81 - Jun 81 6. PERFORMING ORG. REPORT NUMBER
7. AUTHOR(s) A. Kujore, S. B. Chakrabortty, E. A. Starke, Jr.		8. CONTRACT OR GRANT NUMBER(s) N00014-78-C-0270
9. PERFORMING ORGANIZATION NAME AND ADDRESS Fracture and Fatigue Research Laboratory School of Chemical Engineering Georgia Institute of Technology, Atlanta, GA 30332		10. PROGRAM ELEMENT, PROJECT, TASK AREA & WORK UNIT NUMBERS
11. CONTROLLING OFFICE NAME AND ADDRESS Office of Naval Research Department of the Navy, Arlington, VA 22217		12. REPORT DATE July 15, 1981 13. NUMBER OF PAGES 10
14. MONITORING AGENCY NAME & ADDRESS (if different from Controlling Office)		15. SECURITY CLASS. (of this report) Unclassified 15a. DECLASSIFICATION/DOWNGRADING SCHEDULE
16. DISTRIBUTION STATEMENT (of this Report) Unlimited		
17. DISTRIBUTION STATEMENT (of the abstract entered in Block 20, if different from Report)		
18. SUPPLEMENTARY NOTES		
19. KEY WORDS (Continue on reverse side if necessary and identify by block number) Ion plating, ion implantation, fatigue		

20. ABSTRACT (Continue on reverse side if necessary and identify by block number)

The effect of ion implantation (aluminum, boron, chromium) on the tensile and strain or stress controlled fatigue behavior of polycrystalline copper has been studied. The monotonic and cyclic stress-strain relationships, cyclic strain-life and stress-life relationships, cyclic deformation characteristics and crack nucleation behavior of implanted copper are compared with unimplanted copper.

Monotonic and cyclic flow stress are reduced by ion implantation. Life controlled fatigue is improved by ion implantation.

implantation has the greatest effect on both flow-stress reduction and life improvement. Life under stress controlled fatigue may or may not be improved by implantation. Aluminum and chromium implantation produces a significant improvement whereas boron implantation causes a reduction in the resistance to stress cycling.

Nuclear Instruments and Methods 182/183 (1981) 949–958
North-Holland Publishing Company

THE EFFECT OF ION IMPLANTATION ON THE FATIGUE PROPERTIES OF POLYCRYSTALLINE COPPER

A. KUJORE, S.B. CHAKRABORTTY, E.A. STARKE, Jr.
Fracture and Fatigue Research Laboratory, Georgia Institute of Technology, Atlanta, GA 30332, U.S.A.

and

K.O. LEGG
Department of Physics, Georgia Institute of Technology, Atlanta, GA 30332, U.S.A.

The effect of ion implantation (aluminum, boron or chromium) on the tensile and strain or stress controlled fatigue behavior of polycrystalline copper has been studied. The monotonic and cyclic stress–strain relationships, cyclic strain–life and stress–life relationships, cyclic deformation characteristics and crack nucleation behavior of implanted copper are compared with unimplanted copper.

Monotonic and cyclic flow stresses are reduced by ion implantation. Life under strain controlled fatigue is improved by ion implantation. Aluminum implantation has the greatest effect on both flow-stress reduction and life improvement. Life under stress controlled fatigue may or may not be improved by implantation. Aluminum and chromium implantation produces a significant improvement whereas boron implantation causes a reduction in the resistance to stress cycling.

1. Introduction

The fatigue process may be divided into two stages, which are crack initiation and crack propagation. For a defect-free metal, the process of initiation and early crack growth is usually associated with the cyclic deformation behavior of the surface layer. This process is found to occur in conjunction with slip band formation [1,2] in the surface region, or with the incompatibility of deformation between two neighboring grains on the surface [3,4]. Any surface modification which reduces the magnitude or increases the homogeneity and reversibility of cyclic deformation is expected to improve the fatigue crack initiation resistance. It is well known that manufacturing processes, e.g., shot-peening, which produce surface compressive residual stresses have a substantial effect on stress controlled fatigue resistance. However, it has been shown recently that subtle modifications of the surface may also produce large changes in fatigue behavior [5–10].

Chen and Starke [5] have shown that ion plating can have a major effect of the fatigue behavior of copper single crystals. When they plated silver (low stacking fault energy, SFE) on copper, the cyclic deformation behavior of the surface changed toward that of silver. Crack initiation was retarded because of a reduction in the propensity of cross slip compared with the copper substrate and subsequent reduction in slip band formation. Nickel (high SFE) plating had an opposite effect. More recently it has been shown that ion implantation of various species on many metal substrates leads to some spectacular changes in fatigue properties [6–10]. However, a clear understanding of the mechanism for such changes is lacking. The purpose of this work is to study the change in monotonic and cyclic deformation behavior of copper implanted with 3 different species–aluminum, boron and chromium–and to correlate measured mechanical properties with the deformation behavior as modified by ion implantation.

The results obtained here are quantitatively similar to those reported in our prior publications [6,9]. However, previously we used polycrystalline copper samples which had variations in grain size and oxygen content. In the present work, all implanted and non-implanted specimens were made from identical polycrystalline copper material. Therefore direct comparison between the effect of various implanted species is possible. It is expected that all three elements will introduce a similar defect structure but of varying degrees of intensity. Also, boron atoms,

0029-554x/81/0000–0000/$02.50 © North-Holland

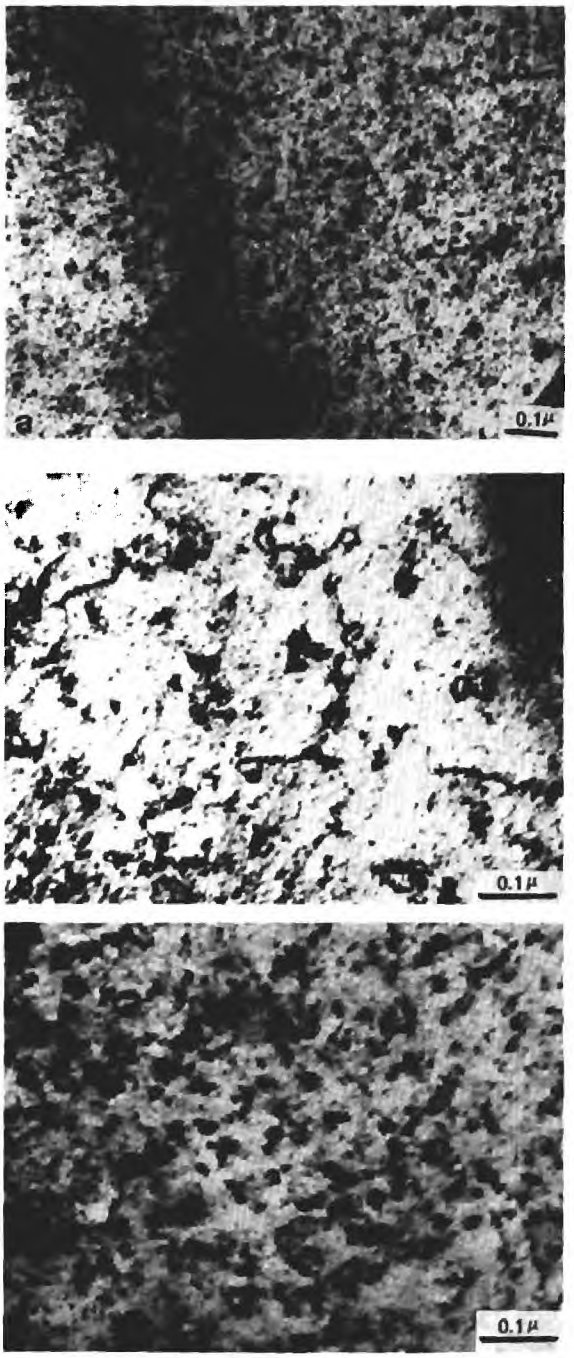

Fig. 2. Transmission electron micrograph of ion implanted surface layers. (a) aluminum implanted, (b) boron implanted, (c) chomium implanted.

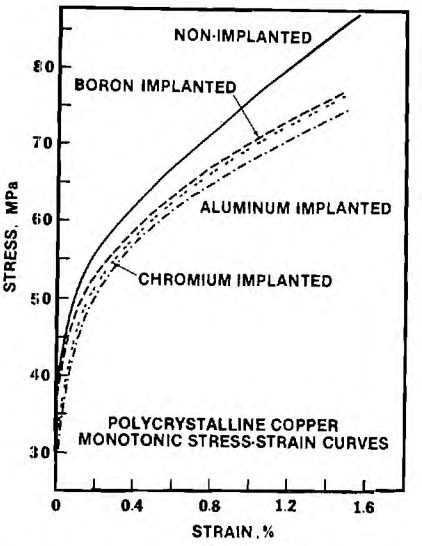

Fig. 3. The effect of ion implantation on monotonic stress–strain curve of polycrystalline copper.

larger effect. Our previous results [6] did not show changes in σ_0 beyond the experimental scatter band. The results given here are from more careful experimentation using microstructurally controlled specimens. Monotonic stress–strain behaviour in all cases (table 1 and fig. 3) was reproduced within ±0.5 MPa using a second set of specimens.

3.3. Cyclic stress–strain response

All materials show considerable cyclic hardening typical of annealed copper (fig. 4). An initial rapid hardening is followed by a saturation stage. The saturation stress versus applied plastic strain amplitude for nonimplanted and implanted metals are plotted in fig. 5. The cyclic flow stress appears to be lowered by ion implantation. Aluminum implantation shows the most significant effect. The relationship between the saturation stress amplitude and the plastic strain amplitude can be described by a function similar to the Lüdwick relationship [13] given by $\sigma_a - \sigma_0' = k'(\epsilon_{pa})^{n'}$, where σ_a is the saturation stress amplitude, ϵ_{pa} is the plastic strain amplitude, σ_0' is the value of σ_a at $\epsilon_{pa} = 0$, k' is the cyclic strength coefficient, and n' is the cyclic strain hardening exponent. The measured values for the cyclic strength coefficient and cyclic strain hardening exponent are given in table 1. Experimental measurement of σ_0' was not made, and it is assumed to be equal to the σ_0 value given in table 1. This should be a good approximation for copper.

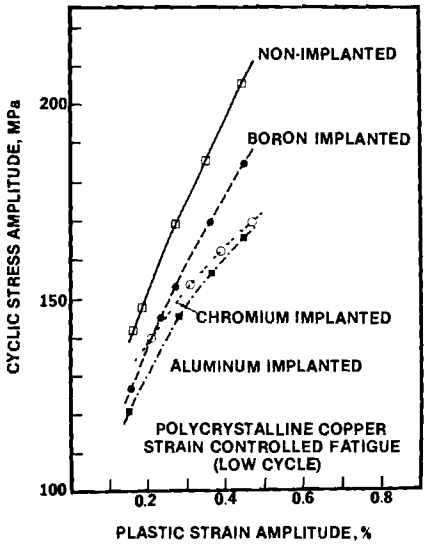

Fig. 5. The effect of ion implantation on cyclic stress–strain relationship of polycrystalline copper.

with a greater improvement at lower stresses. Boron implantation, in contrast, shows a reduction in resistance to cyclic stress, with a greater reduction in life at lower stresses. The limited data on chromium implantation appears to indicate that it improves the cyclic stress resistance almost as well as aluminum implantation.

3.6. Surface observations

Fig. 9 shows scanning electron micrographs of the surfaces of non-implanted and implanted copper after strain controlled fatigue deformation. All micrographs show the presence of persistent slip bands

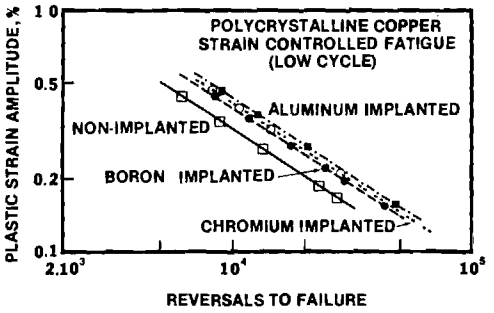

Fig. 6. The effect of ion implantation on cyclic strain–life relationship of polycrystalline copper.

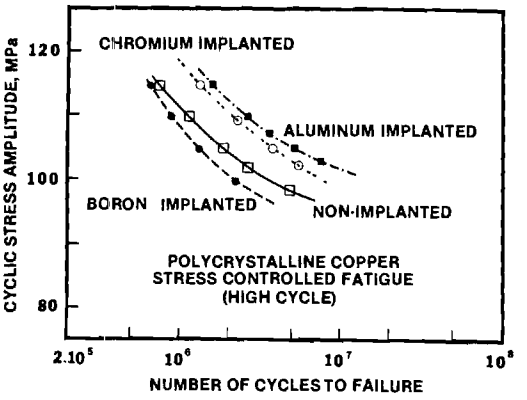

Fig. 7. The effect of ion implantation on cyclic stress–life relationship of polycrystalline copper.

(PSB) and associated intrusions/extrusions. However the propensity of PSB formation appears to be reduced by ion implantation. Aluminum implantation has the most significant effect. Most of the microcracks are at the grain boundaries. Some cracks associated with PSB are also observed, being more frequent for the non-implanted samples and least for the aluminum inplanted samples. Implanted samples show a lower degree of surface rumpling and fewer surface microcracks compared with nonimplanted samples deformed to the same degree. Aluminum implantation appears to have the most significant effect. Transmission electron micrographs (fig. 9) of the saturated surface substructure at $\epsilon_{pa} = 0.3\%$ of aluminum implanted and non-implanted samples show that cell formation occurs for both.

Scanning electron micrographs of the surfaces of nonimplanted and implanted copper after stress controlled fatigue deformation are given in fig. 10. Cracking associated with PSB is more evident than that observed for strain controlled tests (compare with fig. 8). Aluminum implanted samples show the smallest overall fatigue damage. All samples were observed after cycling to failure at the same stress amplitude. Considering the cycles required for failure for the various implanted samples, fig. 10 shows that the life is related to the resistance to microcrack formation.

4. Discussion

The following represents our present understanding of the effect of ion implantation on fatigue behavior of metals. The research is by no means com-

Fig. 9. Transmission electron micrograph of polycrystalline copper deformed at $\epsilon_{pa} = 0.1$. (a) nonimplanted, (b) aluminum implanted.

plete, and studies are being continued to verify some of the conjectures made here.

4.1. Modification by ion implantation

Since the mechanical behavior of ion implanted samples is dependent on the modification of the surfaces, we shall briefly discuss these modifications. The concentration profile for aluminum, boron and chromium ion implantation may be estimated from data available in the literature [16]. The results for such calculations for our samples are given in table 2. The resultant defect profile is expected to be similar but somewhat displaced. Our TEM results and the X-ray analysis by Spooner and co-workers [11,12] indicate that aluminum implantation gives rise to compressive residual surface stresses, a large number of small dislocation loops, and arrays of dislocations. Boron implantation, on the other hand, produces tensile residual stresses [11,12], a smaller number of larger loops, and dislocation arrays. X-ray data on the effect of chromium implantation is not yet available. However, TEM results seem to indicate that the defect structure is very similar to that of the aluminum implanted material. Since the size of the chromium atom is not much different from that of copper, it may be assumed that chromium implantation does not produce any significant residual surface stresses. If the increase in the numbers of atoms by ion implantation forces implant or host atoms into the interstitial sites, creation of compressive residual stresses will be expected. However, with some diffusion (probably enhanced by radiation damage) these form an extra atom layer occupying substitutional sites (such a mechanism is reasonable since TEM studies show that there is sufficient diffusion to create dislocation loops from the initial radiation damage). Therefore, significant compressive stress will not be created due to interstitials. This may explain why boron implanted copper has tensile residual stresses [11,12]. Perhaps most of the boron atoms are in substitutional sites, and since they are considerably smaller than the copper atoms, tensile residual stresses are created.

TEM contrast studies of some of the loops indicate that most are the result of a collapse of clusters of vacancies created by ion bombardment. It appears that since heavier (and larger) Cr and Al atoms have a more efficient transfer of energy than B atoms, the defect structure of Cr and Al implanted surfaces has greater density. Since the foils used for TEM observations are thicker than the damaged layer (which decreases with atomic number), the concentration of defects is actually even higher for Cr and Al implanted samples than it appears in the micrographs. In addition to the defect structure and residual surface stresses, the alloying of the surface material is expected to lower the stacking fault energy (SFE) of this region. It is likely that precipitation of chromium will occur in the chromium implanted samples during fatigue cycling. The effect of lowering SFE will be lost at that stage, and the presence of chromium precipitates has to be considered instead.

4.2. Monotonic and cyclic stress–strain response

The implantation of Al, B, or Cr ions lowers the yield stress and the degree of monotonic and cyclic hardening. The reduction in yield stress and monotonic hardening at low strains is perhaps due to the

flow stresses. The chromium implanted samples have a similar defect structure. However, it appears that Cr precipitation during cycling increases cyclic hardening somewhat by tying up slip dislocations.

4.3. Fatigue crack initiation (FCI)

Under strain controlled fatigue the microcrack formation and eventual failure of the materials follow what is expected from the foregoing discussion of the cyclic hardening behavior. The effect of ion implantation is to improve slip reversibility and homogeneity, and in general this leads to improvement in the low cycle fatigue life, regardless of the exact mechanism of cracking. Fatigue crack initiation in polycrystalline copper has been previously shown to occur along surface grain boundaries at high strains [3,4] and along PSB's emerging on the surface at low strains. Our results are consistent with these observations. However, for our studies both types of cracking are observed because of the intermediate strain range used. Microcrack formation by either mechanism becomes more difficult when the slip is more reversible and more homogeneous. The difference between the FCI resistance of boron and aluminum implanted samples is again due to the difference in defect structure. Aluminum implantation produces the most significant effect because it gives rise to a more intense defect structure. Even though chromium implantation results in a defect structure similar to aluminum, the expected intervention of chromium precipitation decreases the resistance to FCI under what is expected from its defect structure.

Under stress control the ion implanted samples are expected to show improvement in fatigue life due to better slip homogeneity and reversibility. However, other parameters must be considered. Aluminum implanted samples have beneficial compressive surface stress. The compressive stress tends to reduce the more damaging (i.e., tensile) component of the cyclic stress and hence improves the fatigue life. The tensile residual surface stress produced by boron implantation decreases the resistance to stress cycling. The beneficial effects of surface defects due to implantation are overcompensated by the detrimental effects of the residual tensile surface stresses. Chromium implanted samples show fatigue lives similar to aluminum implanted samples, even though beneficial surface residual stresses are not expected. Chromium precipitation may lead to a reduction of cyclic slip at a given stress amplitude and slow down the process of fatigue crack initiation.

We have observed significant changes in monotonic and cyclic flow stresses, and fatigue lives from small alterations of the surface of polycrystalline copper. Most of the trends observed here are at least qualitatively accurate. Our confidence in this is reinforced by qualitative agreement with similar experiments performed earlier [6,9,12]. Experimental uncertainties were reduced by careful microstructural control, by controlled selection of specimens for implantation and by controlled selection of the sequence of mechanical testing. The change in flow stress is significant because this property is traditionally assumed to be a bulk property, and the modified surface layer does not constitute even 0.1% of the bulk. We believe that the main reason for this is that at low strains (either cyclic or monotonic) grains near the free surface deform most and have a major contribution in determining the flow stress. Since surface modification alters the flow characteristics of these grains, the measured flow stresses are substantially altered.

5. Conclusions

1) The surface defect structure of polycrystalline copper due to ion implantation consists of dislocation loops and arrays. The defect structure is more intense for larger and heavier atoms.

2) Monotonic and cyclic flow stresses are reduced by ion implantation. This has been attributed to the availability of slip dislocations and the homogeneity and reversibility of slip as a consequence of the alloying and defect structure in the surface layer.

3) Life under strain controlled fatigue is improved by ion implantation. This is attributed to improvements in the homogeneity and reversibility of slip due to implantation.

4) Under stress controlled conditions, fatigue lives may or may not be improved by ion implantation. When residual tensile surface stresses are present, e.g., due to boron implantation, fatigue life is reduced. Residual compressive stresses along with the effects of surface alloying and defect structure improves the fatigue life, e.g., for the aluminum implanted samples. Chromium implantation also shows marked improvement. This may be attributed to the expected precipitation of chromium along with the presence of defect structures.

This research was sponsored by the Office of Naval Research under Contract N00014-78-C-0270, Dr.

SECURITY CLASSIFICATION OF THIS PAGE *(When Data Entered)*

REPORT DOCUMENTATION PAGE

READ INSTRUCTIONS BEFORE COMPLETING FORM

1. REPORT NUMBER	2. GOVT ACCESSION NO. / 3. RECIPIENT'S CATALOG NUMBER
4. TITLE *(and Subtitle)*: X-ray Scattering Investigation of Microalloying and Defect Structure in Ion Implanted Copper	5. TYPE OF REPORT & PERIOD COVERED: Progress
	6. PERFORMING ORG. REPORT NUMBER: E-19-664
7. AUTHOR(s): S. Spooner	8. CONTRACT OR GRANT NUMBER(s): N00014-78-C-0270
9. PERFORMING ORGANIZATION NAME AND ADDRESS: Fracture & Fatigue Research Laboratory, Georgia Institute of Technology, Atlanta, GA 30332	10. PROGRAM ELEMENT, PROJECT, TASK AREA & WORK UNIT NUMBERS
11. CONTROLLING OFFICE NAME AND ADDRESS: Office of Naval Research, Department of the Navy, Arlington, VA 22217	12. REPORT DATE: August 26, 1981 13. NUMBER OF PAGES: 11
14. MONITORING AGENCY NAME & ADDRESS *(if different from Controlling Office)*	15. SECURITY CLASS. *(of this report)*: Unclassified 15a. DECLASSIFICATION/DOWNGRADING SCHEDULE

16. DISTRIBUTION STATEMENT *(of this Report)*

Unlimited

17. DISTRIBUTION STATEMENT (o ... *from Report)*

18. SUPPLEMENTARY NOTES

19. KEY WORDS *(Continue on rev*

ion plating, ion

20. ABSTRACT *(Continue on re*

The double-crysta ... /sis of radiation described by B. (... nvestigation of aluminum implant ... -ray observations is based on effects ... icroalloy and the presence of dislocation l ... ion damage. The copper crystal with a d ... implanted with aluminum to a dose of 2 x ... 200 keV. The response of the implantec ... 600°C was determined.

DD FORM 1473 EDIT ... JAN 73 ... ied

... IFICATION OF THIS PAGE *(When Data Entered)*

The quantitative use of the x-ray technique to assess implantation effects and the limitations of the technique are discussed.

X-RAY SCATTERING INVESTIGATION OF MICROALLOYING AND DEFECT STRUCTURE IN ION IMPLANTED COPPER

S. Spooner

Fracture and Fatigue Research Laboratory
Georgia Institute of Technology
Atlanta, Georgia 30332

The double-crystal method for x-ray scattering analysis of radiation described by B. C. Larson (1) has been applied to the investigation of aluminum implanted copper. The interpretation of x-ray observations is based on effects of lattice strain in the surface microalloy and the presence of dislocation loops which originate from implantation damage. The copper crystal with a dislocation less than 10^3 cm/cm^3 was implanted with aluminum to a dose of 2×10^{16} ions/cm with energies up to 200 keV. The response of the implanted crystal to annealing at 500 C and 600 C was determined. The quantitative use of the x-ray technique to assess implantation effects and the limitations of the technique are discussed.

This research was sponsored by the Office of Naval Research under Contract N00014-78-C-0270.

X-ray diffraction is an effective method for analyzing radiation damage particularly for quantitative measurement of lattice strain effects associated with defect clusters (1). In recent years there have been a variety of x-ray diffraction investigations of ion implantation damage produced in single crystals based on double-crystal measurements. Komerou et al. (2) observed x-ray scattering Pendellosung interference in rocking curves from Ne^+-implanted garnet films which Speriousu (3) interpreted according to a kinematic diffraction theory incorporating strain and damage distributions as a function of depth. Afanasev et al. (4) have used dynamical theory for calculating the scattering from a silicon crystal with disturbed layers. Yamagishi and Nittono (5) studied Ar^+ ion-implanted copper whiskers with both x-ray topography and a triple-crystal diffraction method to assess lattice strain response with dose and annealing. In the foregoing studies (2-5) no absolute intensity measurements were made so that analysis of structural changes depended mostly upon scattering distribution shape. In the present study, absolute reflectivity measurements are used to study the effects of Al^+-ion damage in copper due to low energy (200 keV) and high dose (2×10^{16} ions/cm^2) using a double-crystal diffraction method. Both surface alloying and implantation damage are under consideration for their important influence on fatigue crack initiation (6). Because radiation damage production of point defect clusters enters our work in a fundamental way, this paper offers an example of the utility of x-ray scattering techniques in radiation damage research.

The principle challenge in this x-ray study was to find an effective x-ray method for investigating the damage and surface alloying effect in an implanted layer which is much thinner than the sampling depth of x-rays. In addition, there was the consideration of which theoretical analysis of scattering intensity would be most appropriate to describe the combined damage and surface alloying scattering effects. This question was approached from two perspectives; (a) use of dynamical theory of diffraction for the analysis of lattice strain due to surface alloying (7,8) and (b) use of kinematic theory for the description of scattering from defect clusters (1). It is shown that the scattering data are dominated by implantation damage defect clusters and that the kinematic theory is most appropriate for the description of scattering in the case at hand. Furthermore, it is shown that a quantitative evaluation of implantation damage can be obtained from the absolute reflectivity measurements made in the double-crystal method.

X-Ray Scattering Models

The structure the implanted region is modeled by placing of point defect clusters within a surface layer which has a lattice parameter that is expanded by implantation alloying. As yet, no single formulation for scattering intensity gives a calculation of the scattering from the combined defect cluster and lattice distortion effects. Instead, we make a calculation for the case of scattering from a defect-free surface alloy on one hand and a calculation for the scattering from defect clusters in a unalloyed matrix on the other hand. The measured x-ray scattering effects are then used to determine the manner in which the two calculations might be applied to represent the scattering from the implanted layer.

For a surface alloy layer free of defects, the dynamical theory of x-ray scattering can be used to calculate the reflectivity of x-rays as a function of crystal rotation in a double-crystal rocking curve. In a two-crystal arrangement, the first crystal which is not implanted is set to maximum reflectivity. The second crystal is rotated about an axis perpendicular to the scattering plane (defined by the incident and reflected

x-ray beams.) The resulting reflectivity curve is the convol[illegible] the reflection characteristic of the first crystal with the reflectivity of the second crystal. Larson (7,8) has adapted, for this surface alloy problem, a method of calculation used by Klar and Rustichelli (9) for neutron scattering from elastically bent crystals. The reflectivity from a crystal is obtained by the computation of the real and imaginary components of the complex scattering amplitude of the reflected radiation. Two coupled differential equations - one for real and one for imaginary components - are integrated numerically. The integration is dependent upon initial values of the amplitude components and the variation in the Bragg angle for the crystalline sublayers due to the elastic lattice distortion arising from bending or composition change. Full algebraic development of the theory can be found in papers by Larson and Barhorst (8) and Klar and Rustichelli (9). The equations requiring integration express the derivatives of the real (X_1) and imaginary (X_2) scattering amplitude components with respect to a variable A which is proportional to depth measured relative to the external surface:

$$\frac{dX_1}{dA}=k(X_1^2-X_2^2+1)+2X_2(X_1-y)-2gX_1 \tag{1}$$

$$\frac{dX_2}{dA}=-(X_1^2-X_2^2+1)+2X_1(kX_2+y)-2gX_2 \tag{2}$$

where k and g are constants which depend on x-ray absorption and the parameter y contains the misset angle, $\Delta\theta$, for the rocking curve as follows:

$$y=C_1\Delta\theta-C_2 \tag{3}$$

where C_1 and C_2 are constants dependent on x-ray scattering parameters tha are fixed for the Bragg diffraction peak under examination. For the case where the lattice parameter varies with A it is shown (8) that

$$y=C_1(\Delta\theta+\varepsilon(A)\tan\theta_B)-C_2 \tag{4}$$

where the variation of the lattice parameter with depth is contained in the strain function $\varepsilon(A)$. In the case at hand, $\varepsilon(A)$ is determined by the composition of the surface alloy as a function of implantation depth.

The method by which the change in relectivity due to surface alloying is calculated does not require integration over the entire crystal thickness. Instead, one uses the well known results (10,11) for the reflectivity from a perfect crystal as a starting point. The real and imaginary components of the scattering amplitude at a set rocking angle are used as initial values for the integration beginning at a depth below the implanted ions. For the integration back to the surface the effects of surface alloying, $\varepsilon(A)$, are allowed to affect the computation of scattering amplitude. A set of these calculations is done for a range of rocking angles where the reflectivity is calculated from,

$$R(\Delta\theta)=X_1^2+X_2^2 \tag{5}$$

where the amplitude components, X_1 and X_2 are evaluated at the reflecting crystal surface. Note that the result is an absolute reflectivity value.

Figure 1 shows the calculated results we have obtained at the reflecting in which 2 atomic percent of aluminum is implanted in copper to a depth of approximately 1000 A. The lattice parameter expansion used in the calculation was taken from the data given on linear lattice strain by King (12) equal to +0.0626 per atomic percent of aluminum in copper. A sharp

subsidiary peak of 1.4 percent reflectivity is seen at a Bragg angle displaced to a lower angle than the substrate Bragg angle corresponding to the expanded lattice parameter. The small peak width is approximately 2 minutes of arc. The reflectivity is the order of the ratio of implanted layer thickness to the x-ray penetration thickness, $1/2\,\mu_o$, where μ_o is the linear absorption parameter.

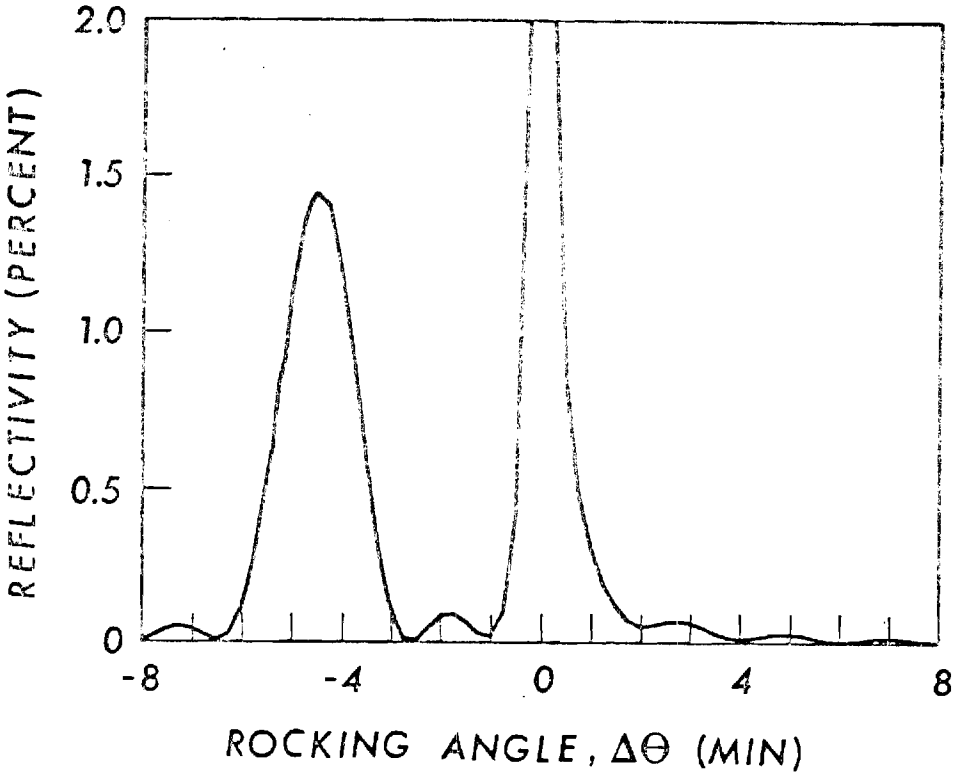

Fig. 1 Calculated reflectivity from a surface implanted to 2 atomic percent of aluminum in copper to a depth of approximately 1000 A The subsidiary peak appears at an angle appropriate for the lattice parameter of this composition.

Consider now the calculation of the scattering from defect clusters in a crystal of uniform lattice parameter. In this case, kinematic diffraction theory is used to calculate the scattering intensity from an isolated defect cluster. The scattering resulting from a collection of defects is the sum of the intensities. This implies that no scattering interference occurs between scattering amplitudes coming from each defect. Larson (1) summarizes the calculation of the scattering intnsity from defect clusters. The experimental geometry used in our experiments is shown in Figure 2 where the scattered x-rays are recieved by a large detector. Each of the scattering vectors is associated with a scattering space vector, q, going from the Bragg spot (at the top) to the surface of the Ewald scattering sphere. In such an experiment, the intensity is averaged over the scattering space vectors, q. q_o is the shortest vector between the Bragg position and the Ewald sphere at a given crystal setting. The measured intensity is called the integral diffuse scattering. The intensity is measured as a function of rocking angle of the crystal in the same geometry used for measurement of dynamical difraction effects described above.

The diffuse scattering from dislocation loops measured close to the Bragg peak is attributed to long range strain fields around the loop and is called [illegible] scattering. Scattering measured farther away from the Bragg

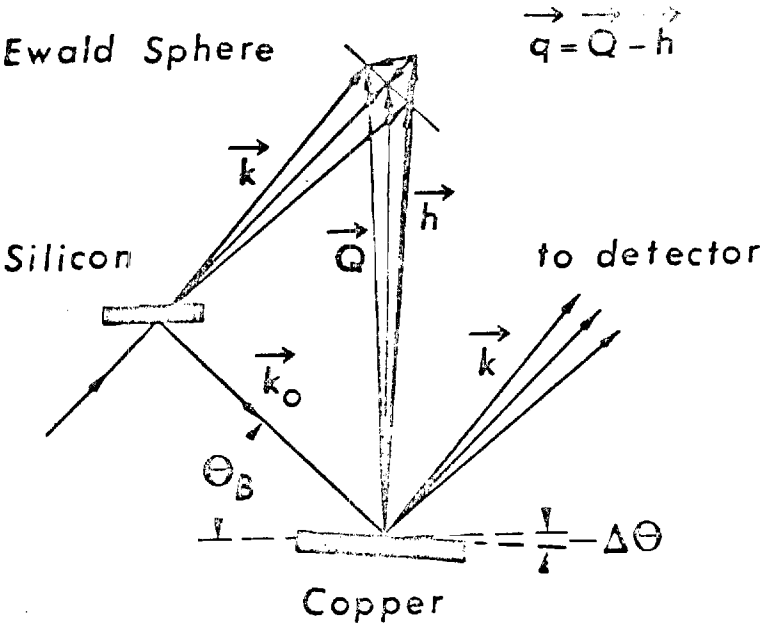

Fig. 2
Scattering geometry for the double crystal method used in this experiment. Upon rocking the crystal the Ewald scattering sphere is swept through the Bragg point. At a fixed crystal setting the diffuse scattering is integrated over a portion of the scattering sphere near the Bragg point.

peak is attributed to short range strain fields and is termed Stokes- Wilson scattering. The diffuse scattering is distributed about the Bragg position in a way dependent on the precise strain field distribution (1,13). The calculation of integral diffuse scattering requires an averaging of the diffuse scattering over the portion of the Ewald scattering sphere which is close to the Bragg position (14). For the scattering from loops of radius R, the Huang scattering smoothly joins the Stokes-Wilson scattering at a scattering parameter $q_o = q_L = \alpha/R$ where $q_o = h\Delta\theta\cos\theta_B$ with d_{hk} spacing, $h = 2\pi/d_{hkl}$, θ_B the Bragg angle for reflection from the hkl planes, $\Delta\theta$, the misset angle of the rocking curve. A symmetric diffuse scattering cross section is defined

$$\sigma_h^s(q_o) = 1/2(\sigma_h^s(-q_o) + \sigma_h^s(q_o)) \tag{6}$$

which is obtained by the average of intensities measure symmetrically above and below the Bragg position ($q_o = 0$). The symmetric diffuse cross sections for Huang and Stokes-Wilson scattering are given by,

(Huang) $$\sigma_h^s(q_o) = (r_e^2 f_h^2 e^{-2M}(h/k)^2 2\pi\tau(b\pi R^2/V_c)^2 \ln(e^{1/2} q_L/q_o) \tag{7}$$

for $q_o < q_L$, and,

(Stokes-Wilson) $$\sigma_h^s(q_o) = (r_e^2 f_h^2 e^{-2M}(h/k)^2 2\pi\tau(b\pi R^2/V_c)^2 q_L^2/2q_o^2 \quad . \tag{8}$$

for $q_o > q_L$, r_e is the Thompson electron radius (2.82×10^{-13} cm), f is the scattering factor, e^{-M} is the Debye-Waller factor, $k = 2\pi/\lambda$, λ= wavelength, α a constant of order 1 which depends on averaging of loop orientations, b= Burgers vector, V_c = atomic volume, The scattering intensity relative to the incident intensity is given by,

$$\frac{I^s(q_o)}{I_o} = \frac{C(R)}{2\mu_o V_c}\sigma_h^s(q_o) \tag{9}$$

where $C(R)/V_c$ is the density of loops of radius R. From Eqns. (7),(8) and (9) one can obtain loop size and density. Note that $(b\pi R^2/V_c)$ equals the number of point defects in the defect cluster.

In summary of the two calculations, the dynamical theory predicts a subsidiary peak which appears at an angle determined by the lattice strain due to alloying. The kinematic theory predicts a diffuse scattering which is proportional to the number and size of loops. Both calculations give the absolute relectivity with no adjustable parameters other than those describing the structure. The dynamical theory calculation depends on the assumption that the surface alloy is crystallographically coherent with the unalloyed crystal. The kinematic theory is likely to be limited in the case of very high defect cluster densities where nonrandom loop distributions may lead to interference between diffuse scattering amplitudes.

Experimental

The calculated strain scattering effects must be measured at small angles near the Bragg diffraction peak of the unaffected crystal. The implant affected region is less than 1 micron and the penetration depth is approxmately 1/2 = 11 microns. It is required that the bulk of the crystal be perfect (mosaic spread less than 1 minute) in order that the small scattering effects can be measured near the Bragg peak. Furthermore, it is required to subtract a significant background due to the tails of the bulk crystal Bragg peak in order to determine the diffuse scattering intensity due to surface alloying and defect clusters. A convenient approach to this measurement is to translate the crystal between an implanted and implantation-free area on the same crystal. Crystals used in these studies were provided by F. W. Young of Oak Ridge National Laboratory. The crystals were grown by the Bridgeman technique, cut to orientation, then annealed at a few degrees below the melting point for two weeks. The crystal pieces were hardened by neutron irradiation and then further cut and shaped by chemical cutting methods (15). The dislocation density measured by etch pit techniques was less than 10^3 cm^{-2} after shaping procedures were completed.

The two-crystal arrangement consisted of a silicon crystal fixed to diffract the Cu K_α radiation onto the implanted copper crystal. The (333) d-spacing (1.0451 A) of silicon happens to match the (222) d-spacing (1.0436 A) of copper very well so that the system is well focussed to give a narrow rocking curve width. The copper crystal is initially aligned to give a sharp maximum in the rocking curve by adjusting the (111) normal about an axis in the scattering plane. When properly adjusted, the full width at half-maximum (FWHM) of the copper rocking curve is 12.5 arc-seconds. The crystal is mounted on a goniostat which can be translated in the plane of the crystal surface so that rocking curves can be made from the implanted area and masked implantation-free areas. In a typical run, the copper crystal is rocked about an axis perpendicular to the scattering plane at a rate of 5 to 20 arc-seconds per minute while x-ray intensities are recorded continuously at 10 second intervals. The x-ray detector has an active receiving area of 5 cm^2 at a distance of 8 cm so that the subtended solid angle (0.08 steradians) integrates the scattering over a large portion of the Ewald sphere in the vicinity of the 222 Bragg peak of copper.

The implantation of aluminum into copper was chosen for these experiments because the ion penetration was favorable and the microalloy concentration was well below the solubility limit of the aluminum in copper. The details of implantation are given elsewhere (19). The implanted layer was 1200 A thick (16) with a composition of 1.8 atomic percent. The distribution of damage over the alloy thickness was estimated on the basis of calculations by Fritzsche (17) and Winterbon (18). The alloy distribution (solid line) and the damage profile (dashed line) are shown in Figure 2.

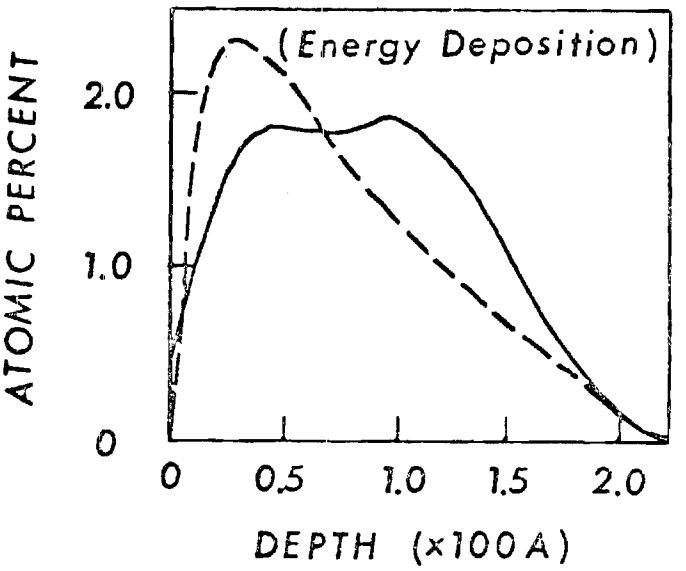

Fig. 3
Distribution of implanted Al^+ ions (solid) and the energy deposition (dashed) for the implantation of 2×10^{16} ion/cm^2 with energies up to 200 keV. Note that damage is concentrated toward the surface and that the damage energy is on a relative scale.

Annealing of the specimens was performed as a means to differentiate the sources of scattering in the implanted layers. The crystals were placed in a vacuum of 10^{-8} Torr at 500 C, 600 C and 900 C for 30 minutes. Annealing at 900 C restored the original structure as seen in the rocking curves.

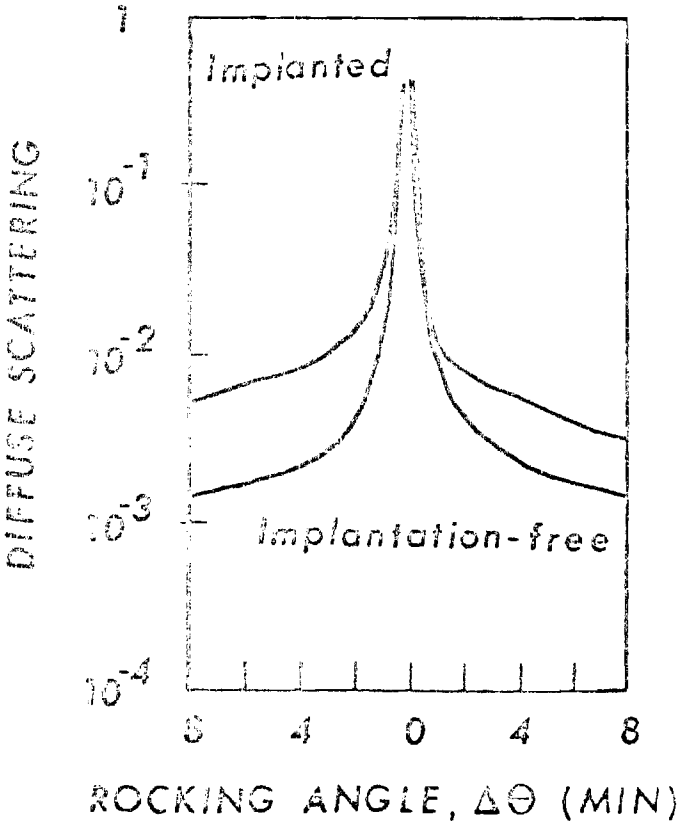

Fig. 4
Rocking curves are shown for the implanted (upper) and implantation-free (lower) crystal. The scattering is expressed as a fraction of the incident beam intensity. Note the larger scattering at low angles.

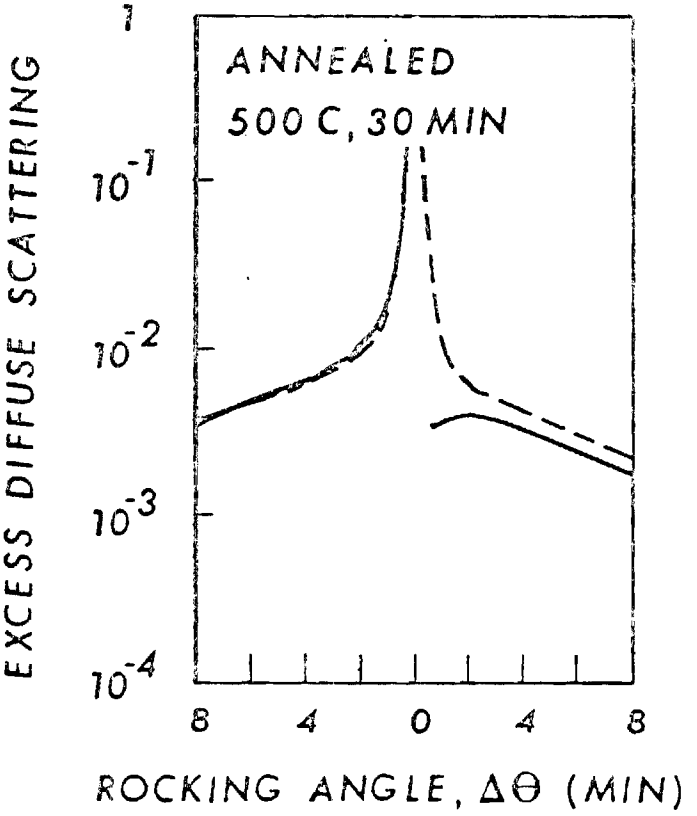

Fig. 5
Excess diffuse scattering intensity for the sample before annealing (dashed) and after annealing (solid) at 500 C. Note that little change in the general level and distribution of the excess intensity occurs upon annealing.

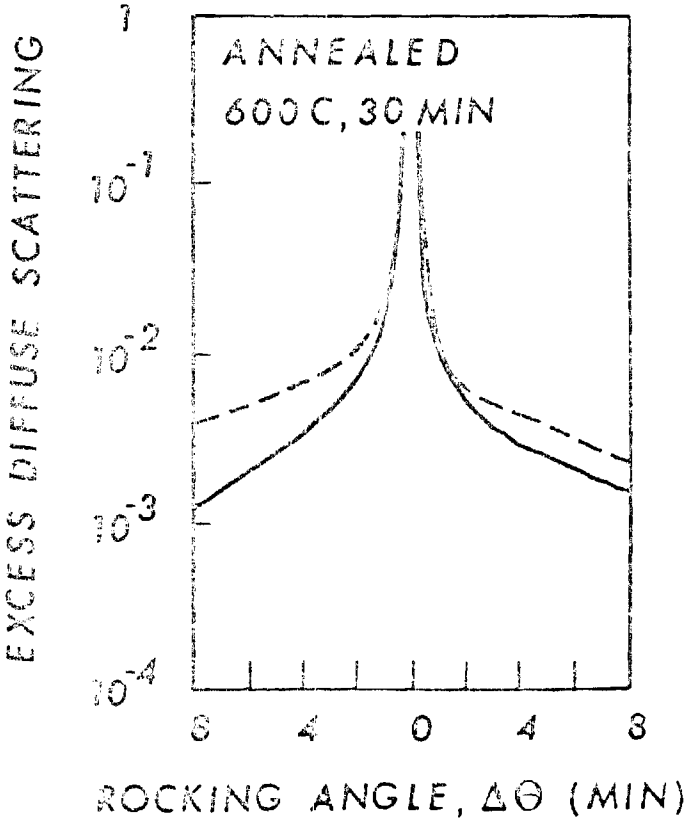

Fig. 6
Excess diffuse scattering intensity for the sample before annealing (dashed) and after annealing (solid) at 600 C. The level and the distribution of the excess intensity changes as a result of the annealing at this temperature.

Results and Discussion

The rocking curves for implantation-free copper and for aluminum implanted copper were measured on the same crystal. These curves are shown in Figure 4. The diffuse scattering from the implanted crystal is more intense on the low angle side of the Bragg peak position. The excess diffuse scattering is calculated by subtraction of the implantation-free rocking curve intensity from the corresponding intensity in the implanted crystal. The excess diffuse scattering for the implanted crystal is shown in Figures 5 and 6 as a dashed line. The effect of 30 minute anneals on the excess diffuse intensity is show in Figure 5 for annealing at 500 C and in Figure 6 for annealing at 600 C. No large change due to annealing occurs at 500 C while for annealing at 600 C, there is a reduction of scattering and scattering becomes more symmetric with respect to the Bragg peak position.

The observation of a higher diffuse scattering at low rocking curve angles can be attributed to the fact that implanted aluminum expands the copper lattice so that Bragg scattering from the implanted region occurs at a lower angle than that for the implantation-free material. The composition of the implanted layer was estimated to be 1.8 atomic percent. The resulting Bragg position would be displaced to lower angle by 4.2 minutes for the 222 reflection from the copper alloy layer.

The diffuse scattering seen on both sides of the main Bragg position can be compared to calculations of the scattering from dislocation loops. In Figure 7 the excess diffuse scattering is plotted versus the log of the rocking angle according to Eqn. (7) for Huang loop scattering. The rocking angle was measured relative to the supposed Bragg position for the alloy.

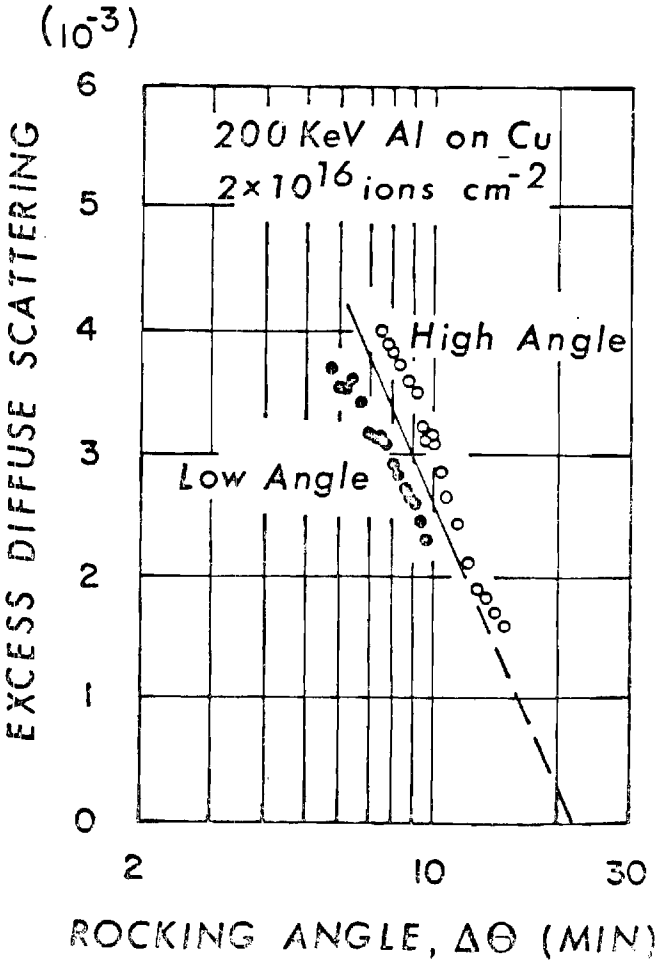

Fig. 7
The excess diffuse scattering from the implanted crystal is plotted versus $\ln(\Delta\theta)$ for the intensity above and below the Bragg position assumed to apply for the implanted region of the crystal.

S. Spooner

Although there is a displacement between the two sets of points, the average of the high angle and low angle intensity is close to a straight line which yields an estimated loop radius of 25 A.

An estimate of the density of loops can be made by comparing measured reflectivity with Eqn. (9). We use a loop radius of 25 A and a reflectivity of 1 percent at $\Delta\theta$= 2 minutes. Substitution of appropriate constants into Eqn. (9) for a 25 A loop size gives

$$\frac{I^s(q_o)}{I_o} = 6.1 \times 10^{-21} \frac{C}{V_c} \ln\left(\frac{44}{\Delta\theta(\text{min})}\right) \qquad (10)$$

from which a value of C/V_c is 5.3×10^{17} loops/cc. (The loops are concentrated by a factor of 40 in the implanted layer since the above calculation assumes the loops to be uniformly distributed).

The failure to observe a sharp Bragg peak associated with the implanted aluminum and the general agreement with scattering levels calculated for loop scattering point to the conclusion that the kinematic theory for diffraction from an implanted crystal containing loops is appropriate. The annealing at 600 C produces symmetrical scattering which suggests that most of the aluminum is removed from the region where loops persist. Thereby the loop scattering now originates in essentially pure copper. The role of aluminum is seen as simply expanding the lattice in a region where loops persist which, by virtue of severe damage, is no longer strictly coherent with the implantation-free crystal.

Conclusions

Analysis of x-ray diffraction in aluminum-ion implanted copper suggests that defect cluster scattering dominates the observed rocking curve intensity. Alloying in the implanted layer contributes through a shifting of the diffuse scattering to lower angles due to the fact that the defect clusters are formed in a region of aluminum-expanded lattice. The formation of a distinct peak predicted by dynamical diffraction theory does not occur, probably because of the intense defect scattering and the widths of the peak from the thin layer. Problems in the analysis of scattering remain in the area of formulating a model of combined alloying and defect cluster scattering as well as description of very high defect cluster scattering. Nevertheless the simplistic interpretation of x-ray scattering observation provides useful insights into the type and quantity of damage as well as the annealing response of the implanted structure. Measurements carried out to larger q_o will be useful in further definition of the defect structure since Bragg scattering from the implantation-free and implanted layer are avoided and the kinematical theory can be assumed. Size distributions an and total point defect densities are more directly measurable at the larger q_o values (1) as well.

Acknowledgements

The author thanks Dr. B. C. Larson and Mr. Jim Barhorst of the Solid State Division of Oak Ridge National Laboratory for their considerable help in the collection of the data and many useful discussions.

References

1. B. C. Larson, "X-ray Studies of Defect Clusters in Copper," J. Appl. Phys., 8, pp. 150-160 (1975).

2. K. Komenou, T. Hirai, K. Asama and M. Sakai, "Crystalline and Magnetic Properties of Ion-Implanted Layer in Bubble Garnet Films,"

3. V. S. Speriosu, B. B. Gibbs and K. Yoshiyama, "X-ray Determination of Strain and Damage Distributions in Ion-Implanted Layers," Appl. Phys. Lett. , 34 , pp. 539-542 (1979).

4. A. M. Afanasev, M. V. Kovalchuck, E. K. Kovev and V. G. Kohn, "X-ray Diffraction in a Perfect Crystal with Disturbed Surface Layer," Phys. Stat. Sol. (a) 42 , pp. 415-422 (1977)

5. H. Yamagishi and O. Nittono, "X-ray Study on Lattice Defects in Ar^+ Ion Implanted Copper Whiskers," Nip. Kinz. Gakk. , 43 , pp. 689-695 (1979).

6. A. Kujore, S. B. Chakrabortty and E. A. Starke, "The Effect of Ion Implantation on the Fatigue Properties of Polycrystalline Copper," Nucl. Instr. Meth., 182/183, pp. 949-958 (1981).

7. B. C. Larson, C. W. White and R. F. Appleton, "Unidirectional Contraction in Boron-Implanted Laser-Annealed Silicon," Appl. Phys. Lett., 32, pp. 801-803 (1978).

8. B. C. Larson and J. F. Barhorst, "X-ray Study of Lattice Strain in Boron Implanted Laser Annealed Silicon," J. Appl. Phys., 51, pp.3181-5 (1980).

9. B. Klar and F. Rustichelli, "Dynamical Neutron Diffraction by Ideally Curved Crystals," Nuovo Cimento, 13B, pp. 249-270 (1973).

10. B. E. Warren, X-ray Diffraction, Chapter 14, pp. 315-354, Addison-Wesley Press, Reading, Mass. (1969).

11. W. H. Zachariasen, Theory of X-ray Diffraction in Crystals, Chapter 3, pp. 83-155, Dover Publications, New York (1967).

12. H. W. King, "Quantitative Size-Factors for Metallic Solid Solutions," J. Mat. Sci, 1, pp. 79-90 (1966).

13. B. C. Larson and W. Schmatz, "Huang-Diffuse Scattering from Dislocation Loops and Cobalt Precipitates in Copper," Phys. Rev. , B10, pp. 2307-2314 (1974).

14. B. C. Larson and F. W. Young, Jr. , "A Comparison of Diffuse Scattering by Defects and Measured in Anomalous Transmission and Near Bragg Reflections," Z. Naturforsch. , 28a, pp. 626-632 (1973).

15. F. W. Young, Jr. , "Etch Pit Studies of Dislocations in Copper Crystals Deformed by Bending. I. Annealed Crystals. II. Irradiated Crystals," J. Appl. Phys. , 33, pp. 3553-3564 (1962).

16. J. Keinonen, M. Hautala, M. Luomajari, A. Antilla and M. Bister, "Ranges of $^{27}Al^+$ Ions in Nine Metals Measured by (p,γ) Resonance Broadening," Rad. Eff. , 39, pp. 189-193 (1978).

17. C. R. Fritzche, "A Simple Method for the Calculation of Energy Deposition Profiles from Range Data of Implanted Ions," Appl. Phys. Lett. , 12, pp. 347-353 (1977).

18. K. B. Winterbon, Ion Implantation Range and Energy Deposition Distributions, Vol. 2, Low Incident Ion Energies, Plenum Press, New York (1975)

19. S. Spooner and K. Legg, "X-ray Diffraction Characterization of Aluminum Ion-Implanted Copper Crystals," Ion Implantation Metallurgy, C. M. Preece and J. K. Hirvonen, eds. TMS AIME, pp. 162-170 (1980).

End of the Year Report
ONR Task Order No. N00014-78-C-0270
September 30, 1981

A. The Effect of Ion Plating and Ion Implantation on the Cyclic Response and Fatigue Crack Initiation of Metals and Alloys

The general goal of this research is to determine the effect of ion implantation and ion plating on the cyclic stress strain response and fatigue crack nucleation of a metal substrate. The coating and substrate materials have been selected in order to separate the various parameters, e.g., crystal structures, SFE, shear modulus, misfit, residual stress, etc., which control deformation behavior and fatigue crack initiation at the surface. The study includes the characterization of the interface region and the implanted or plated layer, and determining the relationship between these structural features and the fatigue crack initiation behavior. We have described our polycrystalline studies in previous reports. During the past year our major effort was concerned with single crystals in order to eliminate grain boundary effects.

Effects of Ion Implantation on Fatigue Behavior of Copper Single Crystals: The effects of ion implantation on low cycle fatigue behavior of copper single crystals oriented for single slip have been investigated. Fatigue crack initiation, stress-life and stress-strain behavior of implanted and non-implanted crystals were studied. Seeded copper single crystals were grown from high purity copper wire by the modified Bridgeman technique. Some of the samples were implanted with Al^+ ions to a dose of 10^{16} ions/cm^2 at 100 KeV. The results of implanted crystals were compared with non-implanted ones.

Aluminum implantation resulted in reduction of cyclic hardening-softening. This is due, in part, to creation of compressive residual stress in the surface and near surface regions. Aluminum implanted crystals showed a low hardening rate in comparison with non-implanted crystals. Scanning electron microscopy studies of slip band characteristics showed that aluminum implanted crystals had a more uniform distribution of deformation bands. Implantation resulted in increased life of crystals in comparison with non-implanted crystals. The defect structure created by ion implantation improves the homogeneity of deformation and this, in general, results in improvement in fatigue life. In addition, microcrack formation and link-up becomes more difficult due to improved reversibility of slip.

Using electron channeling patterns, the extent of damage in the ion implanted region was measured by comparing its back-scattered electron channeling pattern (ECP) with that of a non-implanted surface. The quality of ECP (i.e., contrast, resolution and appearance of various lines) decreases with increasing extent of damage. Because the ECP information comes mainly from a narrow surface layer (<1000Å), and because the damage by implantation is usually in the same narrow layer, this technique should prove to be very valuable for characterizing the damage associated with ion implantation.

The preliminary results of this single crystal study have shown that ion implantation can have beneficial effects on the fatigue life of materials.

B. Implication of ONR Contract Research in Terms of Applied Significance:

Viable structural materials should have an optimum combination of properties like fabricability, strength, fracture toughness, corrosion and fatigue resistance. Often it is difficult to design an alloy which will satisfy the critical demands of an application with respect to all of these properties. Ion implantation and ion plating offer ways of improving surface related properties without any measureable loss in bulk properties. These techniques may harden the surface, delay fatigue, reduce wear and improve corrosion resistance. It is hoped that this research program will aid in understanding these technologically important problems and eventually lead to methods of producing surface modifications for improving properties.

C. Publications, Reports and Talks During 1980-1981

1. S. B. Chakrabortty, A. Kujore and E. A. Starke, Jr., "The Effect of Ion Implantation on Cyclic Stress-Stress Pesponse of Polycrystalline Copper," Thin Solid Films 73 (1980), 209-219.

2. A. Kujore, S. B. Chakrabortty, E. A. Starke, Jr., and K. O. Legg, "The Effect of Ion Implantation on the Fatigue Properties of Polycrystalline Copper," Nuclear Instruments and Methods, 182/183 (1981) 949-958.

3. S. B. Chakrabortty, A. Kujore, E. A. Starke, Jr. and K. O. Legg, "The Effect of Ion Implantation on the Fatigue Behavior of Metals and Alloys," Trans. Nuclear Science 28 (1981) 1812-1815.

4. A. Kujore, S. B. Chakrabortty and E. A. Starke, Jr., Recent Studies of the Effect of Ion Implantation of the Fatigue Behavior of Copper," paper presented at the Fall AIME Meeting, Pittsburgh, PA, October 1980.

5. P. Heydari-Darani and E. A. Starke, Jr., "Effect of Ion Implantation on Low Cycle Fatigue Behavior of Copper Single Crystal," presented at International Conference on Modification of Surface Properties by Ion Implantation, Manchester, U.K. to be published April 1982 in the Conference Proceedings.

D. Other Research Tasks

1. The Effect of Microstructures on the Properties of High Strength Aluminum, AFOSR-78-3471, $140,000 for a one year program.

2. The Investigation of the Effects of Microstructure on the Deformation Modes and Mechanical Properties of Ti-6Al-2Cb-1Ta-0.8Mo, ONR Task Order No. N00014-79-C-0207, $140,000 for a two year period.

3. The Effects of Powder Metallurgical Processing and Intermediate Thermal Mechanical Treatment on the Fatigue Properties of High Strength Aluminum Alloys, USARO Contract No. DAAG 29-80-C-0100, $119,391 for a three year period.

4. Development of High Stiffness Aluminum Alloy from Rapidly Solidified Powders for Aerospace Structural Applications, Lockheed Missile & Space Co. Contract No. HJ80C2630R, $191,000 for a two year period.

Respectfully submitted,

Edgar A. Starke, Jr.
Principal Investigator

X-RAY SCATTERING INVESTIGATION OF MICROALLOYING AND DEFECT STRUCTURE IN ION IMPLANTED COPPER

S. Spooner

Fracture and Fatigue Research Laboratory
Georgia Institute of Technology
Atlanta, Georgia 30332

The double-crystal method for x-ray scattering analysis of radiation described by B. C. Larson (1) has been applied to the investigation of aluminum implanted copper. The interpretation of x-ray observations is based on effects of lattice strain in the surface microalloy and the presence of dislocation loops which originate from implantation damage. The copper crystal with a dislocation less than 10^{5} cm/cm^{3} was implanted with aluminum to a dose of 2×10^{16} ions/cm with energies up to 200 keV. The response of the implanted crystal to annealing at 500 C and 600 C was determined. The quantitative use of the x-ray technique to assess implantation effects and the limitations of the technique are discussed.

This research was sponsored by the Office of Naval Research under Contract N00014-78-C-0270.

Introduction

X-ray diffraction is an effective method for analyzing radiation damage particularly for quantitative measurement of lattice strain effects associated with defect clusters (1). In recent years there have been a variety of x-ray diffraction investigations of ion implantation damage produced in single crystals based on double-crystal measurements. Komenou et al. (2) observed x-ray scattering Pendellosung interference in rocking curves from Ne^+-implanted garnet films which Speriousu (3) interpreted according to a kinematic diffraction theory incorporating strain and damage distributions as a function of depth. Afanasev et al. (4) have used dynamical theory for calculating the scattering from a silicon crystal with disturbed layers. Yamagishi and Nittono (5) studied Ar^+ ion-implanted copper whiskers with both x-ray topography and a triple-crystal diffraction method to assess lattice strain response with dose and annealing. In the foregoing studies (2-5) no absolute intensity measurements were made so that analysis of structural changes depended mostly upon scattering distribution shape. In the present study, absolute reflectivity measurements are used to study the effects of Al^+-ion damage in copper due to low energy (200 keV) and high dose (2×10^{10} ions/cm^2) using a double-crystal diffraction method. Both surface alloying and implantation damage are under consideration for their important influence on fatigue crack initiation (6). Because radiation damage production of point defect clusters enters our work in a fundamental way, this paper offers an example of the utility of x-ray scattering techniques in radiation damage research.

The principle challenge in this x-ray study was to find an effective x-ray method for investigating the damage and surface alloying effect in an implanted layer which is much thinner than the sampling depth of x-rays. In addition, there was the consideration of which theoretical analysis of scattering intensity would be most appropriate to describe the combined damage and surface alloying scattering effects. This question was approached from two perspectives; (a) use of dynamical theory of diffraction for the analysis of lattice strain due to surface alloying (7,8) and (b) use of kinematic theory for the description of scattering from defect clusters (1). It is shown that the scattering data are dominated by implantation damage defect clusters and that the kinematic theory is most appropriate for the description of scattering in the case at hand. Furthermore, it is shown that a quantitative evaluation of implantation damage can be obtained from the absolute reflectivity measurements made in the double-crystal method.

X-Ray Scattering Models

The structure the implanted region is modeled by placing of point defect clusters within a surface layer which has a lattice parameter that is expanded by implantation alloying. As yet, no single formulation for scattering intensity gives a calculation of the scattering from the combined defect cluster and lattice distortion effects. Instead, we make a calculation for the case of scattering from a defect-free surface alloy on one hand and a calculation for the scattering from defect clusters in a unalloyed matrix on the other hand. The measured x-ray scattering effects are then used to determine the manner in which the two calculations might be applied to represent the scattering from the implanted layer.

For a surface alloy layer free of defects, the dynamical theory of x-ray scattering can be used to calculate the reflectivity of x-rays as a function of crystal rotation in a double-crystal rocking curve. In a two-crystal arrangement, the first crystal which is not implanted is set to maximum reflectivity. The second crystal is rotated about an axis perpendicular to the scattering plane (defined by the incident and reflected

x-ray beams.) The resulting reflectivity curve is the convolution of the reflection characteristic of the first crystal with the reflectivity of the second crystal. Larson (7,8) has adapted, for this surface alloy problem, a method of calculation used by Klar and Rustichelli (9) for neutron scattering from elastically bent crystals. The reflectivity from a crystal is obtained by the computation of the real and imaginary components of the complex scattering amplitude of the reflected radiation. Two coupled differential equations - one for real and one for imaginary components - are integrated numerically. The integration is dependent upon initial values of the amplitude components and the variation in the Bragg angle for the crystalline sublayers due to the elastic lattice distortion arising from bending or composition change. Full algebraic development of the theory can be found in papers by Larson and Barhorst (8) and Klar and Rustichelli (9). The equations requiring integration express the derivatives of the real (X_1) and imaginary (X_2) scattering amplitude components with respect to a variable A which is proportional to depth measured relative to the external surface:

$$\frac{dX}{dA}1=k(X_1^2-X_2^2+1)+2X_2(X_1-y)-2gX_1 \tag{1}$$

$$\frac{dX}{dA}2=-(X_1^2-X_2^2+1)+2X_1(kX_2+y)-2gX_2 \tag{2}$$

where k and g are constants which depend on x-ray absorption and the parameter y contains the misset angle, $\Delta\theta$, for the rocking curve as follows:

$$y=C_1\Delta\theta-C_2 \tag{3}$$

where C_1 and C_2 are constants dependent on x-ray scattering parameters tha are fixed for the Bragg diffraction peak under examination. For the case where the lattice parameter varies with A it is shown (8) that

$$y=C_1(\Delta\theta+\varepsilon(A)\tan\theta_B)-C_2 \tag{4}$$

where the variation of the lattice parameter with depth is contained in the strain function $\varepsilon(A)$. In the case at hand, $\varepsilon(A)$ is determined by the composition of the surface alloy as a function of implantation depth.

The method by which the change in relectivity due to surface alloying is calculated does not require integration over the entire crystal thickness. Instead, one uses the well known results (10,11) for the reflectivity from a perfect crystal as a starting point. The real and imaginary components of the scattering amplitude at a set rocking angle are used as initial values for the integration beginning at a depth below the implanted ions. For the integration back to the surface the effects of surface alloying, $\varepsilon(A)$, are allowed to affect the computation of scattering amplitude. A set of these calculations is done for a range of rocking angles where the reflectivity is calculated from,

$$R(\Delta\theta)=X_1^2+X_2^2 \tag{5}$$

where the amplitude components, X_1 and X_2 are evaluated at the reflecting crystal surface. Note that the result is an'absolute reflectivity value.

Figure 1 shows the calculated results we have obtained at the reflecting in which 2 atomic percent of aluminum is implanted in copper to a depth of approximately 1000 A. The lattice parameter expansion used in the calculation was taken from the data given on linear lattice strain by King (12) equal to +0.0626 per atomic percent of aluminum in copper. A sharp

subsidiary peak of 1.4 percent reflectivity is seen at a Bragg angle displaced to a lower angle than the substrate Bragg angle corresponding to the expanded lattice parameter. The small peak width is approximately 2 minutes of arc. The reflectivity is the order of the ratio of implanted layer thickness to the x-ray penetration thickness, $1/2\,\mu_o$, where μ_o is the linear absorption parameter.

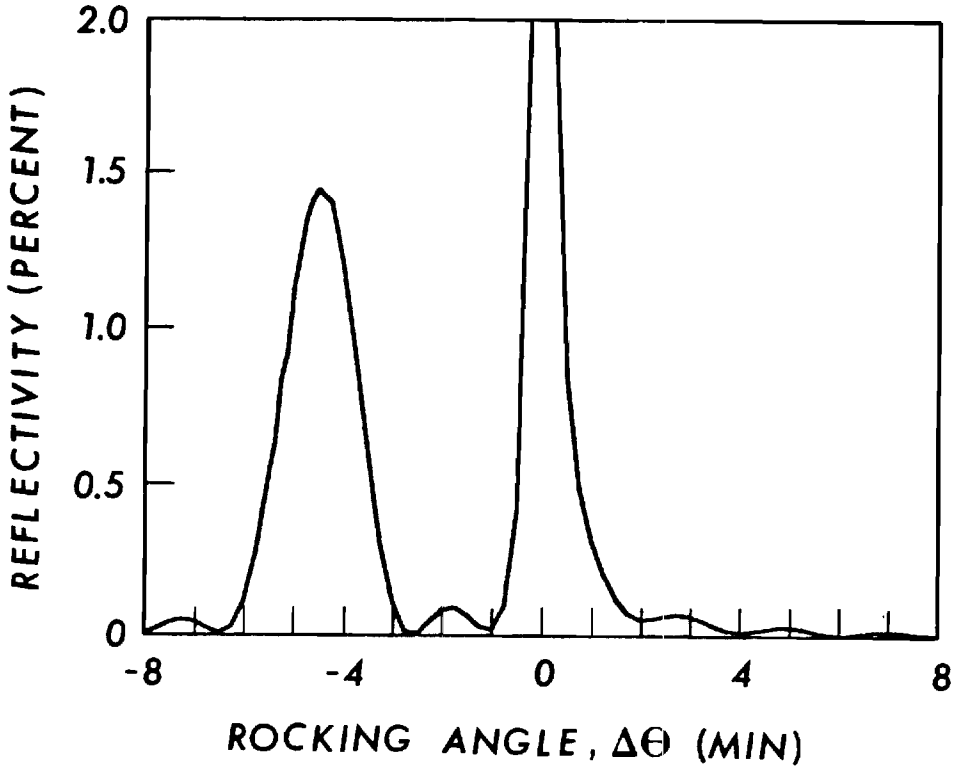

Fig. 1 Calculated reflectivity from a surface implanted to 2 atomic percent of aluminum in copper to a depth of approximately 1000 A The subsidiary peak appears at an angle appropriate for the lattice parameter of this composition.

Consider now the calculation of the scattering from defect clusters in a crystal of uniform lattice parameter. In this case, kinematic diffraction theory is used to calculate the scattering intensity from an isolated defect cluster. The scattering resulting from a collection of defects is the sum of the intensities. This implies that no scattering interference occurs between scattering amplitudes coming from each defect. Larson (1) summarizes the calculation of the scattering intnsity from defect clusters. The experimental geometry used in our experiments is shown in Figure 2 where the scattered x-rays are recieved by a large detector. Each of the scattering vectors is associated with a scattering space vector, q, going from the Bragg spot (at the top) to the surface of the Ewald scattering sphere. In such an experiment, the intensity is averaged over the scattering space vectors, q. q_o is the shortest vector between the Bragg position and the Ewald sphere at a given crystal setting. The measured intensity is called the integral diffuse scattering. The intensity is measured as a function of rocking angle of the crystal in the same geometry used for measurement of dynamical difraction effects described above.

The diffuse scattering from dislocation loops measured close to the Bragg peak is attributed to long range strain fields around the loop and is called Huang scattering. Scattering measured farther away from the Bragg

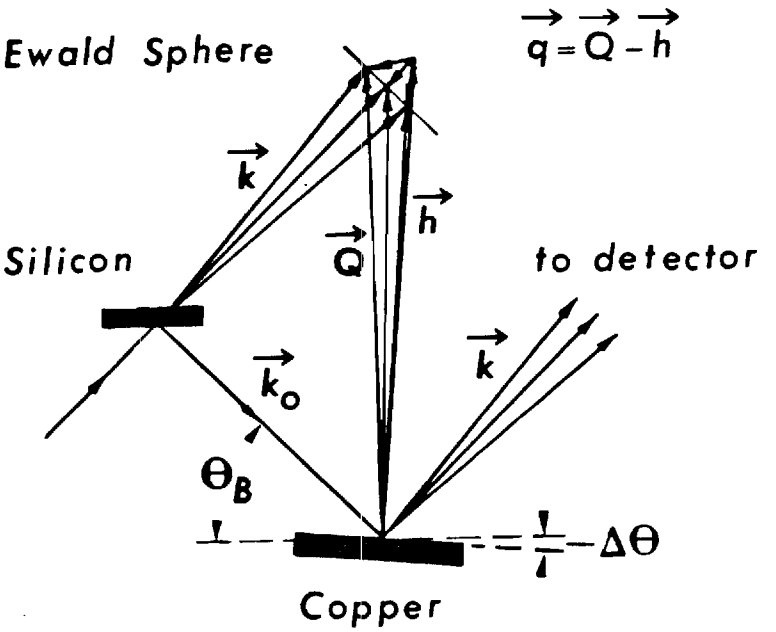

Fig. 2
Scattering geometry for the double crystal method used in this experiment. Upon rocking the crystal the Ewald scattering sphere is swept through the Bragg point. At a fixed crystal setting the diffuse scattering is integrated over a portion of the scattering sphere near the Bragg point.

peak is attributed to short range strain fields and is termed Stokes- Wilson scattering. The diffuse scattering is distributed about the Bragg position in a way dependent on the precise strain field distribution (1,13). The calculation of integral diffuse scattering requires an averaging of the diffuse scattering over the portion of the Ewald scattering sphere which is close to the Bragg position (14). For the scattering from loops of radius R, the Huang scattering smoothly joins the Stokes-Wilson scattering at a scattering parameter $q_o = q_L = \alpha/R$ where $q_o = h\Delta\theta\cos\theta_B$ with d_{hk} spacing, $h = 2\pi/d_{hkl}$, θ_B the Bragg angle for reflection from the hkl planes, $\Delta\theta$, the misset angle of the rocking curve. A symmetric diffuse scattering cross section is defined

$$\sigma_h^s(q_o) = 1/2(\sigma_h^s(-q_o) + \sigma_h^s(q_o)) \tag{6}$$

which is obtained by the average of intensities measure symmetrically above and below the Bragg position ($q_o = 0$). The symmetric diffuse cross sections for Huang and Stokes-Wilson scattering are given by,

(Huang) $$\sigma_h^s(q_o) = (r_e^2 f_h^2 e^{-2M}(h/k)^2 2\pi\tau(b\pi R^2/V_c)^2 \ln(e^{1/2} q_L/q_o) \tag{7}$$

for $q_o < q_L$, and,

(Stokes-Wilson) $$\sigma_h^s(q_o) = (r_e^2 f_h^2 e^{-2M}(h/k)^2 2\pi\tau(b\pi R^2/V_c)^2 q_L^2/2q_o^2 \tag{8}$$

for $q_o > q_L$, r_e is the Thompson electron radius (2.82×10^{-13} cm), f is the scattering factor, e^{-M} is the Debye-Waller factor, $k = 2\pi/\lambda$, λ= wavelength, τ is a constant of order 1 which depends on averaging of loop orientations, b= Burgers vector, V_c = atomic volume, The scattering intensity relative to the incident intensity is given by,

$$\frac{I^s(q_o)}{I_o} = \frac{C(R)}{2\mu_o V_c}\sigma_h^s(q_o) \tag{9}$$

where $C(R)/V_c$ is the density of loops of radius R. From Eqns. (7),(8) and (9) one can obtain loop size and density. Note that $(b\pi R^2/V_c)$ equals the number of point defects in the defect cluster.

In summary of the two calculations, the dynamical theory predicts a subsidiary peak which appears at an angle determined by the lattice strain due to alloying. The kinematic theory predicts a diffuse scattering which is proportional to the number and size of loops. Both calculations give the absolute relectivity with no adjustable parameters other than those describing the structure. The dynamical theory calculation depends on the assumption that the surface alloy is crystallographically coherent with the unalloyed crystal. The kinematic theory is likely to be limited in the case of very high defect cluster densities where nonrandom loop distributions may lead to interference between diffuse scattering amplitudes.

Experimental

The calculated strain scattering effects must be measured at small angles near the Bragg diffraction peak of the unaffected crystal. The implant affected region is less than 1 micron and the penetration depth is approxmately 1/2 = 11 microns. It is required that the bulk of the crystal be perfect (mosaic spread less than 1 minute) in order that the small scattering effects can be measured near the Bragg peak. Furthermore, it is required to subtract a significant background due to the tails of the bulk crystal Bragg peak in order to determine the diffuse scattering intensity due to surface alloying and defect clusters. A convenient approach to this measurement is to translate the crystal between an implanted and implantation-free area on the same crystal. Crystals used in these studies were provided by F. W. Young of Oak Ridge National Laboratory. The crystals were grown by the Bridgeman technique, cut to orientation, then annealed at a few degrees below the melting point for two weeks. The crystal pieces were hardened by neutron irradiation and then further cut and shaped by chemical cutting methods (15). The dislocation density measured by etch pit techniques was less than 10^3 cm^{-2} after shaping procedures were completed.

The two-crystal arrangement consisted of a silicon crystal fixed to diffract the Cu K_α radiation onto the implanted copper crystal. The (333) d-spacing (1.0451 A) of silicon happens to match the (222) d-spacing (1.0436 A) of copper very well so that the system is well focussed to give a narrow rocking curve width. The copper crystal is initially aligned to give a sharp maximum in the rocking curve by adjusting the (111) normal about an axis in the scattering plane. When properly adjusted, the full width at half-maximum (FWHM) of the copper rocking curve is 12.5 arc-seconds. The crystal is mounted on a goniostat which can be translated in the plane of the crystal surface so that rocking curves can be made from the implanted area and masked implantation-free areas. In a typical run, the copper crystal is rocked about an axis perpendicular to the scattering plane at a rate of 5 to 20 arc-seconds per minute while x-ray intensities are recorded continuously at 10 second intervals. The x-ray detector has an active receiving area of 5 cm^2 at a distance of 8 cm so that the subtended solid angle (0.08 steradians) integrates the scattering over a large portion of the Ewald sphere in the vicinity of the 222 Bragg peak of copper.

The implantation of aluminum into copper was chosen for these experiments because the ion penetration was favorable and the microalloy concentration was well below the solubility limit of the aluminum in copper. The details of implantation are given elsewhere (19). The implanted layer was 1200 A thick (16) with a composition of 1.8 atomic percent. The distribution of damage over the alloy thickness was estimated on the basis of calculations by Fritzsche (17) and Winterbon (18). The alloy distribution (solid line) and the damage profile (dashed line) are shown in Figure 3.

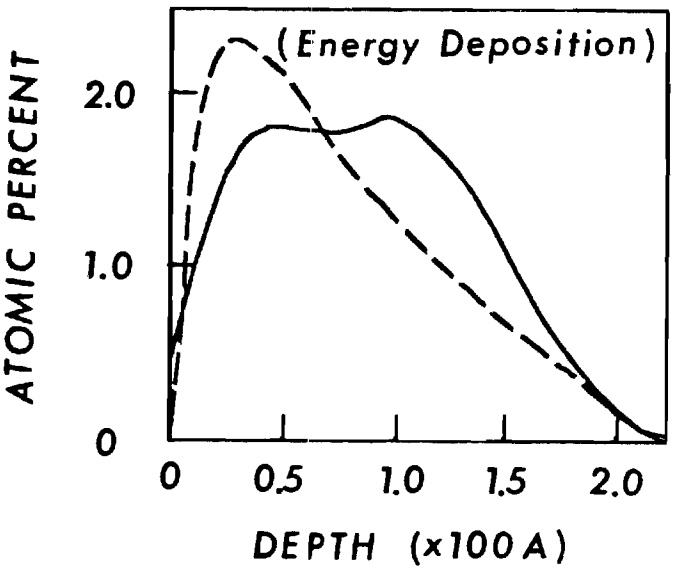

Fig. 3
Distribution of implanted Al^+ ions (solid) and the energy deposition (dashed) for the implantation of 2×10^{16} ion/cm^2 with energies up to 200 keV. Note that damage is concentrated toward the surface and that the damage energy is on a relative scale.

Annealing of the specimens was performed as a means to differentiate the sources of scattering in the implanted layers. The crystals were placed in a vacuum of 10^{-8} Torr at 500 C, 600 C and 900 C for 30 minutes. Annealing at 900 C restored the original structure as seen in the rocking curves.

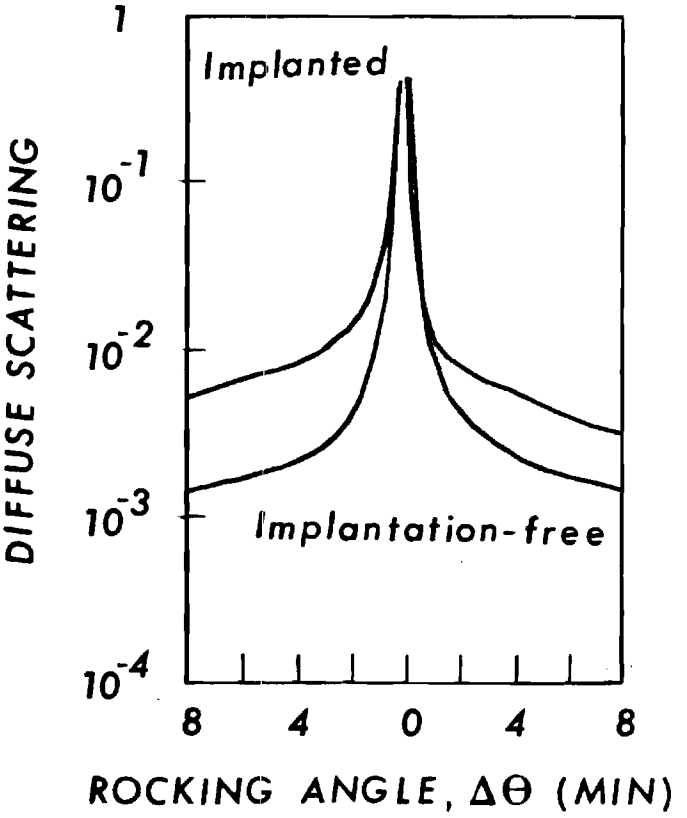

Fig. 4
Rocking curves are shown for the implanted (upper) and implantation-free (lower) crystal. The scattering is expressed as a fraction of the incident beam intensity. Note the larger scattering at low angles.

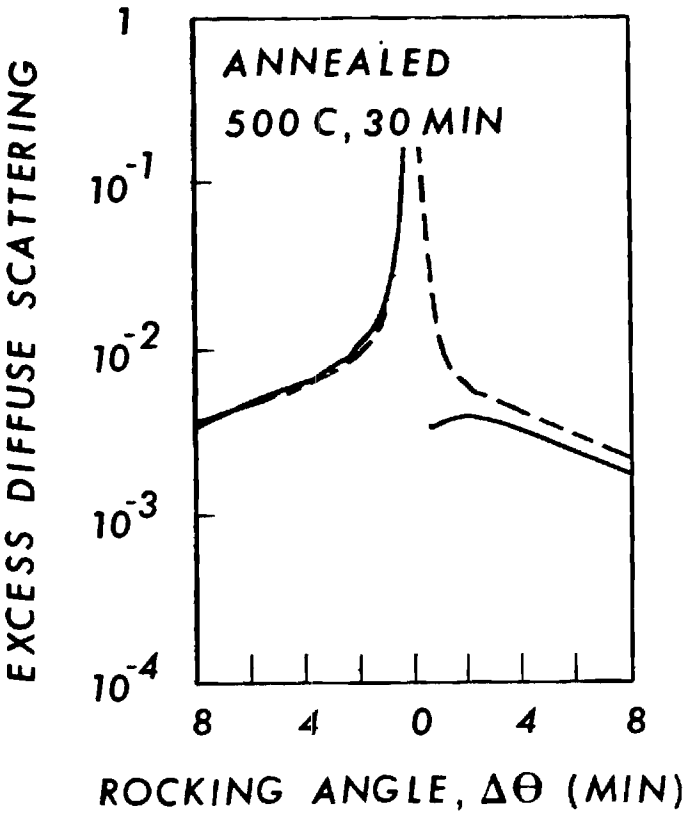

Fig. 5
Excess diffuse scattering intensity for the sample before annealing (dashed) and after annealing (solid) at 500 C. Note that little change in the general level and distribution of the excess intensity occurs upon annealing.

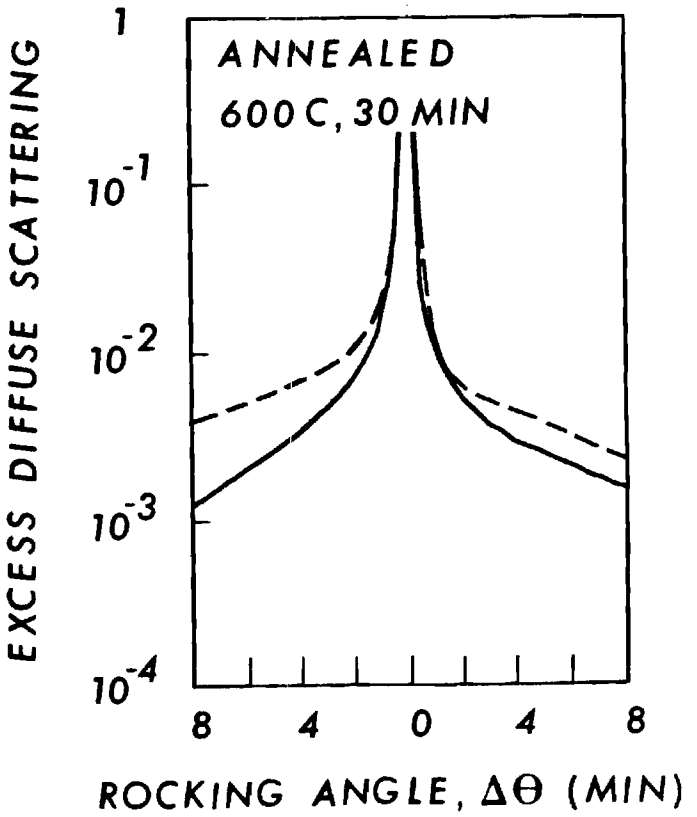

Fig. 6
Excess diffuse scattering intensity for the sample before annealing (dashed) and after annealing (solid) at 600 C. The level and the distribution of the excess intensity changes as a result of the annealing at this temperature.

Although there is a displacement between the two sets of points, the average of the high angle and low angle intensity is close to a straight line which yields an estimated loop radius of 25 A.

An estimate of the density of loops can be made by comparing measured reflectivity with Eqn. (9). We use a loop radius of 25 A and a reflectivity of 1 percent at $\Delta\theta$= 2 minutes. Substitution of appropriate constants into Eqn. (9) for a 25 A loop size gives

$$\frac{I^s(q_o)}{I_o} = 6.1 \times 10^{-21} \frac{C}{V_c} \ln\left(\frac{44}{\Delta\theta(\text{min})}\right) \qquad (10)$$

from which a value of C/V_c is 5.3 x 10^{17} loops/cc. (The loops are concentrated by a factor of 40^c in the implanted layer since the above calculation assumes the loops to be uniformly distributed).

The failure to observe a sharp Bragg peak associated with the implanted aluminum and the general agreement with scattering levels calculated for loop scattering point to the conclusion that the kinematic theory for diffraction from an implanted crystal containing loops is appropriate. The annealing at 600 C produces symmetrical scattering which suggests that most of the aluminum is removed from the region where loops persist. Thereby the loop scattering now originates in essentially pure copper. The role of aluminum is seen as simply expanding the lattice in a region where loops persist which, by virtue of severe damage, is no longer strictly coherent with the implantation-free crystal.

Conclusions

Analysis of x-ray diffraction in aluminum-ion implanted copper suggests that defect cluster scattering dominates the observed rocking curve intensity. Alloying in the implanted layer contributes through a shifting of the diffuse scattering to lower angles due to the fact that the defect clusters are formed in a region of aluminum-expanded lattice. The formation of a distinct peak predicted by dynamical diffraction theory does not occur, probably because of the intense defect scattering and the widths of the peak from the thin layer. Problems in the analysis of scattering remain in the area of formulating a model of combined alloying and defect cluster scattering as well as description of very high defect cluster scattering. Nevertheless the simplistic interpretation of x-ray scattering observation provides useful insights into the type and quantity of damage as well as the annealing response of the implanted structure. Measurements carried out to larger q_o will be useful in further definition of the defect structure since Bragg scattering from the implantation-free and implanted layer are avoided and the kinematical theory can be assumed. Size distributions an and total point defect densities are more directly measurable at the larger q_o values (1) as well.

Acknowledgements

The author thanks Dr. B. C. Larson and Mr. Jim Barhorst of the Solid State Division of Oak Ridge National Laboratory for their considerable help in the collection of the data and many useful discussions.

References

1. B. C. Larson, "X-ray Studies of Defect Clusters in Copper," J. Appl. Cryst. , 8 ,pp. 150-160 (1975).

2. K. Komenou, I. Hirai, K. Asama and M. Sakai, "Crystalline and Magnetic Properties of an Ion-Implanted Layer in Bubble Garnet Films," J. Appl. Phys. , 49 ,pp. 5816-5822 (1978).

Results and Discussion

The rocking curves for implantation-free copper and for aluminum implanted copper were measured on the same crystal. These curves are shown in Figure 4. The diffuse scattering from the implanted crystal is more intense on the low angle side of the Bragg peak position. The excess diffuse scattering is calculated by subtraction of the implantation-free rocking curve intensity from the corresponding intensity in the implanted crystal. The excess diffuse scattering for the implanted crystal is shown in Figures 5 and 6 as a dashed line. The effect of 30 minute anneals on the excess diffuse intensity is show in Figure 5 for annealing at 500 C and in Figure 6 for annealing at 600 C. No large change due to annealing occurs at 500 C while for annealing at 600 C, there is a reduction of scattering and scattering becomes more symmetric with respect to the Bragg peak position.

The observation of a higher diffuse scattering at low rocking curve angles can be attributed to the fact that implanted aluminum expands the copper lattice so that Bragg scattering from the implanted region occurs at a lower angle than that for the implantation-free material. The composition of the implanted layer was estimated to be 1.8 atomic percent. The resulting Bragg position would be displaced to lower angle by 4.2 minutes for the 222 reflection from the copper alloy layer.

The diffuse scattering seen on both sides of the main Bragg position can be compared to calculations of the scattering from dislocation loops. In Figure 7 the excess diffuse scattering is plotted versus the log of the rocking angle according to Eqn. (7) for Huang loop scattering. The rocking angle was measured relative to the supposed Bragg position for the alloy.

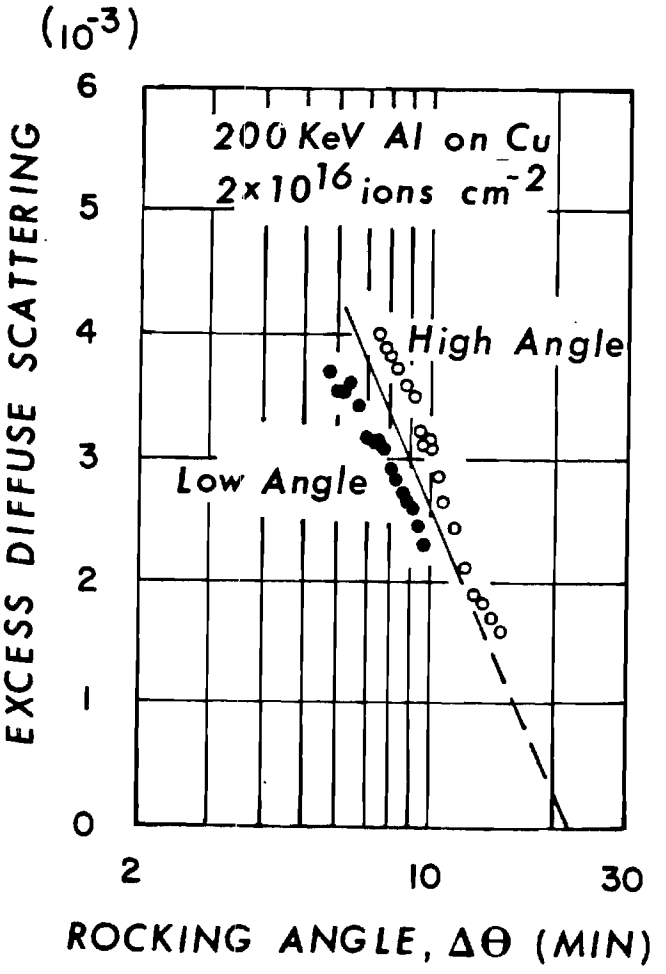

Fig. 7
The excess diffuse scattering from the implanted crystal is plotted versus $\ln(\Delta\theta)$ for the intensity above and below the Bragg position assumed to apply for the implanted region of the crystal.

3. V. S. Speriousu, H. L. Glass and T. Kobayashi, X-ray Determination of Strain and Damage Distributions in Ion-Implanted Layers," Appl. Phys. Lett. , 34 , pp. 539-542 (1979).

4. A. M. Afanasev, M. V. Kovalchuck, E. K. Kovev and V. G. Kohn, "X-ray Diffraction in a Perfect Crystal with Disturbed Surface Layer," Phys. Stat. Sol. (a) 42 , pp. 415-422 (1977)

5. H. Yamagishi and O. Nittono, "X-ray Study on Lattice Defects in Ar^+ Ion Implanted Copper Whiskers," Nip. Kinz. Gakk. , 43 , pp. 689-695 (1979).

6. A. Kujore,S. B. Chakrabortty and E. A. Starke, "The Effect of Ion Implantation on the Fatigue Properties of Polycrystalline Copper," Nucl. Instr. Meth., 182/183, pp. 949-958 (1981).

7. B. C. Larson, C. W. White and B. R. Appleton, "Unidirectional Contraction in Boron-Implanted Laser-Annealed Silicon," Appl. Phys. Lett., 32, pp. 801-803 (1978).

8. B. C. Larson and J. F. Barhorst, "X-ray Study of Lattice Strain in Boron Implanted Laser Annealed Silicon," J. Appl. Phys., 51, pp.3181-5 (1980).

9. B. Klar and F. Rustichelli, "Dynamical Neutron Diffraction by Ideally Curved Crystals," Nuovo Cimento, 13B, pp. 249-270 (1973).

10. B. E. Warren, X-ray Diffraction, Chapter 14, pp. 315-354, Addison-Wesley Press, Reading, Mass. (1969).

11. W. H. Zachariasen, Theory of X-ray Diffraction in Crystals, Chapter 3, pp. 83-155, Dover Publications, New York (1967).

12. H. W. King, "Quantitative Size-Factors for Metallic Solid Solutions," J. Mat. Sci, 1, pp. 79-90 (1966).

13. B. C. Larson and W. Schmatz, "Huang-Diffuse Scattering from Dislocation Loops and Cobalt Precipitates in Copper," Phys. Rev. , B10, pp. 2307-2314 (1974).

14. B. C. Larson and F. W. Young, Jr. , "A Comparison of Diffuse Scattering by Defects and Measured in Anomalous Transmission and Near Bragg Reflections," Z. Naturforsch. , 28a, pp. 626-632 (1973).

15. F. W. Young, Jr. , "Etch Pit Studies of Dislocations in Copper Crystals Deformed by Bending. I. Annealed Crystals. II. Irradiated Crystals," J. Appl. Phys. , 33, pp. 3553-3564 (1962).

16. J. Keinonen, M. Hautala, M. Luomajari, A. Antilla and M. Bister, "Ranges of $^{27}Al^+$ Ions in Nine Metals Measured by (p,γ) Resonance Broadening," Rad. Eff. , 39, pp. 189-193 (1978).

17. C. R. Fritzche, "A Simple Method for the Calculation of Energy Deposition Profiles from Range Data of Implanted Ions," Appl. Phys. Lett. , 12, pp. 347-353 (1977).

18. K. B. Winterbon, Ion Implantation Range and Energy Deposition Distributions, Vol. 2, Low Incident Ion Energies, Plenum Press, New York (1975)

19. S. Spooner and K. Legg, "X-ray Diffraction Characterization of Aluminum Ion-Implanted Copper Crystals," Ion Implantation Metallurgy, C. M. Preece and J. K. Hirvonen, eds. TMS AIME, pp. 162-170 (1980).